AIS and VDES Ranging - measurements results

GA5.3/5.4 project report

Issue: 2.0

Issue Status: Approved

Issue Date: 24/10/2021

	Name	Partner	Signature
Provided	Krzysztof Bronk	NIT	
Review	Stefan Gewies	DLR	
Approval	Stefan Gewies	DLR	

Document Information

Project Title	R-Mode Baltic
Work Package No.	GA 5.3/5.4
Document Title	AIS and VDES Ranging - measurements results
Description	The major topic of the document is the analysis of the measurement results of AIS and VDES ranging
Date	24.10.2021
Lead Author	NIT
Lead Author's Contact Information	National Institute of Telecommunications Wireless Systems and Networks Department Telephone: (+48) 58 341 71 21 E-mail: K.Bronk@itl.waw.pl
Contributing Author(s)	Krzysztof Bronk, Patryk Koncicki, Rafał Niski, Błażej Wereszko
Approval	Yes

Track Changes

Issue	Date	Pages	Change	Author, Company
1.0	16/12/2019	69	Draft	NIT
2.0	19/03/2020	82	Draft	NIT

This report was created within the framework of the **R-Mode Baltic** project, which aims to develop and demonstrate a new maritime backup system for Position, Navigation and Time (PNT) purposes based on R-Mode technology. Within the project life time of three years the project consortium develops solutions for R-Mode transmitter and receiver prototypes, for independent time synchronisations of broadcasting stations and for a testbed concept and its deployment. The dissemination of R-Mode technology is supported by work in international standardisation bodies. The world's first operational testbed for a transnational R-Mode system will be completed by the project in 2020.

The R-Mode Baltic project is co-financed by the European Regional Development Fund within the Interreg Baltic Sea Region Programme.

This report is available for download on the project website https://www.r-mode-baltic.eu/.

Contents

List of Tables

List of Figures

Abbreviations

AIS	Automatic Identification System
AWGN	Additive White Gaussian Noise
BER	Bit Error Rate
BLER	Block Error Rate
CRC	Cyclic Redundancy Check
GMSK	Gaussian Minimum Shift Keying
GNSS	Global Navigation Satellite System
GPS	Global Positioning System
LPF	Low-pass filter
NRZI	Non Return to Zero Inverted
PNT	Position, Navigation and Time
R-Mode	Ranging Mode
SDR	Software Defined Radio
TOA	Time of Arrival
USRP	Universal Software Radio Peripheral
VDES	VHF Data Exchange System
PNT	Position, Navigation and Time
R-Mode	Ranging Mode
MOG	Maritime Office in Gdynia
VHF	Very High Frequency
VDES	VHD Data Exchange System
AIS	Automatic Identification System
SOTDMA	Self-organized time-division multiple access
ITDMA	Incremental Division Multiple Access
CRC	Cyclic Redundancy Code
QPSK	Quadrature Phase Shift Keying
MCS	Modulation and Coding Scheme
FEC	Forward Error Correction
AWGN	Additive white Gaussian noise
QAM	Quadrature Amplitude Modulation
PSK	Phase Shift Keying
SWR	Standing Wave Ratio
VSWR	Voltage Standing Wave Ratio
RRC	Root Raised Cosine

SNR	Signal to Noise Ratio
RMS	Root Mean Square
GNSS	Global Navigation Satellite Systems
EGNOS	European Geostationary Navigation Overlay Service

1 Introduction

The following report summarises the activities of the National Institute of Telecommunications in the R-Mode's GAs 5.3 and 5.4. The major topic of the document is the analysis of the measurement results of AIS and VDES ranging. This report is a continuation and supplement to the report entitled "AIS Ranging and Positioning - concept and signal design", therefore there will be some references to this report in the text.

The report is comprised of six chapters (including this introduction).

The second chapter describes the assumptions of measurement campaigns. It presents general concept of measurements, AIS and VDES message structures, base station technical parameters and calibration.

The next, third chapter, provides a detailed description of the software implementation of the AIS and VDES systems (transmitter, channel, receiver) as well as the hardware platform prepared for the measurement campaigns.

The fourth chapter is dedicated to the analysis of the measurement campaign results. During two measurement campaigns carried out in summer and autumn, ranging tests were performed using AIS and VDES systems. Authors conducted a comparative analysis of the obtained results.

In the fifth chapter, some final remarks are included, mostly regarding the future tasks to be carried out by the National Institute of Telecommunication in the R-Mode project.

In the last chapter, authors introduced conclusions and plans for the next measurement campaign scheduled to take place at the Baltic Sea in the spring 2020.

2 Measurement methodology

2.1 General concept of measurement campaigns

The measurement campaigns at sea were carried out in cooperation with the Maritime Office in Gdynia (MOG). For the purpose of the measurements, the MOG provided its VHF antenna installation located on the tower near the entrance to the port in Gdynia. This specific location was used for the R-Mode testbed's transmitter (Tx) installation. The aim of the measurements was to test, in real conditions, designed system and its possibility to determine the distance between the terminal at sea and the base station on the shore.

The main goal of the measurements is the analysis of the impact of the maritime radio VHF channel on the ranging accuracy when using time-based methods (this analysis will be performed for different weather conditions). In order to eliminate some sources of errors, the rubidium oscillators were installed on both ends of the radio link.

Additionally, the exact location of the transmitting station was determined via RTK measurements. An important element of the measurements was the logging of the vessel position determined using the GNSS+EGNOS receiver. The fixed position was converted to the distance to the transmitting station and was the reference value for the collected measurement values. It allowed to determine the final ranging accuracy of the R-Mode test-bed. For this purpose the GNSS u-blox EVK-M8 (multisystem GNSS + EGNOS receiver) was used and was register the most important parameters such as: UTC time, coordinates, velocity, course, and DOP values.

The receiving (Rx) station was installed on the Stena Line ferryboat running between Gdynia and Karlskrona. This solution allowed to obtain diversified results (for different distances between the transmitter and the receiver) without the need to rent a vessel, which will reduce the costs of the entire operation. Additionally, the measurement results were recorded each time for a situation when the vessel moves away from the R-Mode station and when it approaches it. Figure 2-1 presents Stena Line Gdynia-Karlskrona route.

Figure 2-1: Stena Line Gdynia-Karlskrona route

As part of the preparations for the planned measurement campaigns in the Baltic Sea, a measurement stand including a transmission and reception side was designed. Appropriate schemes for AIS and VDES was presented in Chapter 3.

Figures 2-2 and 2-3 show, accordingly, the receiving side of the measurement stand and Rx antennas installed on the ferry.

Figure 2-2: The receiving side of the measurement stand installed on the ferry

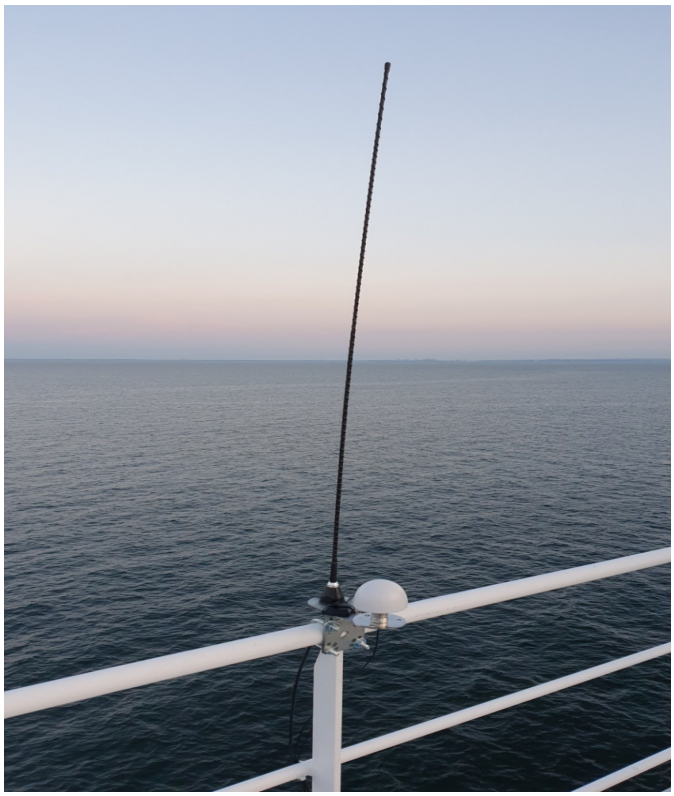

Figure 2-3: The VHF and GNSS antennas installed on the ferry

In 2019, two measurement campaigns were carried out:

- 17-18 June 2019 - based on AIS transmission,
- 15-16 November 2019 - based on VDES transmission.

The results obtained and their analysis are presented in Chapter 4.

2.2 Base station technical parameters

During the tests, 4 neighboring channels were used with a width of 25 kHz each (channels No. 2024, 2084, 2025, 2085 with center frequencies from 161.800 MHz to 161.875 MHz) provided for the VDES [4-4] system (VHF Data Exchange System). NIT obtained a temporary permit from the President of Polish Office of Electronic Communications (Decision No. DZC.WML.5101.3255.2018.2) to use the above-mentioned radio channels for testing the R-Mode system in the area of the Bay of Gdańsk and the Polish territorial waters of the Baltic Sea. In the figure 2-4 the R-Mode base station designed by NIT was presented.

Figure 2-4: Designed R-Mode base station installed in the MOG spot in Port Gdynia

In the figure 2-5 the MOG tower with VHF antenna installation and also a part of calibration stand is depicted.

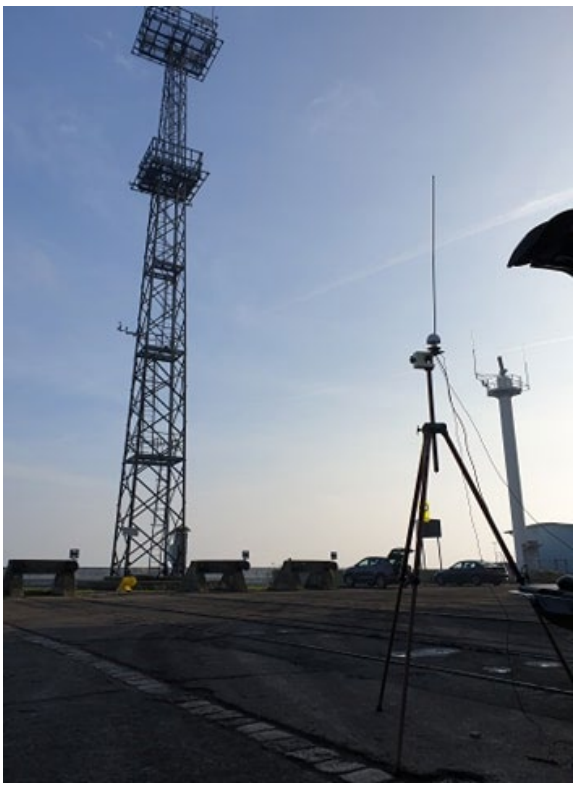

Figure 2-5: MOG tower with VHF antenna installation and a part of calibration stand

The table 2-1 contains the most important technical parameters of the R-Mode test station, whereas in table 2-2 the receiver technical parameters are presented.

Table 2-1: Technical parameters of the R-Mode test station

Location	N 54° 31' 45,36" E 18° 33' 34,48"
Height of the antenna	28 m a.s.l.
Frequency of the transmitter	161.8375 MHz
Antenna type	Radmor 32812/1
Antenna radiation pattern	Omni-directional antenna
Antenna gain	2.15 dBi
Cable attenuation	8.5 dB
ERP power	14.8 dBW
Transmitting device	• National Instruments USRP 2920 / USRP 2954 • Power amplifier POPEK ELEKTRONIK PEA02-2-50 • Baseband filter PROFCOM BPF 2/2-250
Modulation used	• GMSK (according to ITU-R M.1371-5) • Pi/4-QPSK (according to ITU-R M.2092)

Table 2-2: Technical parameters of the R-Mode test receiver

Sensitivity	-107 dBm
The minimum value of the useful field strength	14 dBμV/m
The maximum value of the interference field strength	12 dBμV/m
Height of the antenna	4 m a.s.l.

Report shows the expected useful ranges determined in accordance with the ITU-R propagation model P.1546-5 [5-1], on the basis of the assumed parameters.

The measured EIRP power of the transmitter at the location in Gdynia was 41.25 dBm for the AIS transmission.

2.3 AIS message structure

One of the basic R-Mode project assumptions is the usage of the Automatic Identification System's (AIS) standard messages for ranging measurements. The project requirements indicate the AIS Message 26 should be used [2-1]. The multiple slot binary Message 26 is primarily intended for scheduled binary data transmissions by applying either the SOTDMA or ITDMA access schemes. This multiple slot binary message can contain up to 1 004 data bits (using 5 slots) depending on the coding method used for the content, and the destination indication of broadcast or addressed. The table 2-3 presents the Message 26 structure tailored to the project purposes [2-2].

Table 2-3: AIS Message 26 structure [2-2]

Parameter	Number of bits	Description
Message ID	6	Identifier for Message 26; always 26
Repeat indicator	2	Used by the repeater to indicate how many times a message has been repeated; default = 0
Source ID	30	MMSI number of source station
Destination indicator	1	0 = Broadcast (no Destination ID field used)
Binary data flag	1	1 = binary data coded as defined by using the 16-bit Application identifier
Binary data	104	Application identifier - 16 bits
		Application binary data - 88bits
Binary data added by 2nd slot	224	Allows for 32 bits of bit-stuffing
Binary data added by 3rd slot	224	Allows for 32 bits of bit-stuffing
Binary data added by 4th slot	224	Allows for 32 bits of bit-stuffing
Binary data added by 5th slot	224	Allows for 32 bits of bit-stuffing
Spare	4	Needed for byte alignment
Communication state selector flag	1	0 = SOTDMA communication state follows 1 = ITDMA communication state follows
Communication state	19	SOTDMA communication state if communication state selector flag is set to 0, or ITDMA communication state if communication state selector flag is set to 1
Maximum number of bits	Maximum 1 064	

The table 2-4 contains the maximum number of binary data-bits for settings of destination indicator and coding method flags, such that the message does not exceed the indicated number of slots.

Table 2-4: Maximum number of AIS Message 26 data bits [2-2]

Destination indicator	Binary data flag	Binary data (maximum bits)				
		1-slot	2-slot	3-slot	4-slot	5-slot
0	1	88	312	536	760	984

In the transmission part of the AIS system, the structure of the data frame has been defined (Fig. 2-6.), [4-1].

Ramp Up 8 bits	Training sequence 24 bits	Start flag 8 bits	Data 1064 bits	CRC16 16 bits	End flag 8 bits

Figure 2-6: The structure of the implemented frame for the AIS system

In the AIS system the frame consists of the following blocks [4-1]:

- a ramp up sequence which is responsible for activating the power detector,
- a training sequence, which allows the correlator in the receiver to properly determine the start of the frame,
- a start flag, which is used to detect the start of the transmission packet,
- a data block with the checksum CRC-16,
- an end flag which is used to detect the end of the transmission packet.

2.4 VDES message structure

In the second measurement campaign, the VDES frame structure was used [2-3]. For the VDES-TER layer with 100 kHz band and π/4-QPSK modulation, the following parameters were used from table 2-5:

Table 2-5: VDE-TER Link ID parameters

PL format #	TER-MCS-1.25	TER-MCS-3.25	TER-MCS-5.25	TER-MCS-1.50	TER-MCS-2.50	TER-MCS-3.50	TER-MCS-1.100	TER-MCS-3.100	TER-MCS-5.100	
Link Config ID	11	12	14	14	15	16	17	18	19	kHz
Channel BW	25			50			100			
Roll off filtering	0,3									
Signal BW	25			49,9			99,8			kHz
Symbol rate	19,2			38,4			76,8			ksps
PAPR (example)	3,82	4,4	6,7	3,82	4,4	6,7	3,82	4,4	6,7	dB
Minimum high output average	12,5	11	6,5	12,5	11	6,5	12,5	11	6,5	Watt

power										
Burst size	1									slot
Guard time	0,83									ms
Burst duration	25,8									Ms
Symbols/burst	496			992			1984			symbols
Ramp-up/down	8/8			16/16			32/32			symbols
Ramp-up/down	0.41/0.41									ms
Syncword size	27									symbols
Syncword modulation	PI/4 QPSK (00/11 only)									
Link Config ID size	16 (32,6 block code)									symbols
Link Config ID modulation	PI/4 QPSK									
Net symbols/burst	437			917			1877			symbols
Channel bits	874	1311	1748	1834	2751	3668	3754	5631	7508	bits
Padding + FEC tail	10 +0	3 +12	8 +12	30 +12	51 +12	72 +12	0 +10	243 +12	8 +12	bits
FEC decoder input symbols	432			896			1872	1792	1872	symbols
FEC decoder input bits	864	1296	1728	1792	2688	3584	3744	5376	7488	Bits

FEC output bits	432	972	1296	896	2016	2688	1872	4032	5616	Bits
FEC output bytes	54	122	162	112	252	336	234	504	702	bytes
Modulation	PI/4 QPSK	8PSK	16QAM	PI/4 QPSK	8PSK	16QAM	PI/4 QPSK	8PSK	16QAM	
FEC rate	½	3/2	¾	½	¾	¾	½	¾	¾	
E_S/N_0 on AWGN	1	7,9	10,2	1	7,9	10,2	1	7,9	10,2	dB
$C/(N_o+I_0)$ threshold	43,8	50,7	53	46,8	53,7	56	49,9	56,8	59,1	dBHz
Minimum CQI value	42						48		84	dBHz

In the transmission part of the VDES system, the structure of the data frame has been defined (Fig. 2-7.).

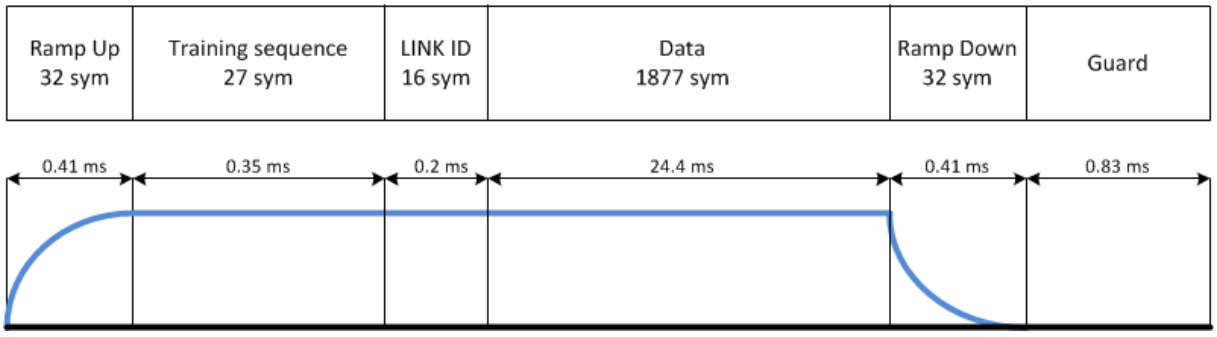

Figure 2-7: The structure of the implemented frame for the VDES system

In the VDES system the frame consists of the following blocks:

- A ramp up sequence which is responsible for activating the power detector,
- a training sequence, which allows the correlator in the receiver to properly determine the start of the frame,
- a LINK ID, defines the channel configurations (table 2-6),
- a data block with the checksum CRC-16,
- an ramp down which is used to detect the end of the transmission packet,
- a guard, time consists of the ramp down time from full power to −50 dBc of less than or equal to 416 μs. The remaining time is for delay and jitter.

The Link ID defines the channel configurations. The Link ID is used to index the table of channel configurations. The Link ID consists of 6 bits (D0, D1, D2, D3, D4, D5) encoded into a sequence of 32 bits using biorthogonal (32,6) code. The code is a first order Reed-Muller code with generator matrix: The code shall be bit scrambled using the scrambling word 11000010111000101000111001001111. This results in the Link ID coding of table 2-6.

Table 2-6: Link ID code words for VDES

Link Conf ID	Bit-scrambled code word	Link Conf ID	Bit-scrambled code word
0	11 00 00 10 11 10 00 10 10 00 11 10 01 00 11 11	32	01 00 00 00 00 00 10 11 01 10 01 11 11 01 10 01
1	11 00 01 10 11 10 00 10 11 11 00 01 10 11 00 00	33	01 00 01 00 00 00 10 11 00 01 10 00 00 10 01 10
2	11 00 10 10 10 01 11 01 10 00 11 10 10 11 00 00	34	01 00 10 00 01 11 01 00 01 10 01 11 00 10 01 10
3	11 00 11 10 10 01 11 01 11 11 00 01 01 00 11 11	35	01 00 11 00 01 11 01 00 00 01 10 00 11 01 10 01
4	11 01 00 01 11 10 11 01 00 00 00 01 01 00 00 00	36	01 01 00 11 00 00 01 00 11 10 10 00 11 01 01 10
5	11 01 01 01 11 10 11 01 01 11 11 10 10 11 11 11	37	01 01 01 11 00 00 01 00 10 01 01 11 00 10 10 01
6	11 01 10 01 10 01 00 10 00 00 00 01 10 11 11 11	38	01 01 10 11 01 11 10 11 11 10 10 00 00 10 10 01
7	11 01 11 01 10 01 00 10 01 11 11 10 01 00 00 00	39	01 01 11 11 01 11 10 11 10 01 01 11 11 01 01 10
8	11 10 00 01 01 01 00 01 10 11 11 01 01 11 11 00	40	01 10 00 11 10 11 10 00 01 01 01 00 11 10 10 10
9	11 10 01 01 01 01 00 01 11 00 00 10 10 00 00 11	41	01 10 01 11 10 11 10 00 00 10 10 11 00 01 01 01
10	11 10 10 01 00 10 11 10 10 11 11 01 10 00 00 11	42	01 10 10 11 11 00 01 11 01 01 01 00 00 01 01 01
11	11 10 11 01 00 10 11 10 11 00 00 10 01 11 11 00	43	01 10 11 11 11 00 01 11 00 10 10 11 11 10 10 10
12	11 11 00 10 01 01 11 10 00 11 00 10 01 11 00 11	44	01 11 00 00 10 11 01 11 11 01 10 11 11 10 01 01
13	11 11 01 10 01 01 11 10 01 00 11 01 10 00 11 00	45	01 11 01 00 10 11 01 11 10 10 01 00 00 01 10 10
14	11 11 10 10 00 10 00 01 00 11 00 10 10 00 11 00	46	01 11 10 00 11 00 10 00 11 01 10 11 00 01 10 10
15	11 11 11 10 00 10 00 01 01 00 11 01 01 11 00 11	47	01 11 11 00 11 00 10 00 10 10 01 00 11 10 01 01
16	10 00 00 11 00 11 01 11 01 01 10 11 00 01 10 10	48	00 00 00 01 11 01 11 10 10 11 00 10 10 00 11 00
17	10 00 01 11 00 11 01 11 00 10 01 00 11 10 01 01	49	00 00 01 01 11 01 11 10 11 00 11 01 01 11 00 11
18	10 00 10 11 01 00 10 00 01 01 10 11 11 10 01 01	50	00 00 10 01 10 10 00 01 10 11 00 10 01 11 00 11
19	10 00 11 11 01 00 10 00 00 10 01 00 00 01 10 10	51	00 00 11 01 10 10 00 01 11 00 11 01 10 00 11 00
20	10 01 00 00 00 11 10 00 11 01 01 00 00 01 01 01	52	00 01 00 10 11 01 00 01 00 11 11 01 10 00 00 11

21	10 01 01 00 00 11 10 00 10 10 10 11 11 10 10 10	53	00 01 01 10 11 01 00 01 01 00 00 10 01 11 11 00
22	10 01 10 00 01 00 01 11 11 01 01 00 11 10 10 10	54	00 01 10 10 10 10 11 10 00 11 11 01 01 11 11 00
23	10 01 11 00 01 00 01 11 10 10 10 11 00 01 01 01	55	00 01 11 10 10 10 11 10 01 00 00 10 10 00 00 11
24	10 10 00 00 10 00 01 00 01 10 10 00 00 10 10 01	56	00 10 00 10 01 10 11 01 10 00 00 01 10 11 11 11
25	10 10 01 00 10 00 01 00 00 01 01 11 11 01 01 10	57	00 10 01 10 01 10 11 01 11 11 11 10 01 00 00 00
26	10 10 10 00 11 11 10 11 01 10 10 00 11 01 01 10	58	00 10 10 10 00 01 00 10 10 00 00 01 01 00 00 00
27	10 10 11 00 11 11 10 11 00 01 01 11 00 10 10 01	59	00 10 11 10 00 01 00 10 11 11 11 10 10 11 11 11
28	10 11 00 11 10 00 10 11 11 10 01 11 00 10 01 10	60	00 11 00 01 01 10 00 10 00 00 11 10 10 11 00 00
29	10 11 01 11 10 00 10 11 10 01 10 00 11 01 10 01	61	00 11 01 01 01 10 00 10 01 11 00 01 01 00 11 11
30	10 11 10 11 11 11 01 00 11 10 01 11 11 01 10 01	62	00 11 10 01 00 01 11 01 00 00 11 10 01 00 11 11
31	10 11 11 11 11 11 01 00 10 01 10 00 00 10 01 10	63	00 11 11 01 00 01 11 01 01 11 00 01 10 11 00 00

2.5 Time and spectral characteristics of AIS and VDES signals

This chapter presents the time and spectral characteristics of AIS and VDES signals. The Hann window was used for both signal cases. The main reason for its use is the reduction of spectral leakage. The main disadvantage of using this window is a power loss of 4 dB. The Hanna window function is described in the following formula 2-1:

$$w(u) = 0{,}5\left(1 - \cos\left(\frac{2\pi n}{N-1}\right)\right) \quad (2\text{-}1)$$

where:

n - sample value,

N - number of all samples.

The figure 2.8 shows the characteristics of the Hann window.

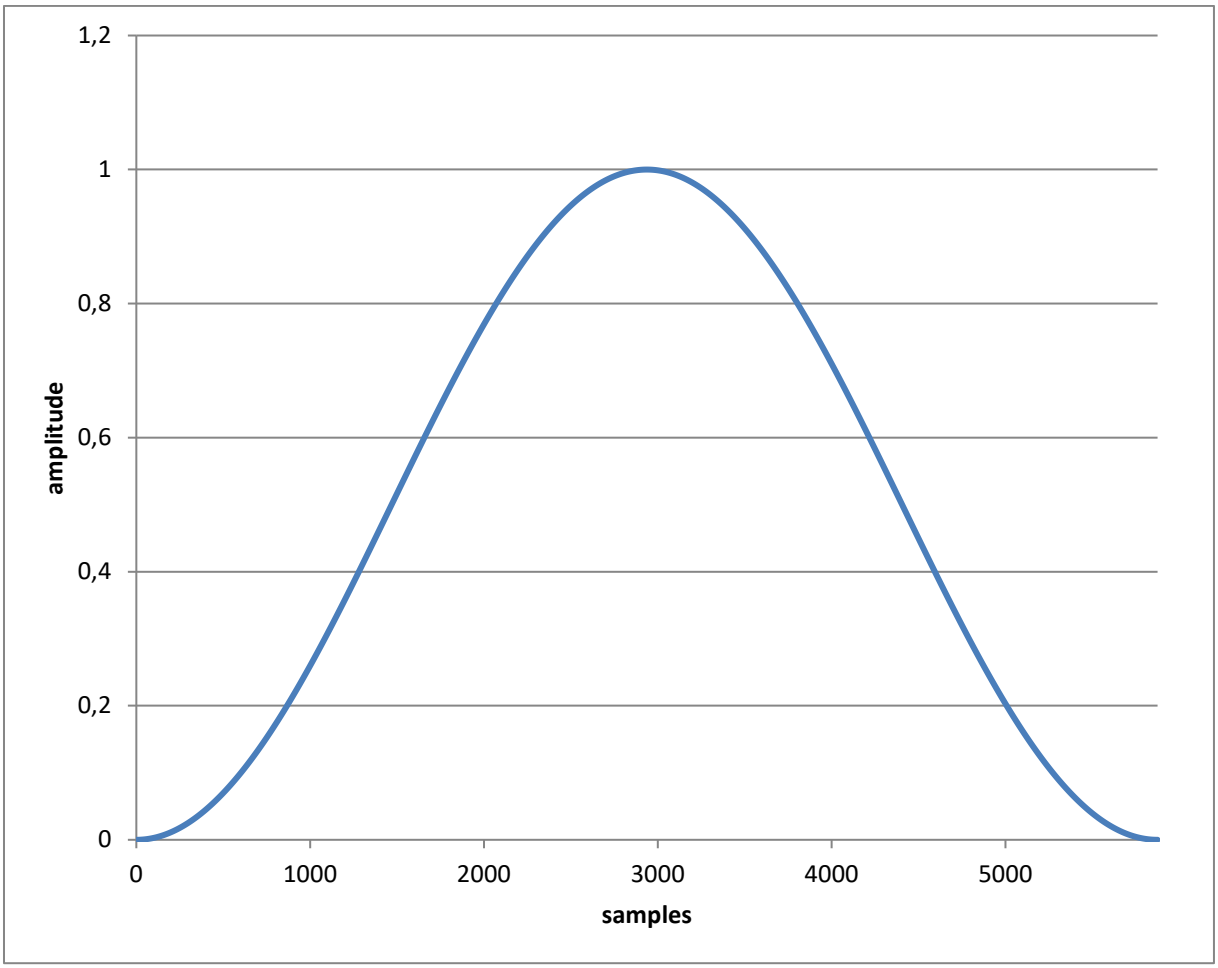

Figure 2-8: Hann Window

Figure 2-9 shows the time characteristics of the AIS signal. This signal was broadcast in the first measurement campaign.

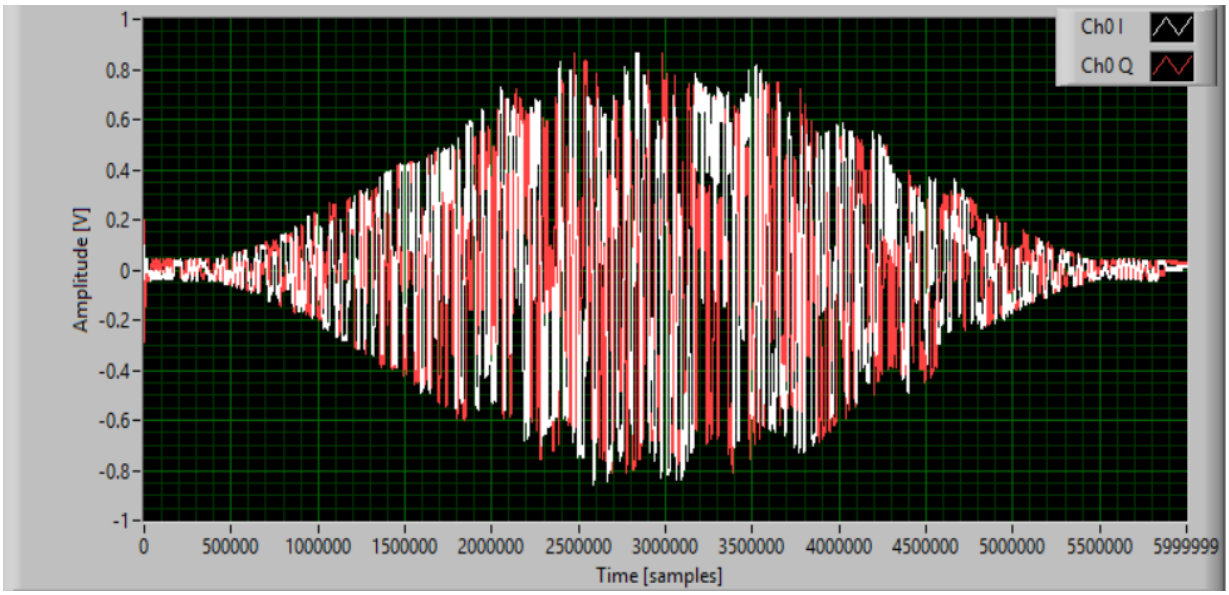

Figure 2-9: Time characteristics of the AIS signal

Figure 2-10 shows the spectral characteristics of the AIS signal. The obtained shape of the AIS signal spectrum is the result of GMSK modulation and the use of Gaussian filter.

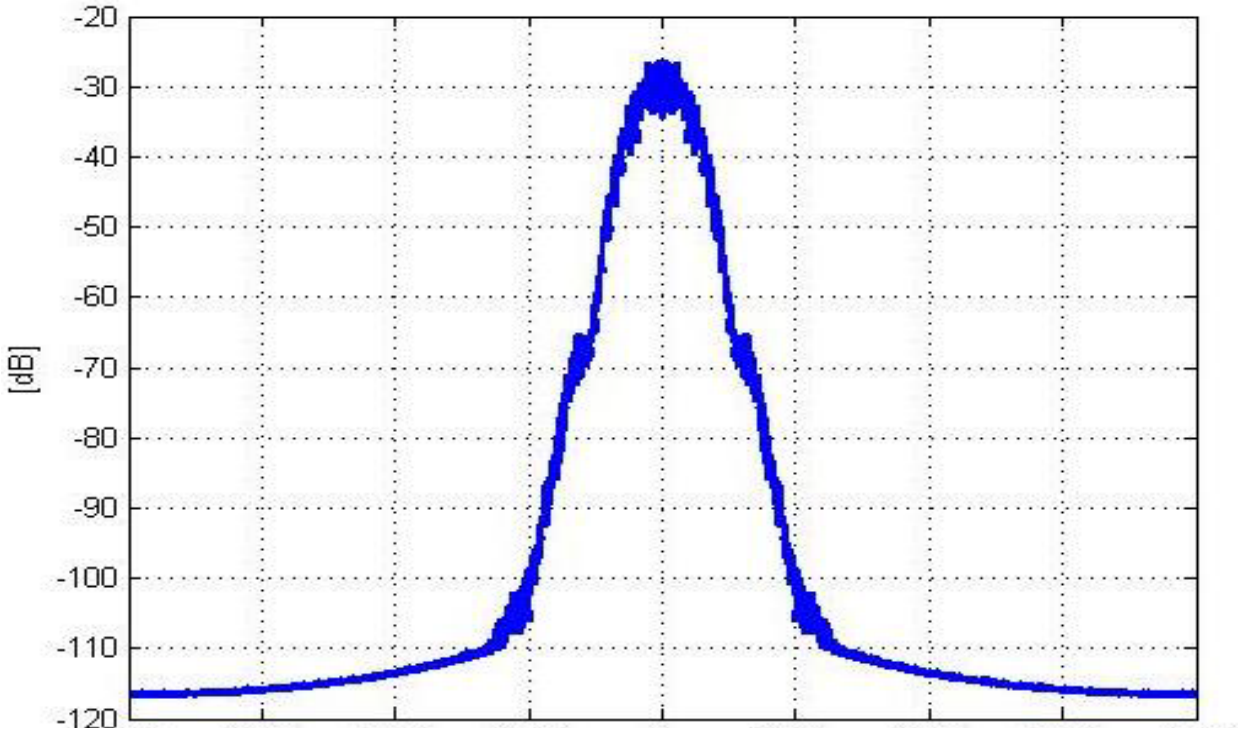

Figure 2-10: Spectrum of the AIS signal

Figure 2-11 shows the time characteristics of the VDES signal. This signal was broadcast in the second measurement campaign.

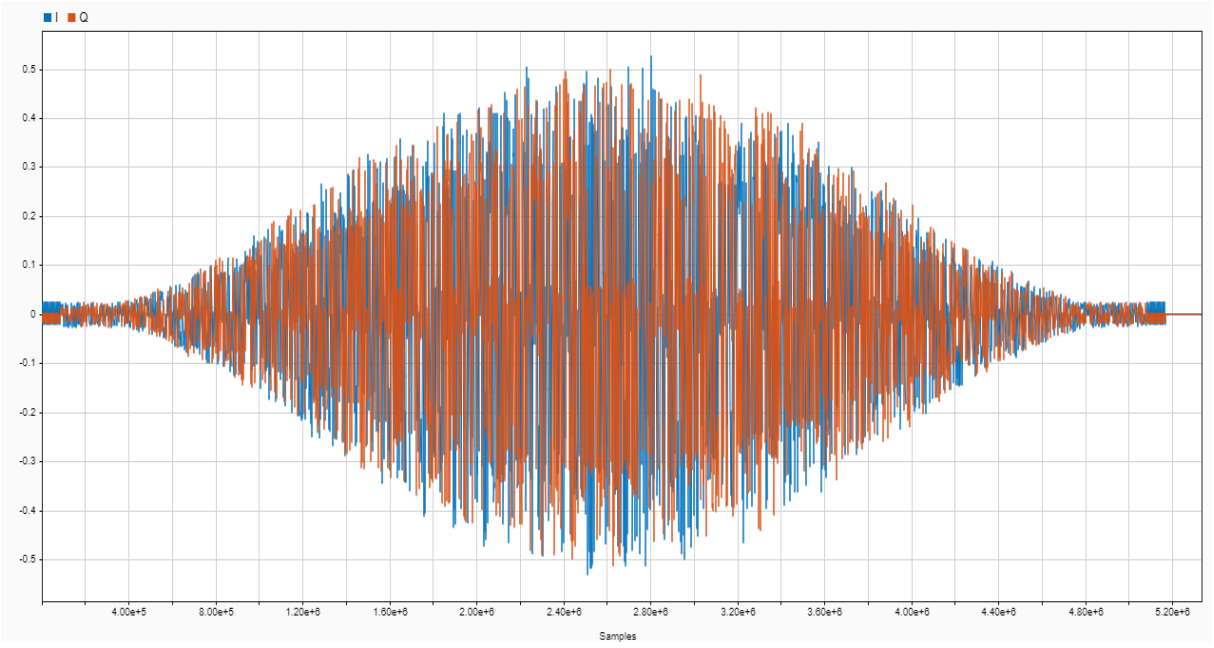

Figure 2-11: Time characteristics of the VDES signal

Figure 2-12 shows the spectral characteristics of the VDES signal.

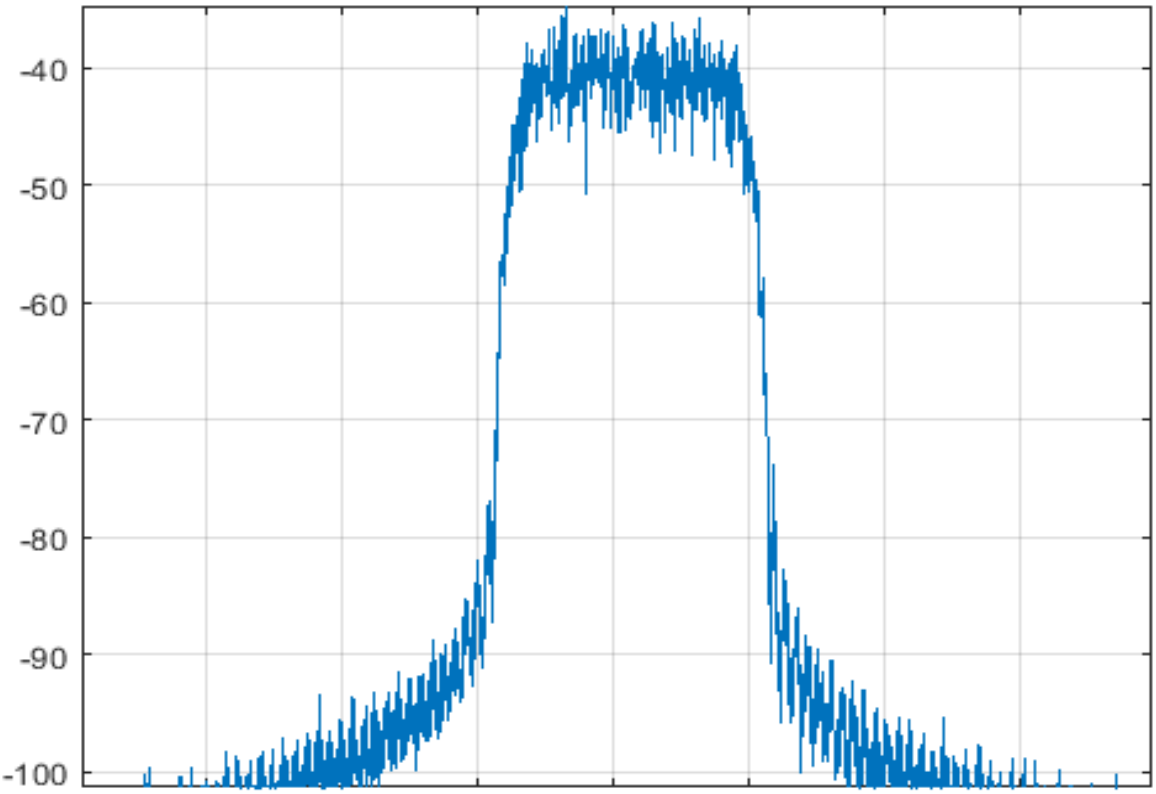

Figure 2-12: Spectrum of the VDES signal

2.6 Calibration measurements

Calibration and test measurements were carried out in three places:

- calibration measurements in the port of Gdynia (at a point about 30 meters from the transmitting antenna and at a point about 450 meters from the transmitting antenna),
- test measurements at NIT in Gdańsk about 17.45 km from the transmitting antenna,
- test measurements on Hel approximately 19.7 km away from the transmitting antenna.

2.6.1 Calibration measurements for the first measurement campaign

The first tests of the system operation correctness for the measurement campaign were carried out at NIT in Gdańsk. The purpose of these tests was to check the correct operation of the AIS system. Radio transmission and cable transmission were checked. The figures 2-13 and 2-14 below show the transmitting station at the front and back.

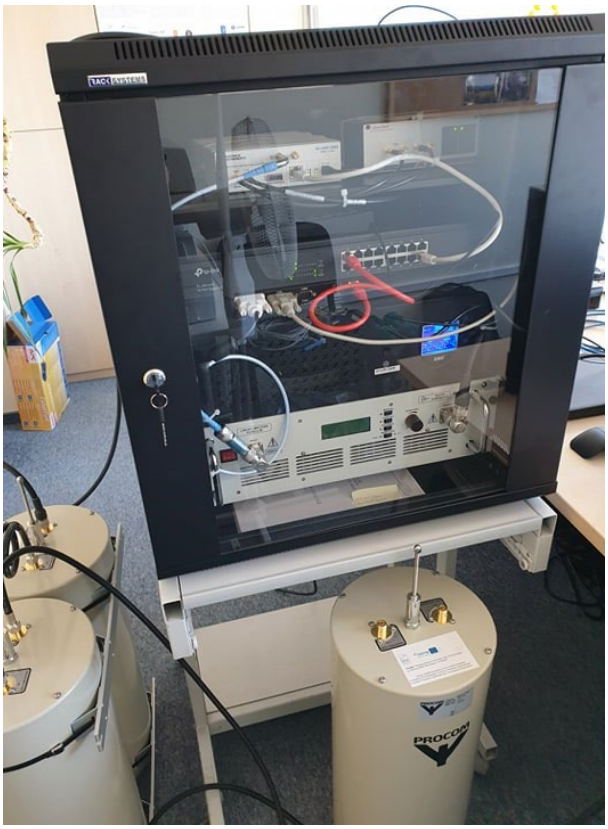

Figure 2-13: Front of the transmitting station

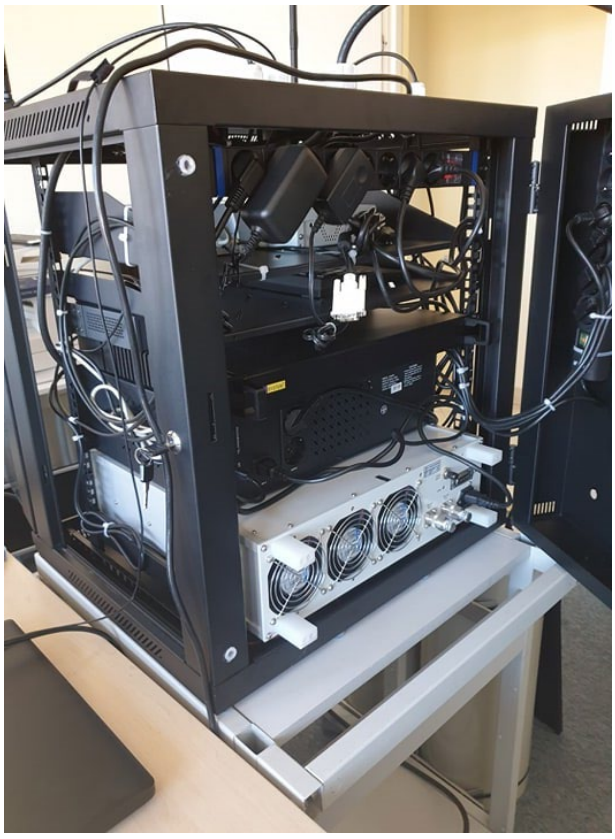

Figure 2-14: Back of the transmitting station

Tests carried out at NIT allowed for checking the correct implementation of the correlation module. It was also possible to check the correctness of the GMSK signal design. In the figure 2-15 and figure 2-16 below, the signal spectrum and channel power measurements for the AIS system are presented.

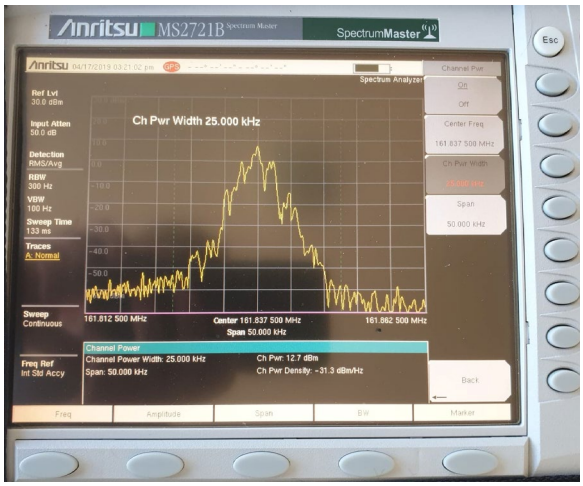

Figure 2-15: Channel power measurements

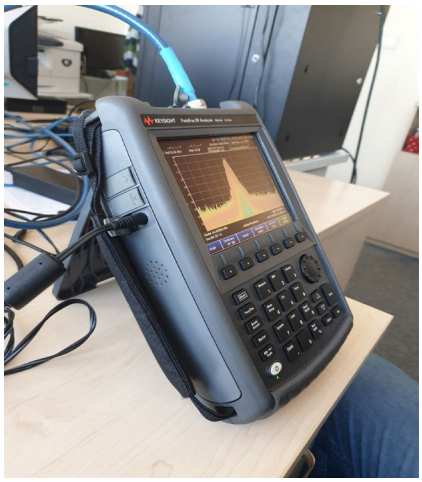

Figure 2-16: Spectrum of the AIS signal

The second stage was the installation of a broadcasting station in the port of Gdynia. Below is a picture 2-17 of the broadcast station installation already in place.

Figure 2-17: Installation of the transmitting station in Gdynia

In order to perform an accurate calibration, a number of calibration tests were performed, including:

- cable length measurement (fig. 2-18),

- antenna path matching measurement (fig. 2-19),
- cable loss measurement (fig. 2-20).

For a radio (transmitter in our case) to deliver power to an antenna, the impedance of the radio and transmission line must be well matched to the antenna's impedance. The parameter VSWR is a measure that numerically describes how well the antenna is impedance matched to the radio or transmission line it is connected to.

VSWR stands for Voltage Standing Wave Radio, and is also referred to as Standing Wave Ratio (SWR). VSWR is a function of the reflection coefficient, which describes the power reflected from the antenna.

When an antenna is not matched to the receiver, power is reflected (so that the reflection coefficient, is not zero). This causes a "reflected voltage wave", which creates standing waves along the transmission line.

The higher the VSWR parameter, the bigger the mismatch. In our case, this parameter is very small and it is correct.

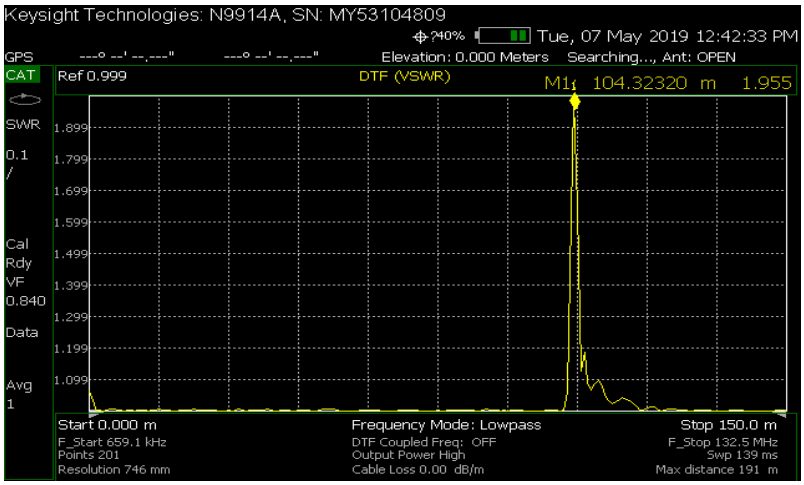

Figure 2-18: Cable length measurement

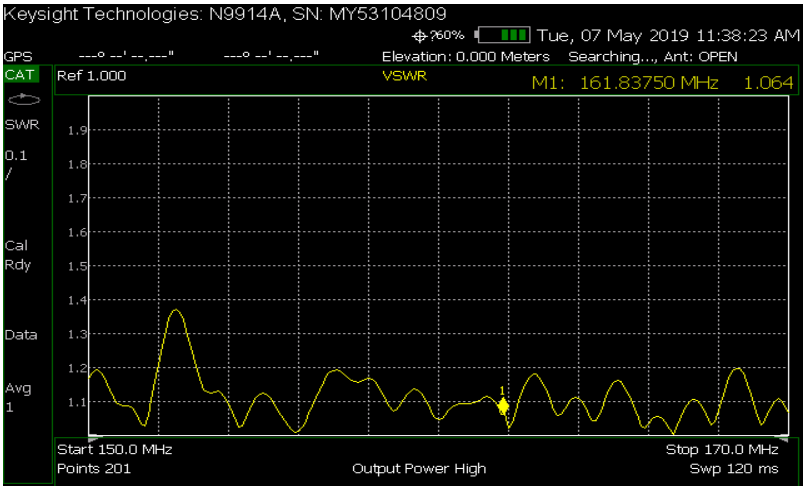

Figure 2-19: Antenna path matching measurement

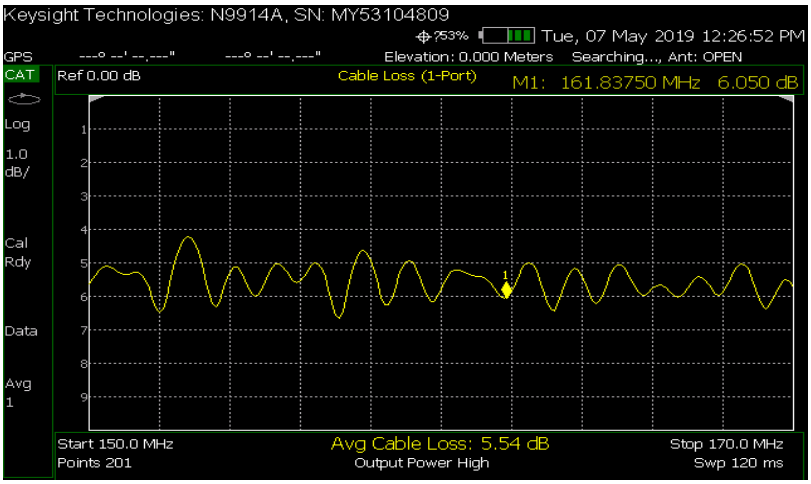

Figure 2-20: Cable loss measurement

Calibration measurements for the AIS system in the port of Gdynia were taken at two points. Thanks to this, it was possible to determine what number of samples could be considered as a correction value in the correlator to determine the exact position. The diagram 2-21 below shows the scenario of the performed calibration measurements.

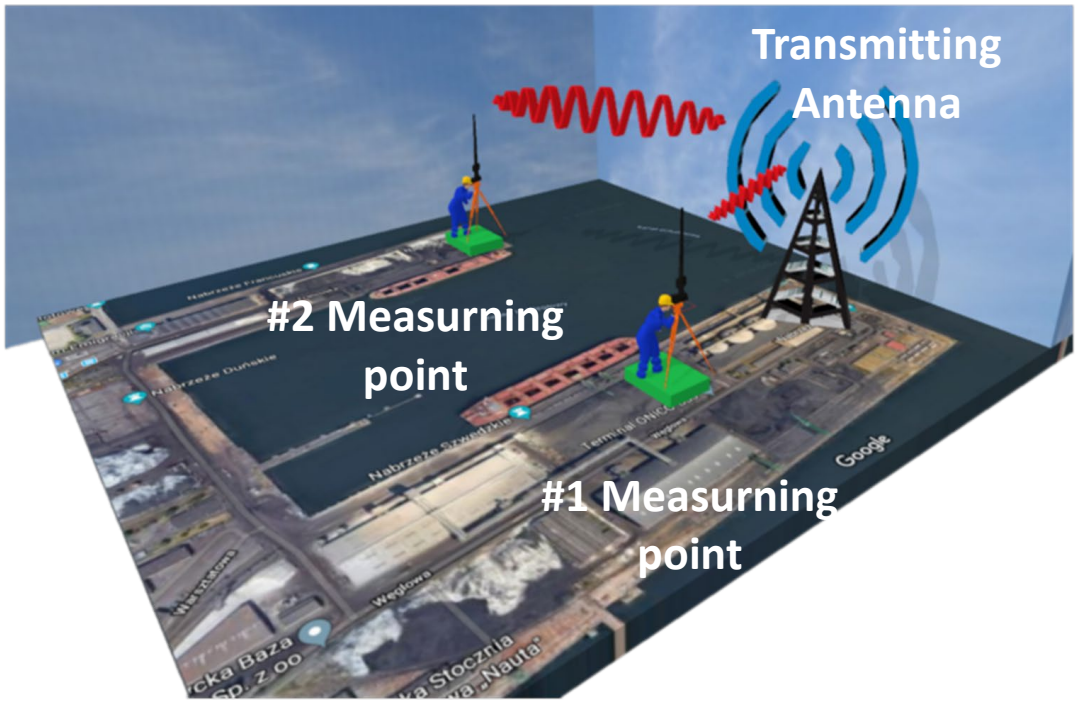

Figure 2-21: Calibration measurements

The table 2-7 below shows the values in the form of the number of samples obtained during calibration. For the AIS system, it was assumed from previous calculations that one sample corresponds to 6 m. From the obtained data it can be calculated that 0 m is adopted for the correction value of 5120 samples.

Table 2-7: Calibration measurements - the correct number of samples for the AIS system

Measurning point	Number of samples	Distance
1	5125	~ 32 m
2	5195	~ 454 m

Below are some photos from the calibration measurements taken in Gdynia before the first measurement campaign (figure 2-22, 2-23, 2-24, 2-25).

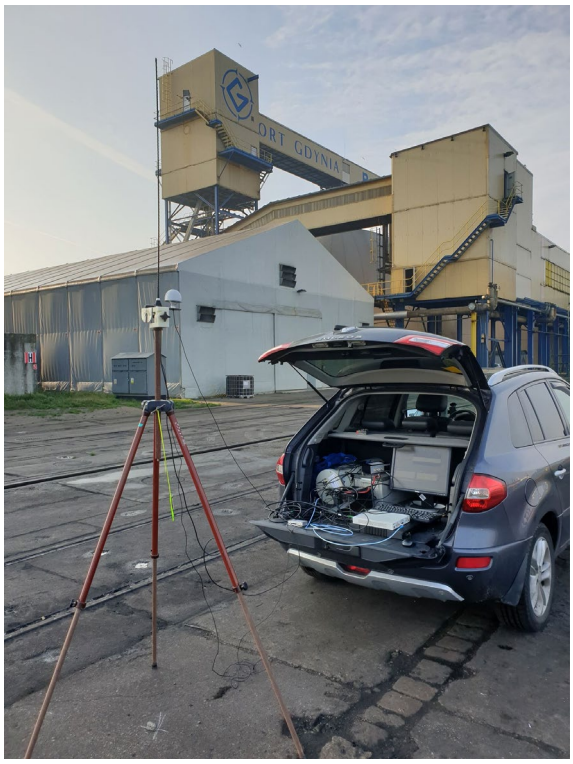

Figure 2-22: Calibration measurements in Gdynia (1/4)

Figure 2-23: Calibration measurements in Gdynia (2/4)

Figure 2-24: Calibration measurements in Gdynia (3/4)

Figure 2-25: Calibration measurements in Gdynia (4/4)

The third measurements as test measurements were carried out on Hel (figure 2-27). One of the results was checking the correct operation of the correlator as shown in the figure 2-26.

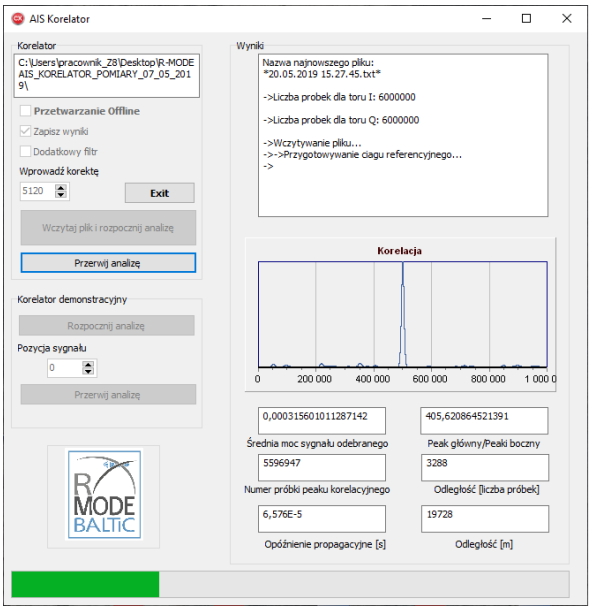

Figure 2-26: Calibration measurements on Hel - correlation

After processing the test files from Hel, the correlator calculated a distance of 19.72 km. This result coincided with the actual distance between the transmitting station located in Gdynia and the measuring point located on Hel.

Figure 2-27: Calibration measurements on Hel

2.6.2 Calibration measurements for the second measurement campaign

The second calibration measurements were carried out this time for the VDES system. Calibration measurements had to be carried out again mainly due to the purchase and replacement of the new USRP platform. In order to check the correctness of signal design for the physical VDES layer, a number of tests were carried out at NIT in Gdańsk. The first test measurements were carried out for low output power on USRP. test results are shown in the figures 2-28 and 2-29.

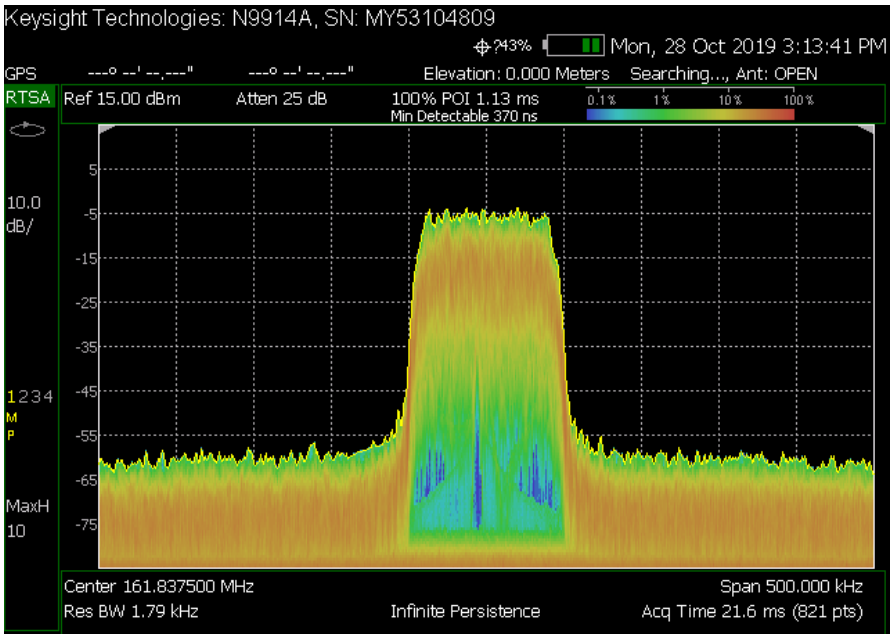

Figure 2-28: USRP output signal – Low power output (1/2)

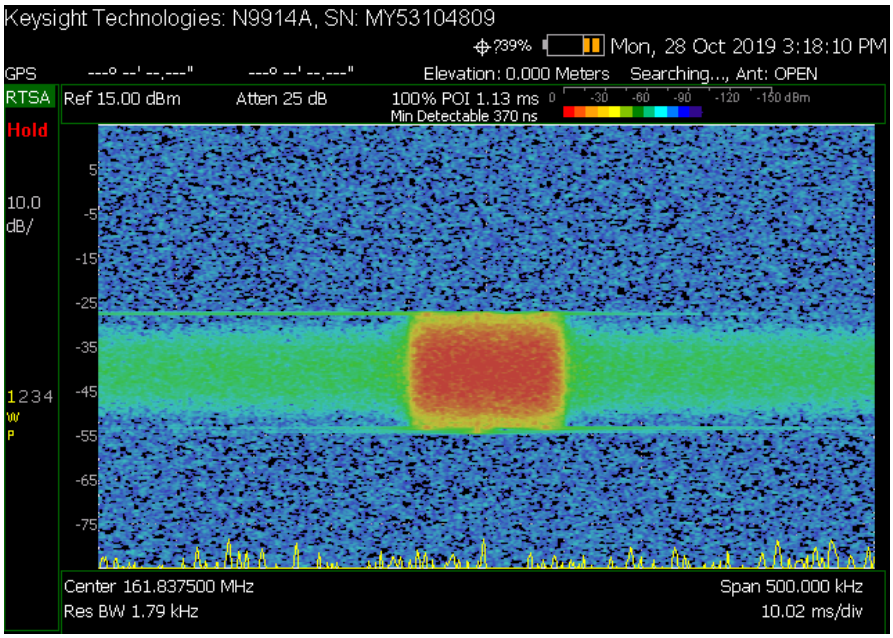

Figure 2-29: USRP output signal – Low power output (2/2)

After checking the correctness of VDES signal transmission and reception, the new USRP platform was taken to the transmitting station in the port of Gdynia. The new USRP platform was replaced on site. There, the high power output tests of station were carried out. The results are presented below in the figure 2-30 and 2-31.

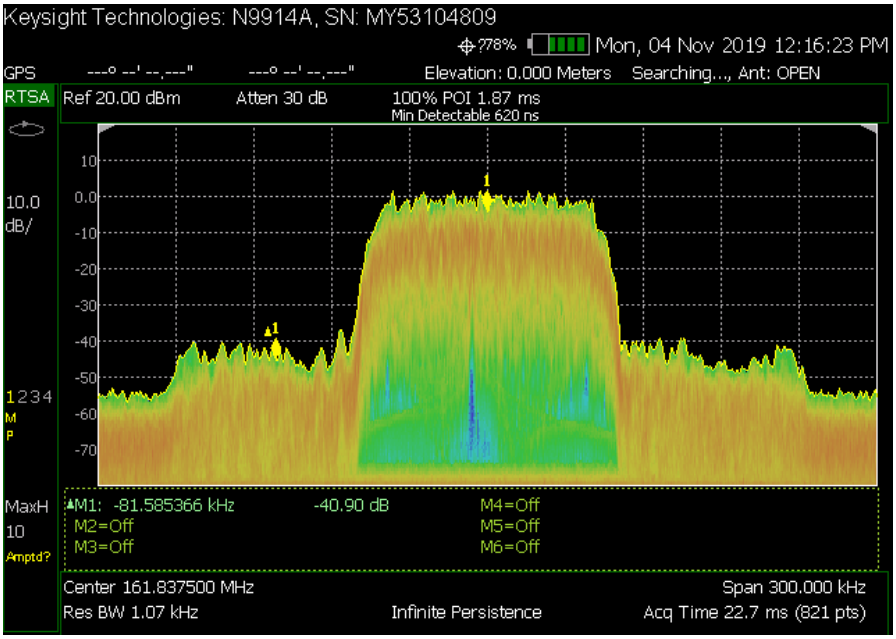

Figure 2-30: Station output signal – High power output

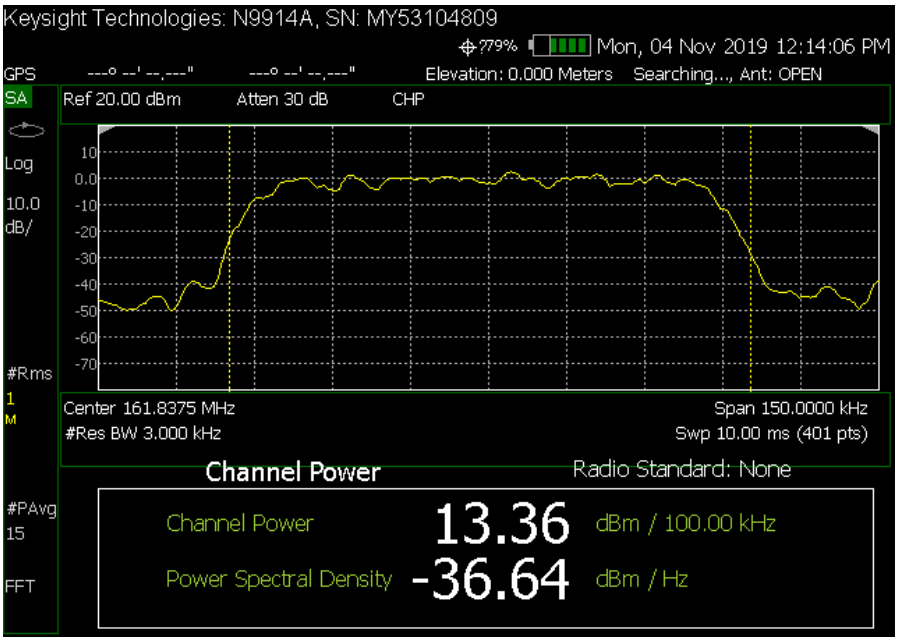

Figure 2-31: Channel Power station

Then radio reception tests were carried out. As a result, below is a radio signal spectrogram from the station in Gdynia (fig. 2-32) and from NIT in Gdańsk (fig. 2-33). In particular, you can see other AIS signals from ships.

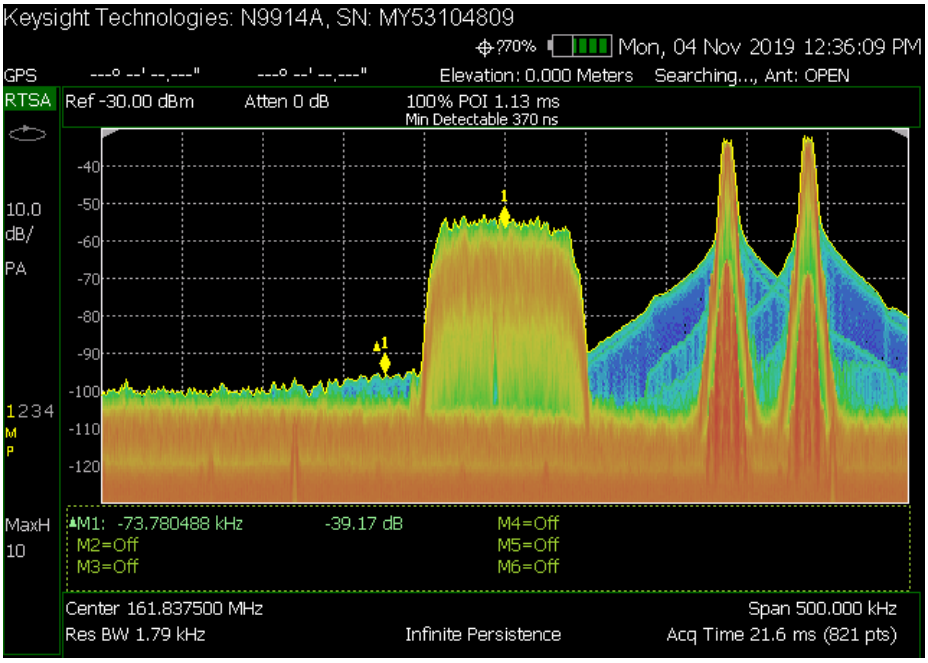

Figure 2-32: Radio signal spectrogram along with AIS signals (station in Gdynia)

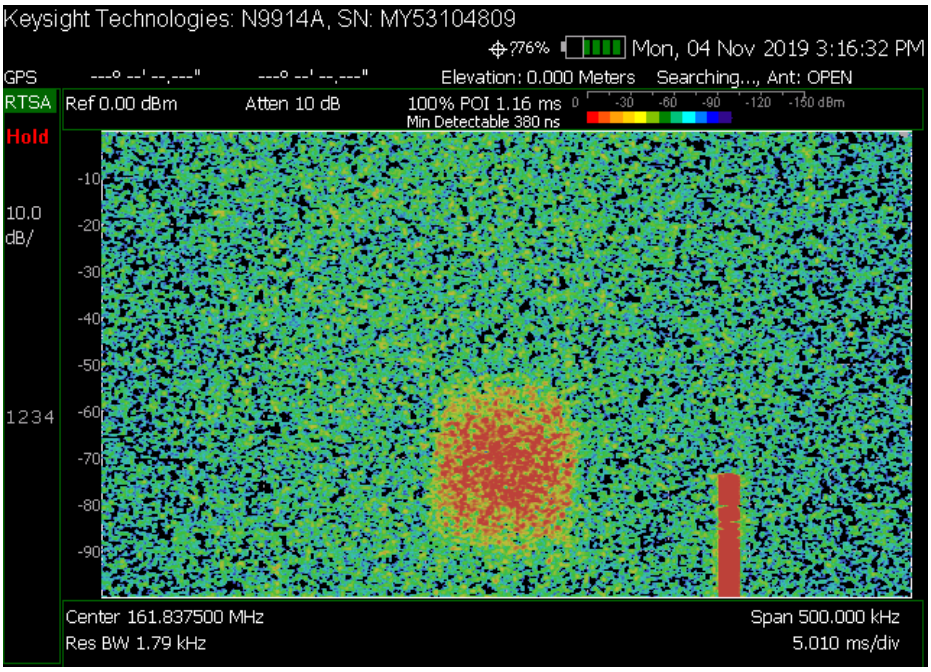

Figure 2-33: Radio signal spectrogram along with AIS signals (NIT in Gdańsk)

For testing purposes, the signal was received at NIT in Gdańsk (fig. 2-34). Below is the correlation result (fig. 2-35) and the VDES signal over time (fig. 2-36).

Figure 2-34: Signal reception test in Gdańsk

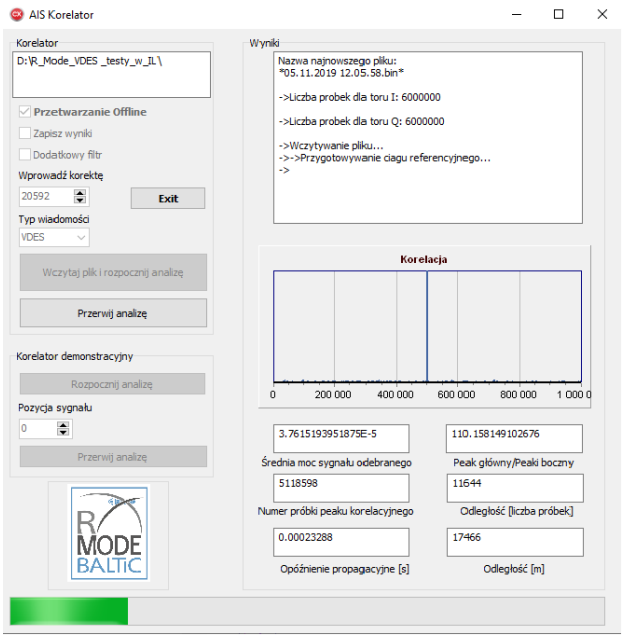

Figure 2-35: Signal correlation

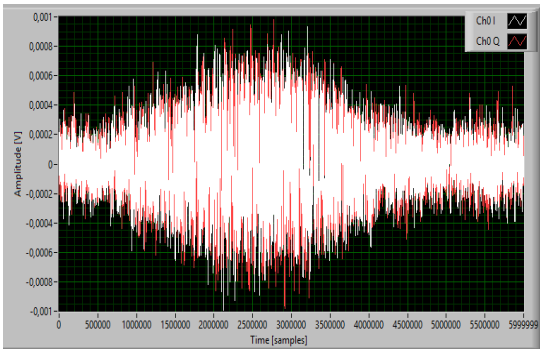

Figure 2-36: VDES signal received - time characteristics

After testing the signal and the transmitting station, calibration measurements were taken in the port of Gdynia. Calibration tests took place before the second measurement campaign. Calibration measurements for the VDES system in the port of Gdynia were taken at two points. Thanks to this, it was possible to determine what number of samples could be considered as a correction value in the correlator to determine the exact position. The diagram 2-37 below shows the scenario of the performed calibration measurements.

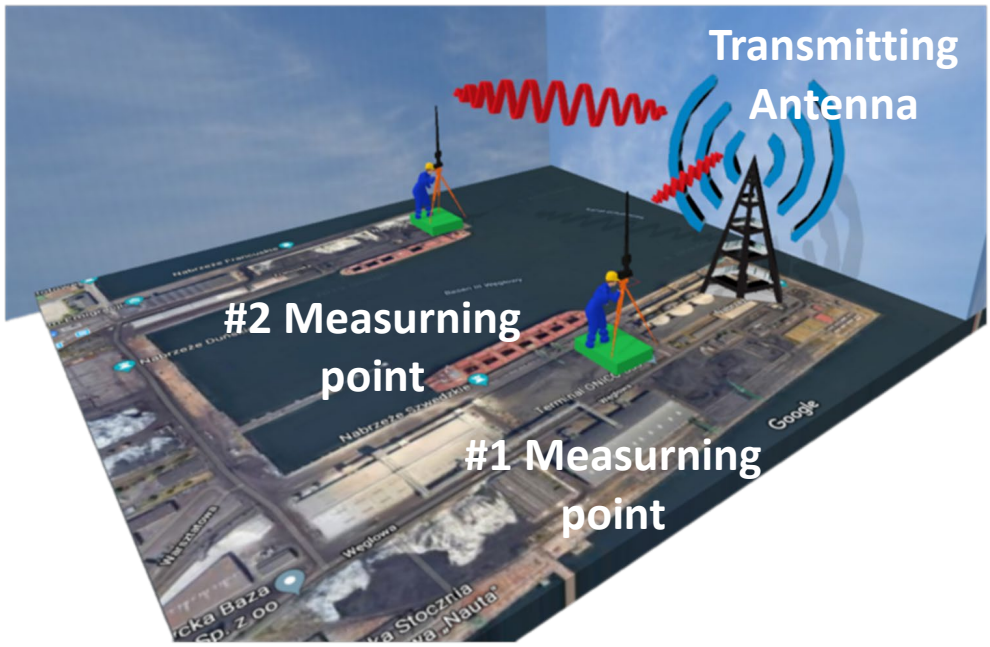

Figure 2-37: Calibration measurements - second measurement campaign

The table 2-8 below shows the values in the form of the number of samples obtained during calibration. For the VDES system, it was assumed from previous calculations that one

sample corresponds to 1.5 m. From the obtained data it can be calculated that 0 m is adopted for the correction value of 21957 samples.

Table 2-8: Calibration measurements - the correct number of samples for the VDES system

Measurning point	Number of samples	Distance
1	21978	~ 32 m
2	22258	~ 454 m

Below are some photos from the calibration measurements taken in Gdynia before the second measurement campaign (figure 2-38, 2-39, 2-40, 2-41).

Figure 2-38: Second calibration measurements in Gdynia (1/4)

Figure 2-39: Second calibration measurements in Gdynia (2/4)

Figure 2-40: Second calibration measurements in Gdynia (3/4)

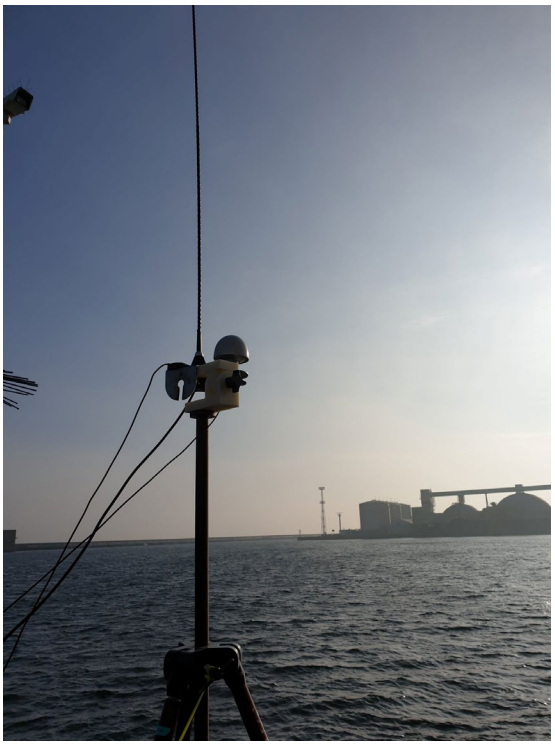

Figure 2-41: Second calibration measurements in Gdynia (4/4)

3 R-Mode system implementation

3.1 Hardware implementation

Due to the fact that the scheme of the measuring stand for the second campaign has been modified, in relation to the first measurement campaign, this chapter presents the diagrams of both configurations, detailing the differences.

3.1.1 Test-bed for the AIS transmission

The diagrams of the transmitting and receiving parts of the test-bed for AIS transmission are illustrated in Figures 3-1 and 3-2, respectively.

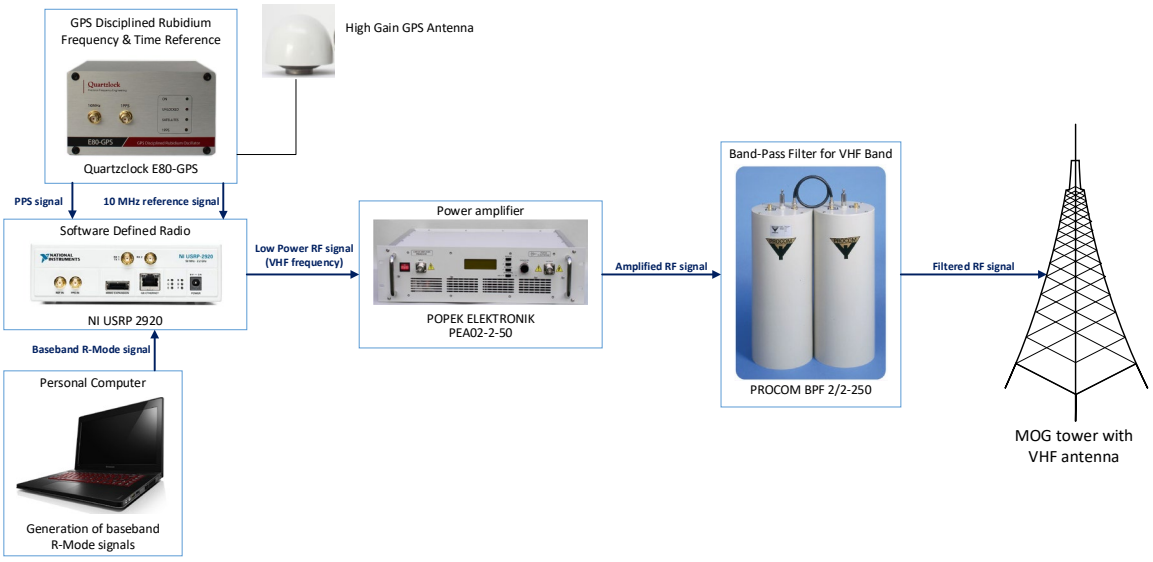

Figure 3-1: Test-bed Transmitter diagram for the AIS transmission

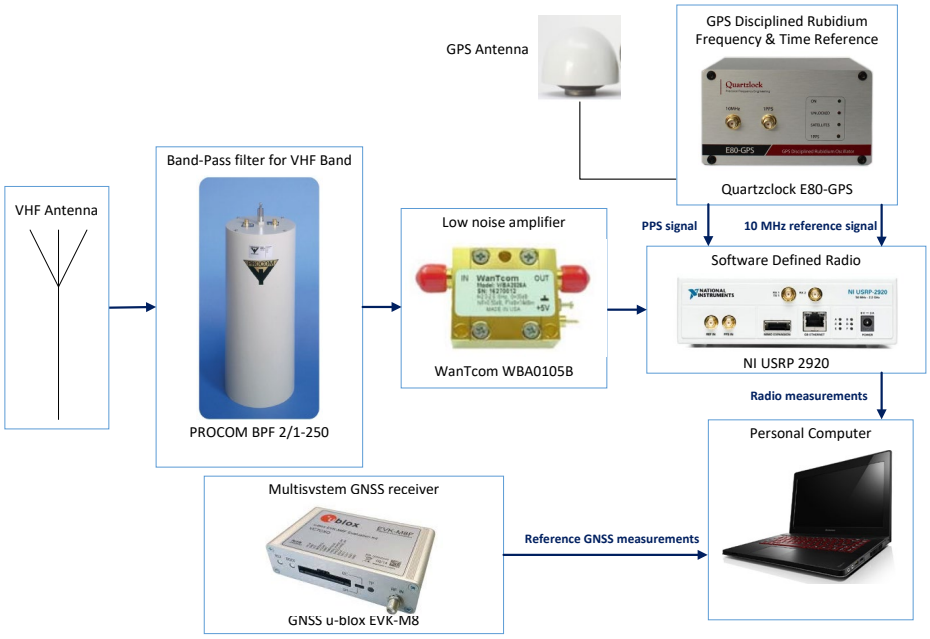

Figure 3-2: Test-bed Receiver diagram for the AIS transmission

The main elements of the developed measurement system are NI USRP 2920 software defined radios, responsible for transmitting and receiving generated test signals, as well as external rubidium Quartzlock E80 GPS oscillators that provide a stable source of frequency and time (both devices are characterized in detail in [XXX]). This is particularly important for ongoing studies involving the measurement of radio signal propagation time. External oscillators are also used to synchronize the transmitter and receiver part of the system, which will allow to examine the influence of the propagation environment on the distance measurements. In addition to these elements, the measuring sites consist of appropriate bandpass filters, a power amplifier and antennas.

In addition to providing an accurate source of time and frequency for the USRP devices, the rubidium oscillator is also used to synchronization between the transmitting and receiving part of the measurement system.

3.1.2 Test-bed for the VDES transmission

To improve performance and accuracy of distance determination, new USRP modules and a new software (described in the next subchapter) were used. The diagrams of the transmitting and receiving parts of the test-bed for VDES transmission are illustrated in Figures 3-3 and 3-4, respectively.

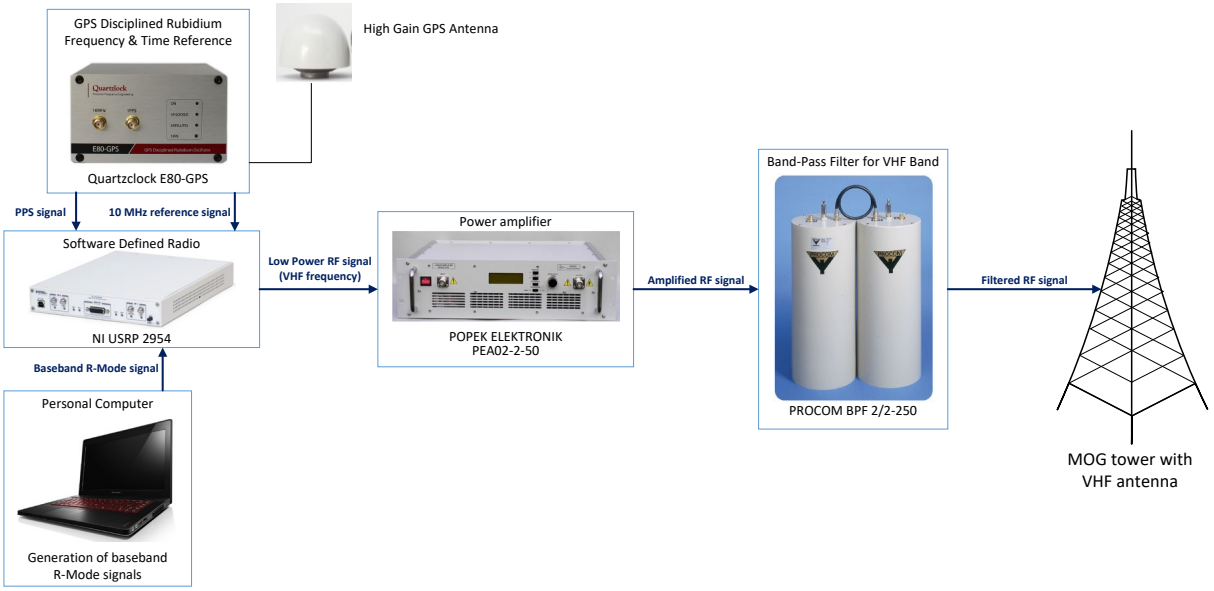

Figure 3-3: Test-bed Transmitter diagram for the VDES transmission

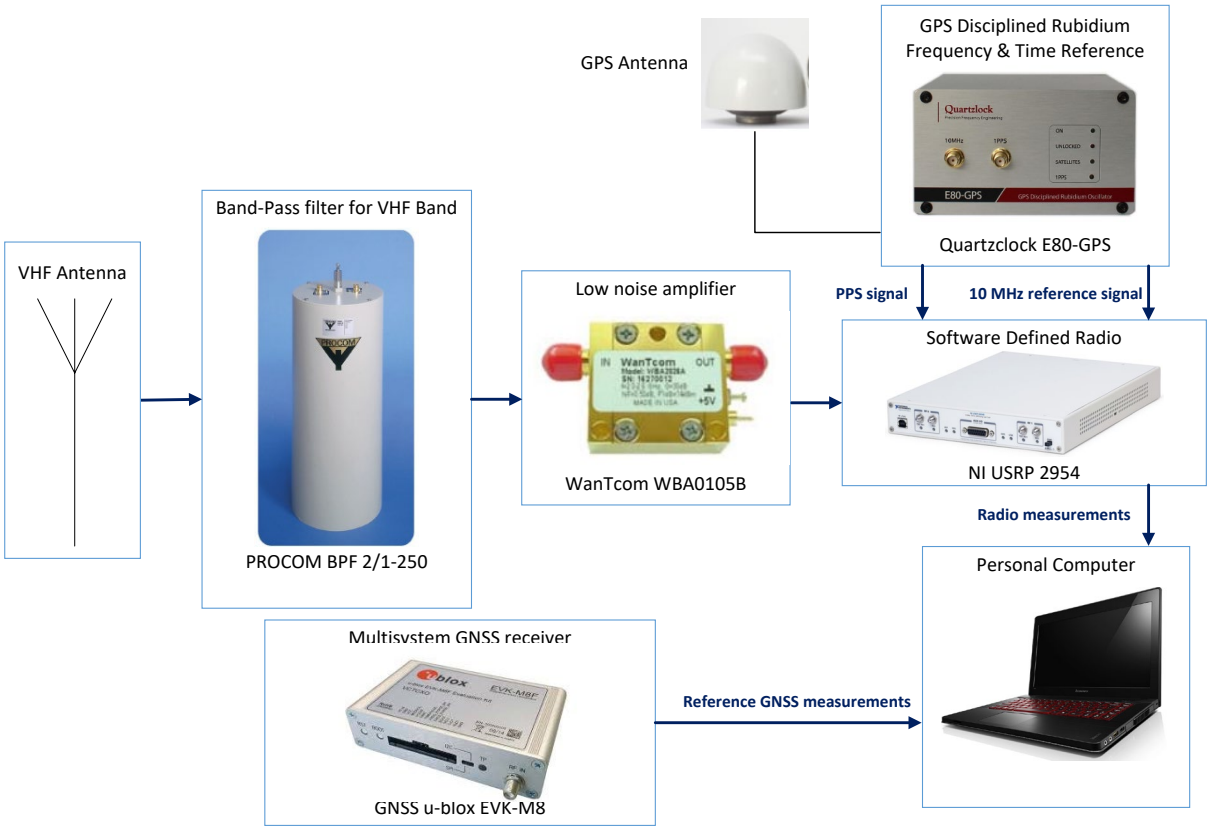

Figure 3-4: Test-bed Receiver diagram for the VDES transmission

The most important parameters of the new USRP 2954 model are specified below.

USRP 2954 transmitter parameters [4-2]:

- Frequency range: 10 MHz to 6 GHz,
- Frequency step: <1 kHz,
- Maximum output power: 50 mW to 100 mW (17 dBm to 20 dBm),
- Gain range: 0 dB to 31.5 dB,
- Gain step: 0.5 dB,
- Frequency accuracy:
    - 25 ppb (not locked to GPS),
    - 5 ppb (locked to GPS),
- Maximum instantaneous real-time bandwidth: 160 MHz,
- Maximum I/Q sample rate: 200 MS/s,
- Digital-to-analog converter (DAC):
    - 2 channels,
    - Resolution: 16 bit,
    - Spurious-free dynamic range (sFDR): 80 dB.

USRP 2954 receiver parameters [4-2]:

- Frequency range: 10 MHz to 6 GHz,
- Frequency step: <1 kHz,
- Gain range: 0 dB to 37.5 dB,
- Gain step: 0.5 dB,
- Maximum input power: -15 dBm,
- Noise figure: 5 dB to 7 dB,
- Frequency accuracy:
    - 25 ppb (not locked to GPS),
    - 5 ppb (locked to GPS),
- Maximum instantaneous real-time bandwidth: 160 MHz,
- Maximum I/Q sample rate: 200 MS/s,
- Analog-to-digital converter (ADC):
    - 2 channels,
    - Resolution: 14 bit,
    - Spurious-free dynamic range (sFDR): 88 dB.

The most important advantages of the USRP 2954 module compared to the old one in the context of ranging measurements are:

- maximum I/Q sample rate 200 MS/s (1 sample will correspond to 1.5 m),
- better A/D converter resolution,
  frequency accuracy: 25 ppb (not locked to GPS) - but it was also used an external source of frequency and time using PPS and frequency reference inputs.

3.2 Software implementation

This chapter will present changes compared to previous implementation work on the AIS system. The modulation applied to the VDES physical layer will be described. The software created for the correlation of signals based on which it was possible to determine the position was also described. In addition, there will also be a description of the filters designed for the needs of the project.

3.2.1 USRP application

In the R-Mode system the distance between base station and mobile station on the ship is determined using the TOA method which is based on the measurement of radio signal propagation time. Therefore, the key issue is to ensure transmission and reception start of R-Mode messages in precisely defined moments of time. For this purpose, the triggers are utilized in the USRP modules. They are used for generation and acquisition synchronization to the timestamp specified by the 'Start Trigger Time' properties. The 'Start Trigger' occurs when the onboard device timer reaches the timestamp specified by the user. Therefore, the operation of setting the trigger and data transmission/reception must be performed periodically - in a loop.

Applications have the following features:

- full configurability of radio parameters,
- reading/writing signals from/to the file in the form of IQ samples,
- possibility of graphical signal presentation,
- automation of measurements,
- monitoring of application work and logging of configuration and possible errors.

In report [xxx] the flowcharts of the transmitting and receiving applications are illustrated. The schemes of the measurement applications for the VDES transmission has not changed, only some modifications were necessary:

- A new 64-bit version of LabView plus new USRP Driver,
- AIS signal covered 5 time slots, while VDES - one slot,
- The single VDES transmission measurement file has 22.8 MB (due to the higher IQ rate and better resolution), while AIS transmission measurement file had 11.4 MB,
- Different frequency of receiving messages. Due to the higher performance of USRP 2954, the recording of samples for VDES transmission was performed every second (for the AIS transmission - every 4 seconds). The measuring signal was transmitted, in both cases, every 3 seconds. So, for VDES the useful signal was recorded in 1 of 3 samples and for AIS – in 1 of 12 samples.

During the first measurement campaign, the signal transmission was carried out each time at the beginning of the UTC second (in the slot number 0). However, some measurements had to be rejected due to other transmissions (interferences) appearing in the slots used for transmission. In order to minimize interferences, an analysis of the AIS slots occupancy was made, based on data collected by the Maritime Office in Gdynia from the area of the Bay of Gdańsk, shown in the picture 3-5.

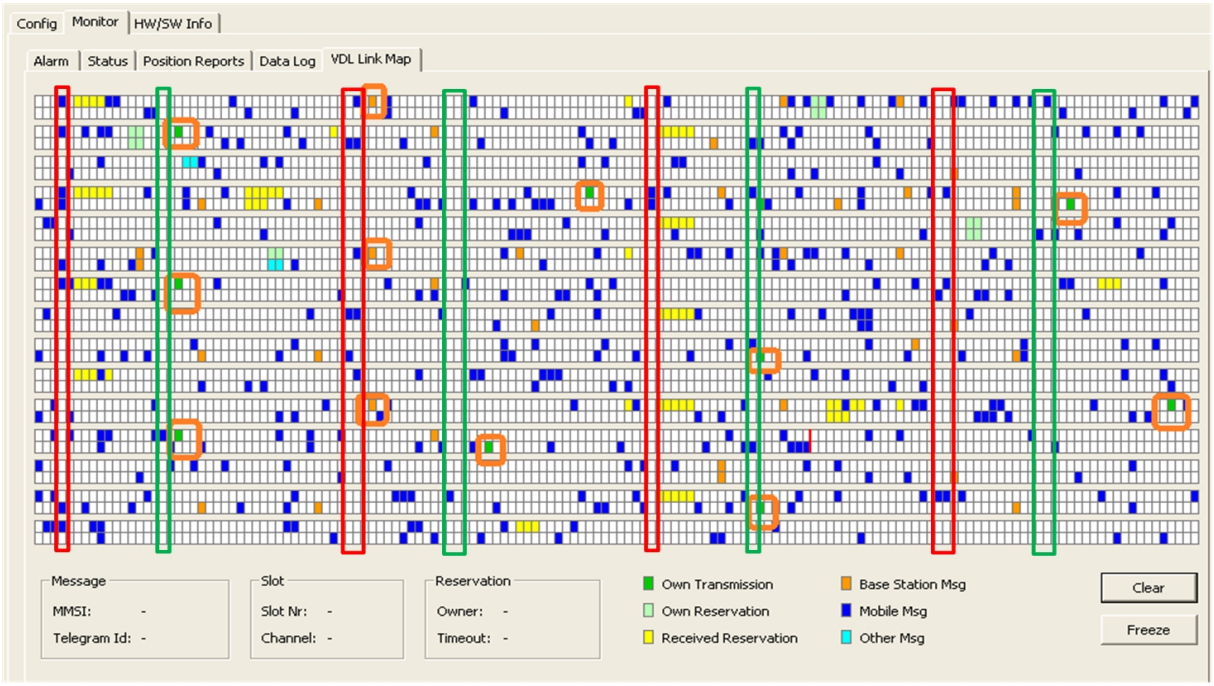

Figure 3-5: The occupancy of AIS slots registered in the Bay of Gdańsk area

During analysis there were searched the time slots not used by base stations and not reserved for other transmissions (we have no influence on ships transmissions). Slot number 3 (80 ms after UTC second start) was selected, because adjacent slots were also not used.

3.2.2 VDES physical layer in the R-Mode project

The main changes that were made to the software were a change in modulation for the needs of the VDES system. The entire software implementation for the AIS system was described in the first report. The following are all changes to the software for the implementation of the VDES system:

- Modulation π/4 QPSK,
- RRC filter 100 kHz,
- Data rate 76,8 ksym/s,
- Using a Gold sequence of length 1877 symbols.

The input bit stream is partitioned by a serial-to-parallel converter into two parallel data streams $m_{I,k}$ and $m_{Q,k}$, each with a symbol rate equal to half that of incoming bit rate. The *k th* in-phase and quadrature pulses, I_k and Q_k, are produced at the output of the signal mapping circuit over time $kT \leq t \leq (k+1)T$. Both I_k, Q_k are passed through root raised cosine (*RRC*) rolloff pulse shaping filters, in order to reduce the bandwith occupancy. Then they are multiplied by the carrier and summed (fig. 3-6).

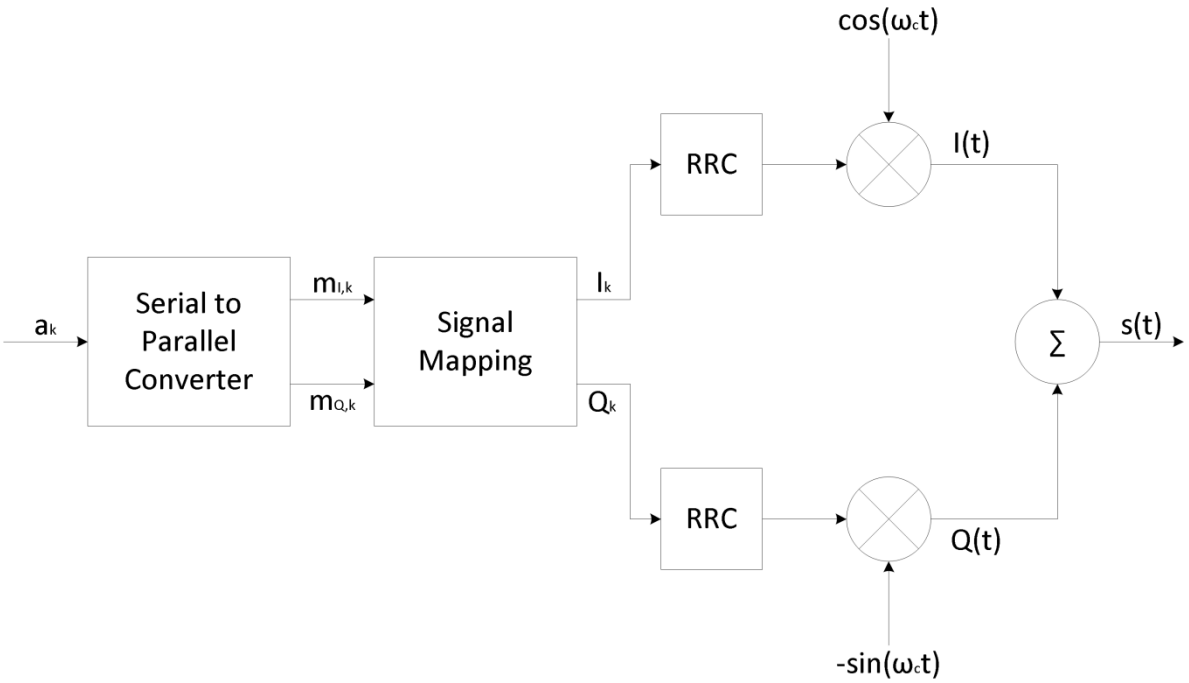

Figure 3-6: Modulator π/4 QPSK

Below is a constellation for modulation π/4 QPSK (fig. 3-7):

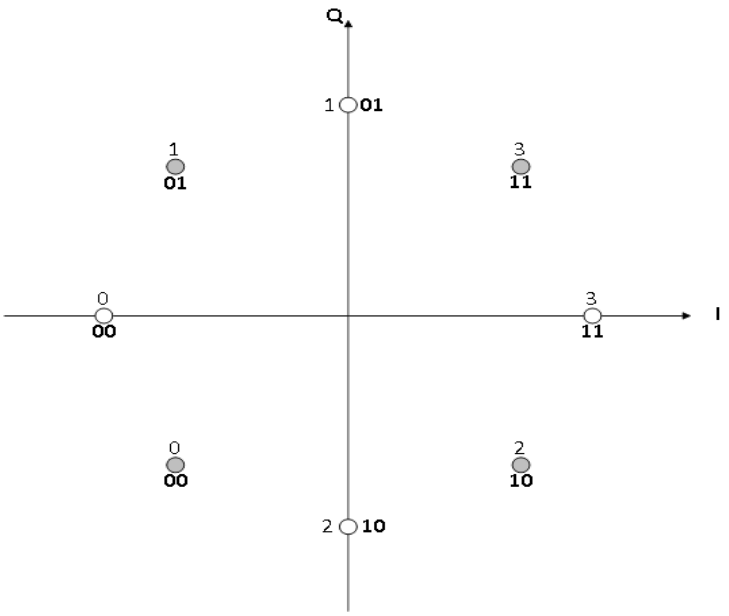

Figure 3-7: Signal constellation for modulation π/4 QPSK

3.3 Signal correlation application

The application for correlating the received signal is presented below. The application contains all modules that were described in the first report. One of the most important modules that the correlation application contains are:

- loading files from the selected path,

- processing files offline from any path,
- online file processing (implementation of the module that selects the latest file from the selected path). When the USRP platform saves the latest measurement file in a given location, the correlation application downloads and processes it,
- saving the most important data, e.g. SNR, calculated position, maximum peak position, correlation peak to side peak ratio, processing time,
- the option of enabling a low-pass filter as part of improving positioning,
- introducing the sample correction that was determined on the calibration measurements,
- the ability to interrupt file analysis at any time without the risk of losing previously processed data,
- saving files with a correlation graph for later analysis.

The application's instruction manual is presented below (fig. 3-8).

The 'AIS Korelator' application can operate in two modes:

- Offline,
- Online.

Below are the steps that will allow you to properly operate the program, which will allow you to get the results of processed data and save the results to files.

1. OFFLINE operation mode

This mode allows you to process any number of files that are contained in a specific folder. The application in turn will analyze each data file located in a given location.

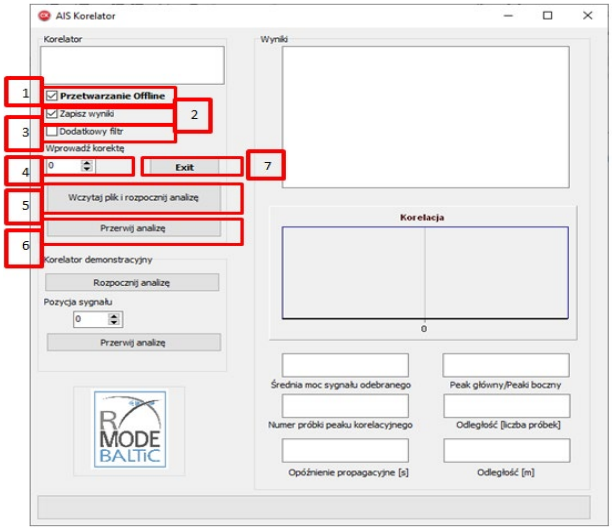

Figure 3-8: Signal correlation application – offline mode

1. If files are to be processed in offline mode - the option 'offline processing' should be selected before loading the files and starting the analysis

2. If the obtained results and a fragment of the correlation graph are to be saved in a file - the 'Save results' option should be checked before loading the files and starting the analysis.

3. If you want to activate an additional low-pass filter - you should select the 'Additional filter' option before loading the files and starting the analysis.

4. Enter the correction here as the number of samples that was determined during system calibration.
5. Choose the folder in which to analyze the files

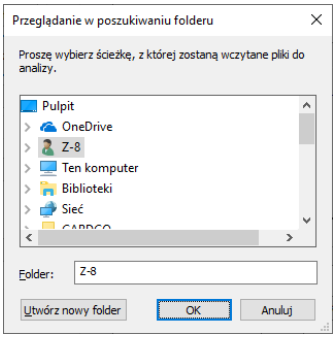

6. If you want to stop the data analysis, press the 'Stop analysis' button. This will result in a trouble-free program termination. If the button is turned on when analyzing a downloaded file, then the program will complete the analysis of the file, after which it will end its operation and will not download the next file.

7. Press this button if you need to immediately turn off the program. The program will be canceled immediately.

2. ONLINE mode of operation

This mode allows you to process the file whose creation date was the earliest (fig. 3-9). Until the program is interrupted, the application downloads each time from a given location.

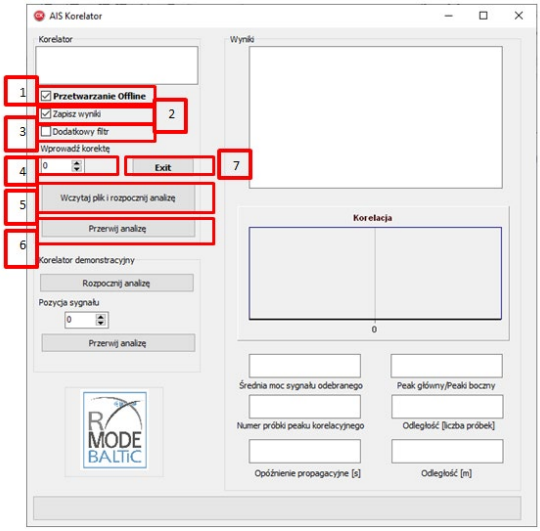

Figure 3-9: Signal correlation application – online mode

1. If files are to be processed in online mode - the option 'offline processing' should be deselected before loading the files and starting the analysis.

2. If the obtained results and a fragment of the correlation graph are to be saved in a file - the 'Save results' option should be checked before loading the files and starting the analysis.

3. If you want to activate an additional low-pass filter - you should select the 'Additional filter' option before loading the files and starting the analysis.

4. Enter the correction here as the number of samples that was determined during system calibration.

5. Choose the folder in which to analyze the files

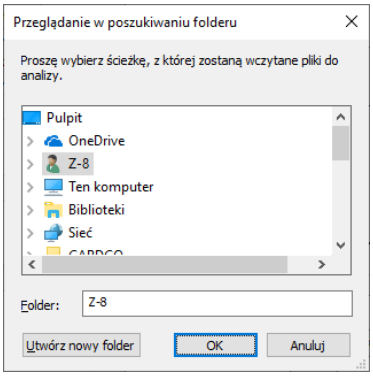

6. If you want to stop the data analysis, press the 'Stop analysis' button. This will result in a trouble-free program termination. If the button is turned on when analyzing a downloaded file, then the program will complete the analysis of the file, after which it will end its operation and will not download the next file.

7. Press this button if you need to immediately turn off the program. The program will be canceled immediately.

The photo below shows in visual form the operation of the signal correlation application (fig. 3-10).

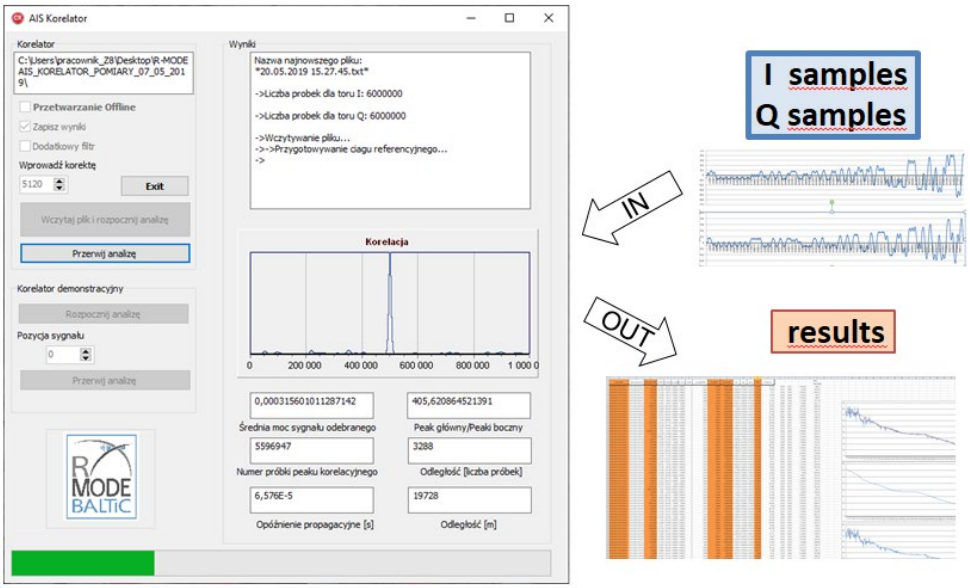

Figure 3-10: Signal correlation application – visualisation

Below (fig. 3-11) are the correlation charts that were obtained in the signal correlation application. This is the case for the AIS signal.

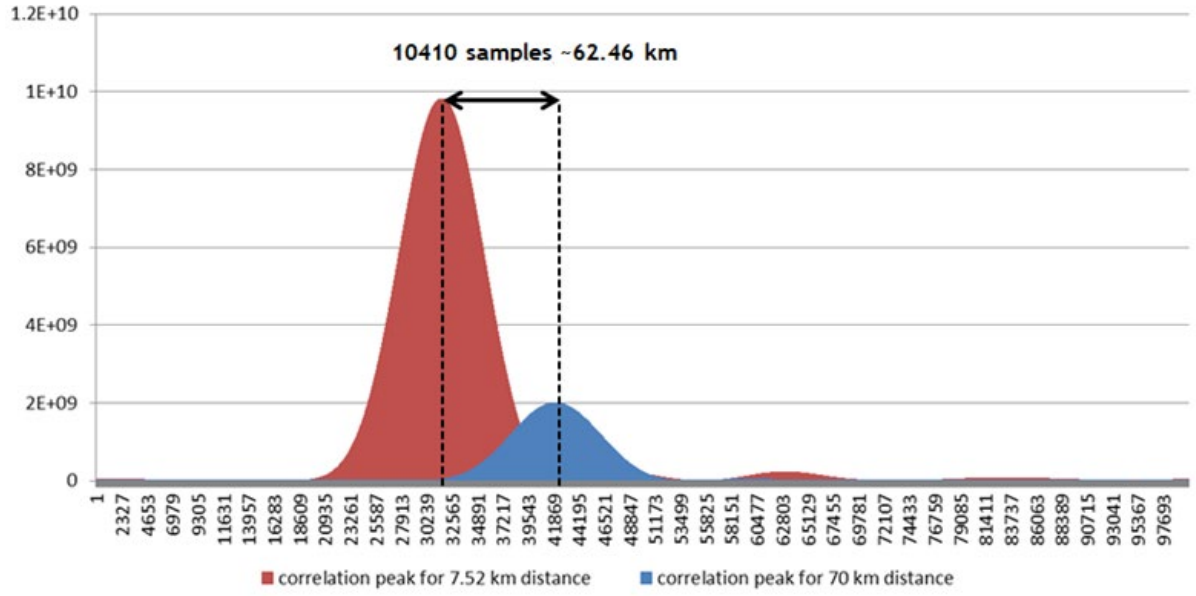

Figure 3-11: Correlation peak found (100 000 samples) – an example for AIS

Figure 3-12 shows the correlation peak for the VDES signal. Figure 3-13 shows the same peak but in zoom.

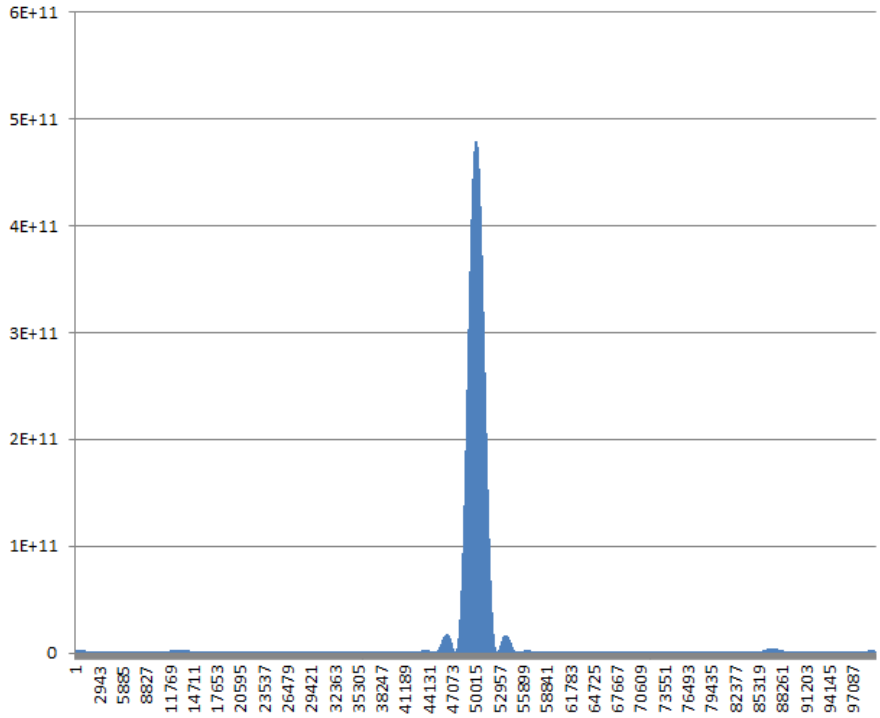

Figure 3-12: Correlation peak found (100 000 samples) – an example for VDES

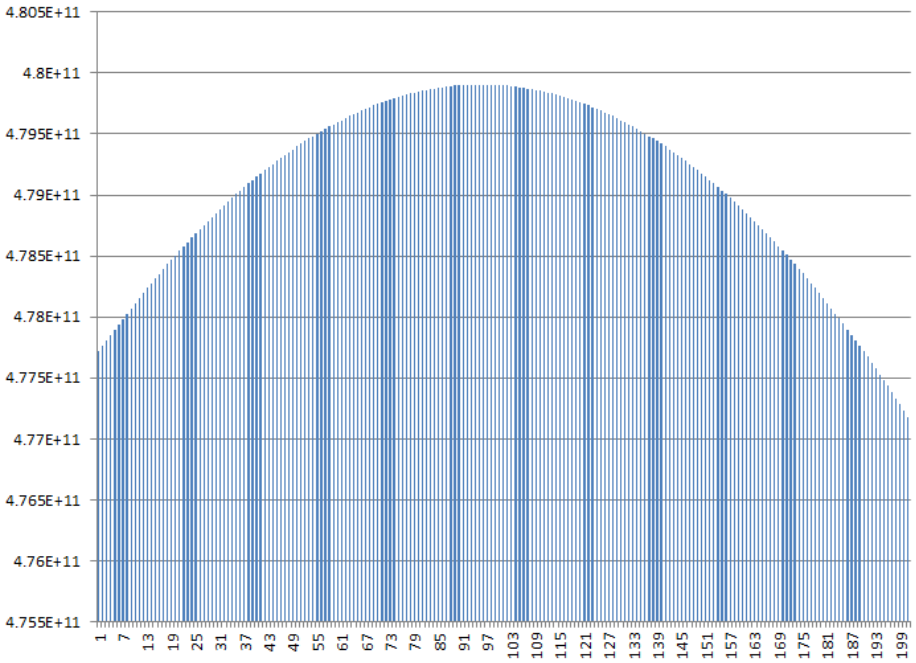

Figure 3-13: Correlation peak in zoom

3.4 Designed filters

For the needs of the project in order to determine position more accurately, low-pass filters were designed for AIS system and VDES system. The filters were designed using the Filter Designer tool, which is available in the MATLAB environment.

Below are the peak correlations for a small ratio of signal power to the noise power (fig. 3-14). Without the filter, the peak is 'jagged', making it difficult to determine the distance with high accuracy in the next steps.

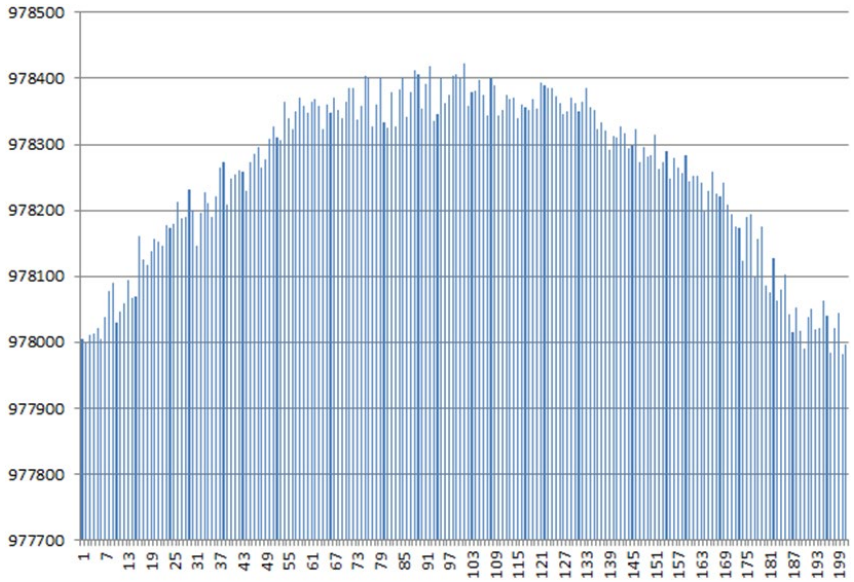

Figure 3-14: Correlation peak before applying the filter

The following filter has been designed for the designed signal for AIS (fig. 3-15).

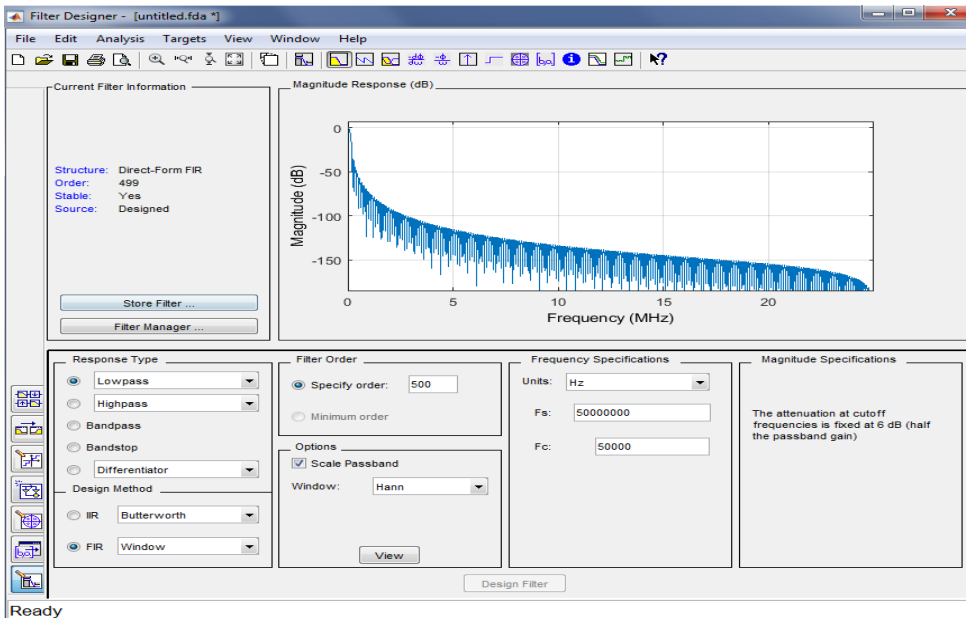

Figure 3-15: Designed filter for AIS signal

Below is the version for 500 (fig. 3-16) and 1000 taps (fig. 3-17).

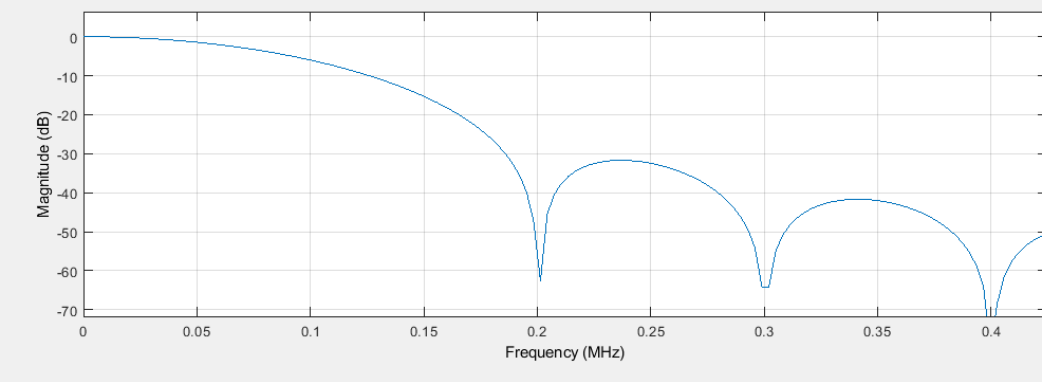

Figure 3-16: 500 tap filter for AIS

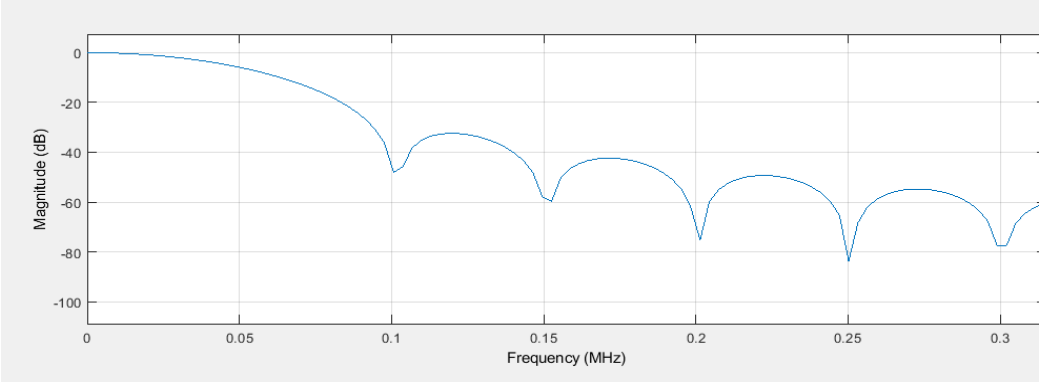

Figure 3-17: 1000 tap filter for AIS

As a result of the above filter, the correlation peak after filtration is shown below (fig. 3-18).

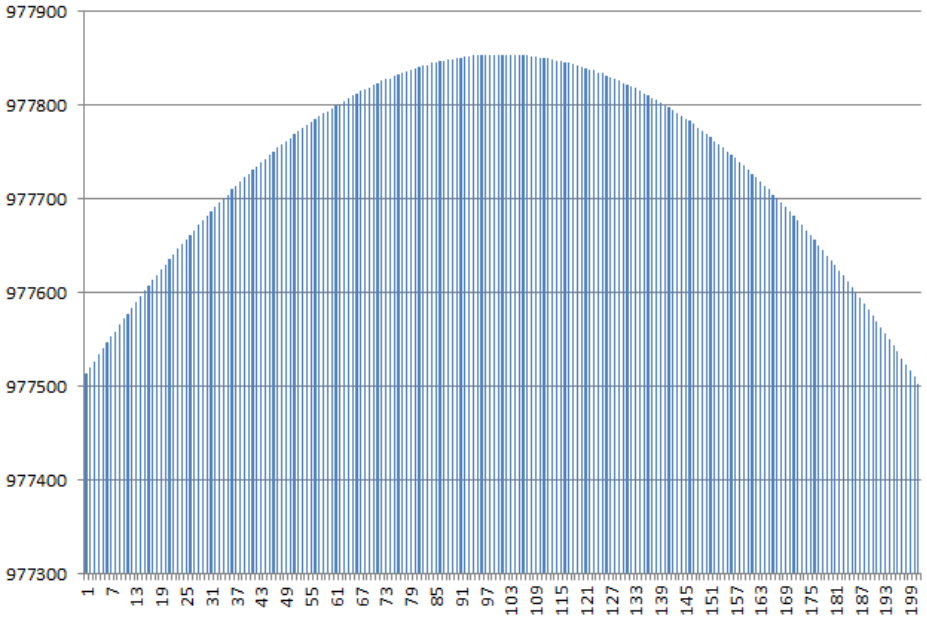

Figure 3-18: Correlation peak after applying the filter

The VDES signal bandwidth is four times wider. Below is the filter design for the VDES system. Figure 3-19 shows the filter characteristics enlarged. Because of the wider bandwidth compared to signal AIS, applied 2000 in the filter taps in order to improve the filtration efficiency (fig. 3-20).

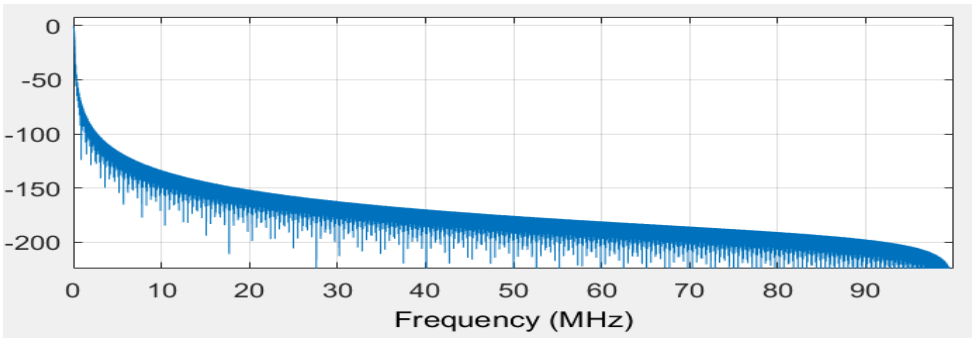

Figure 3-19: Designed filter for VDES signal

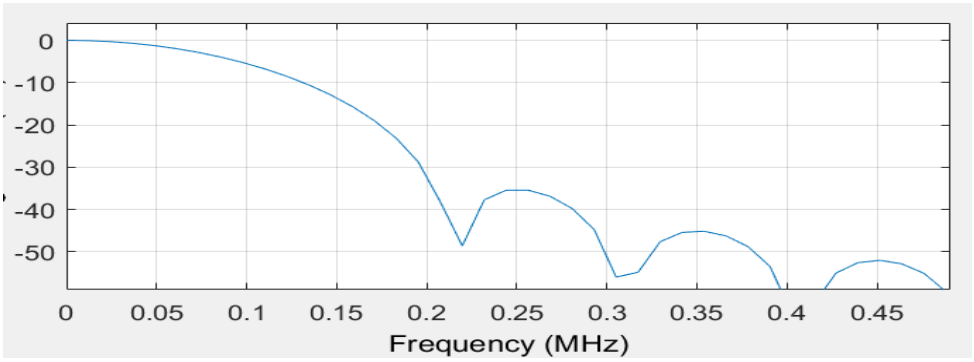

Figure 3-20: 2000 tap filter for VDES

The enlarged correlation peak for VDES signals before (fig 3-21) and after (fig. 3-22) filtration is shown below.

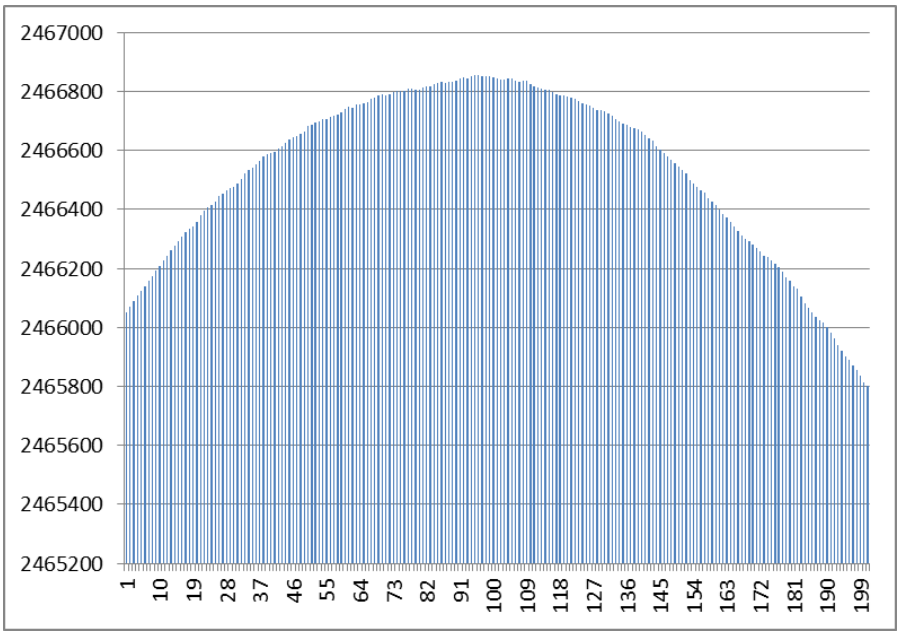

Figure 3-21: Correlation peak before applying the filter for VDES signal

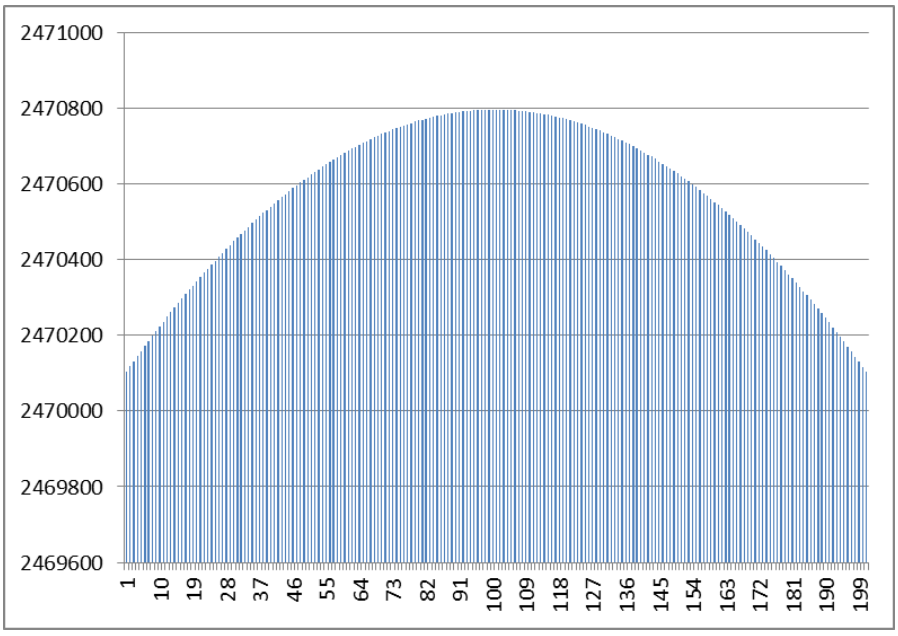

Figure 3-22: Correlation peak after applying the filter for VDES signal

The use of a low-pass filter resulted in smoothing the correlation peak. It allows for greater accuracy in determining the distance from the transmitter to the receiver. The use of a filter also increases the SNR value by about 6 dB.

4 Analysis of the measurement campaign results

This chapter describes the results of two measurement campaigns. The results include:

- route measurement chart to Karlskrona,
- route measurement chart for Gdynia,
- SNR measurement chart,
- graph of measurements of the ratio of the main peak to the side peaks,
- accuracy error graph,
- RMS curves for all measurements,
- RMS curves for the water environment,
- RMS curves for the terrestrial environment,
- impact of the width of the Hel peninsula on the RMS,
- map with accuracy errors in the measurement campaign,
- comparison of results from the AIS campaign with the VDES campaign.

4.1 Analysis of results from the AIS measurement campaign

The measurements took place on 17-18 June 2019. The table 4-1 below shows the number of files and their size, which has been processed by the application for signal correlation.

Table 4-1: Number and size of processed files for AIS

Route	Number of files	File size
Gdynia – Karlskrona	4540	55,9 GB
Karlskrona - Gdynia	3628	41,1 GB

However, the table 4-2 gives the exact start and end times of the measurements.

Table 4-2: Time of processed files for AIS

Route	Start time	End time
Gdynia – Karlskrona	22:38:44	03:40:17
Karlskrona - Gdynia	18:10:32	22:11:33

4.1.1 Analysis on the Gdynia - Karlskrona route

Below is the result in the form of the distance from the transmitting antenna from Gdynia to the receiving antenna located on the ferry. Figure 4-1 shows the distances that were obtained by processing the files in the application for signal correlation. Figure 4-2 shows the route measurements based on GNSS and EGNOS.

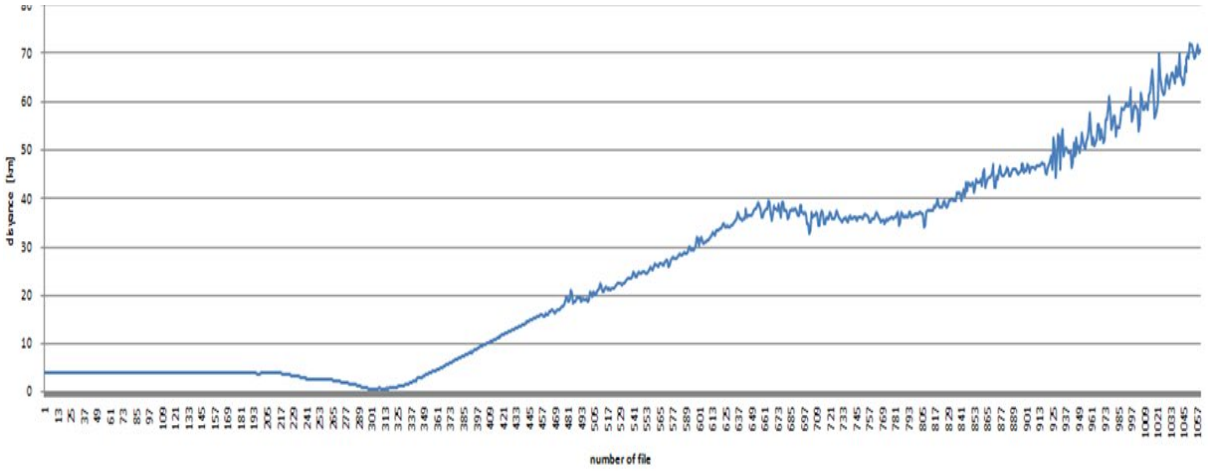

Figure 4-1: Route measurement after correlation application processing

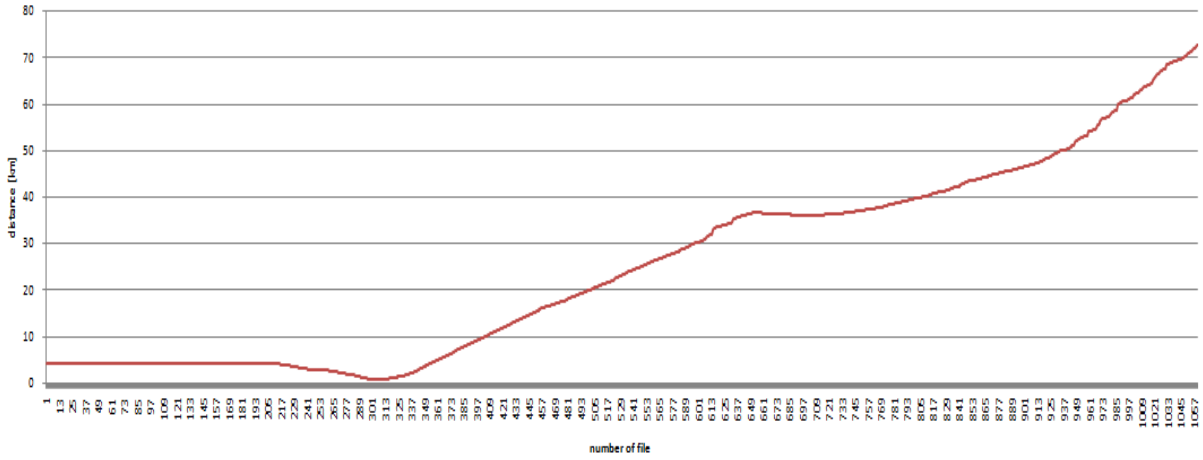

Figure 4-2: Route measurement based on GNSS and EGNOS

In order to better compare the results obtained, the charts have been superimposed in order to see the differences. The chart is presented below (fig. 4-3):

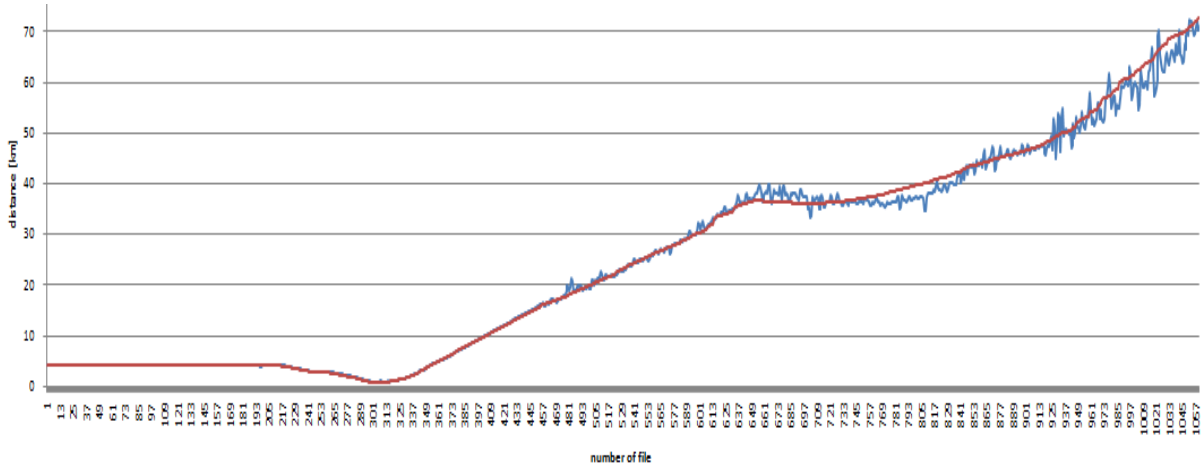

Figure 4-3: Route measurement - superimposed charts to see differences

Based on the above results, it can be seen that the charts overlap up to 20 km. This means that for this place the obtained distance measurement accuracy will be the best. However, the further route shows deviations. This indicates that the accuracy was lower. The results also show that it was possible to obtain a range of about 72 km for the AIS system. Up to this point, the signals were correlated and the distance from the transmitting antenna was calculated. Outside this zone, signals could not be correlated, making it impossible to determine further positions.

You will also notice that only files containing a useful signal are included in the results. Files in which noise was detected were rejected and were not included in the results.

The next step presents the obtained SNR values on the Gdynia-Karlskrona route. Below is a graph of this relationship (fig. 4-4).

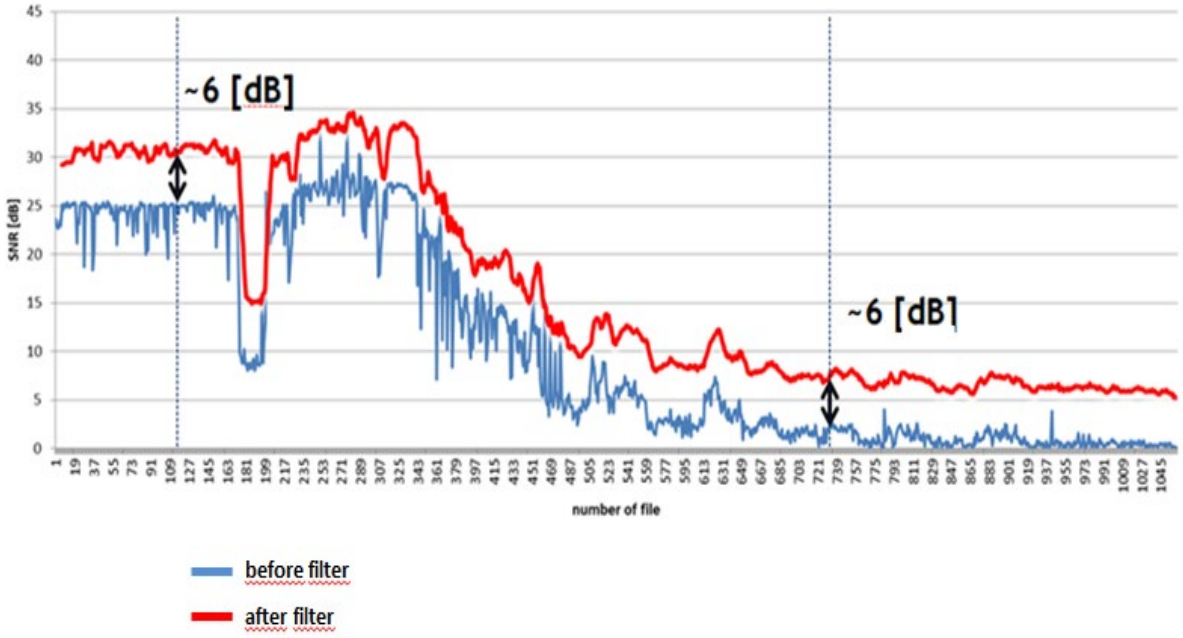

Figure 4-4: Measurements SNR at the Gdynia-Karlskrona route

The above graph shows the ratio of useful signal power to noise power. It can also be seen that, after using an additional low-pass filter, an additional 6 dB was gained in the analysis. You can see how the signal strength level fell just behind the Hel Peninsula.

The 'hole' in the power drop that was generated at the beginning of the measurements at the port could have been caused by the fact that signals from other vessels could have been received at the same frequency. After careful analysis, it was noted that at the same time it also broadcast a marine radio with a weather program. These factors could have influenced such a visible worsening of the SNR.

The ratio of the main correlation peak to side peaks was also analyzed. It can be seen on the graph (fig. 4-5) that this value deteriorated as the distance increased. The better value of this ratio, the better distance accuracy could be obtained based on correlation.

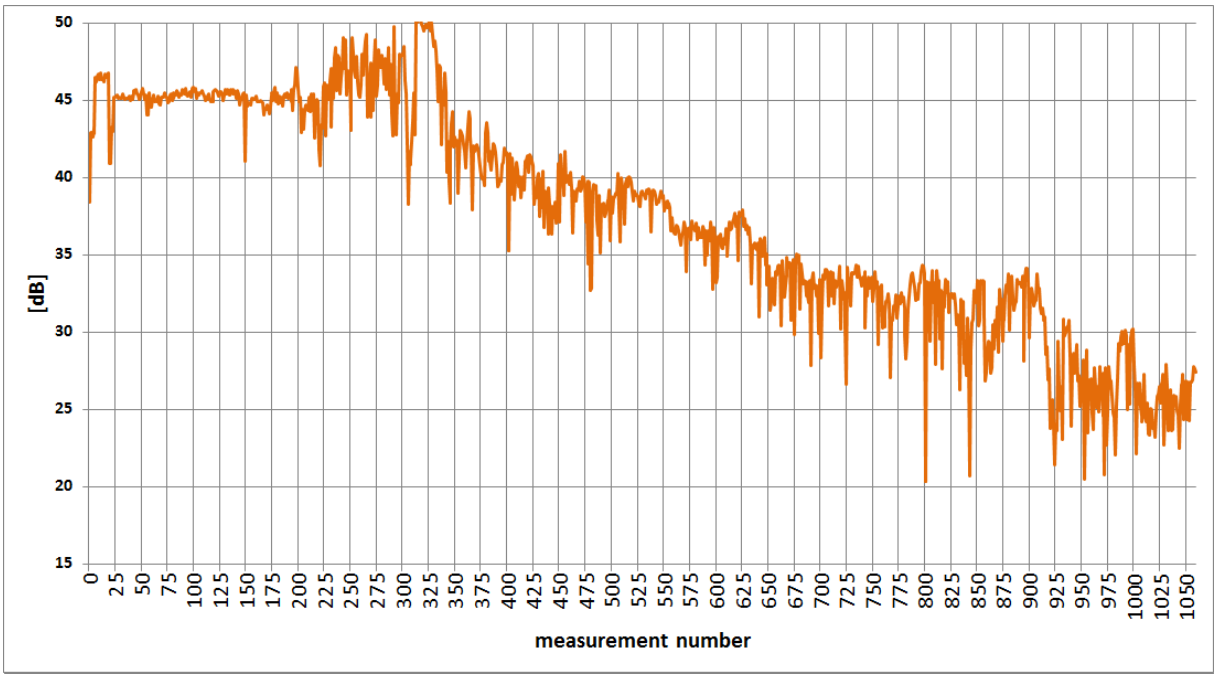

Figure 4-5: Ratio of correlation peak to side peaks

4.1.2 Analysis on the Karlskrona – Gdynia route

Below is the result in the form of the distance from the transmitting antenna from Gdynia to the receiving antenna located on the ferry. Figure 4-6 shows the distances that were obtained by processing the files in the application for signal correlation. Figure 4-7 shows the route measurements based on GNSS and EGNOS.

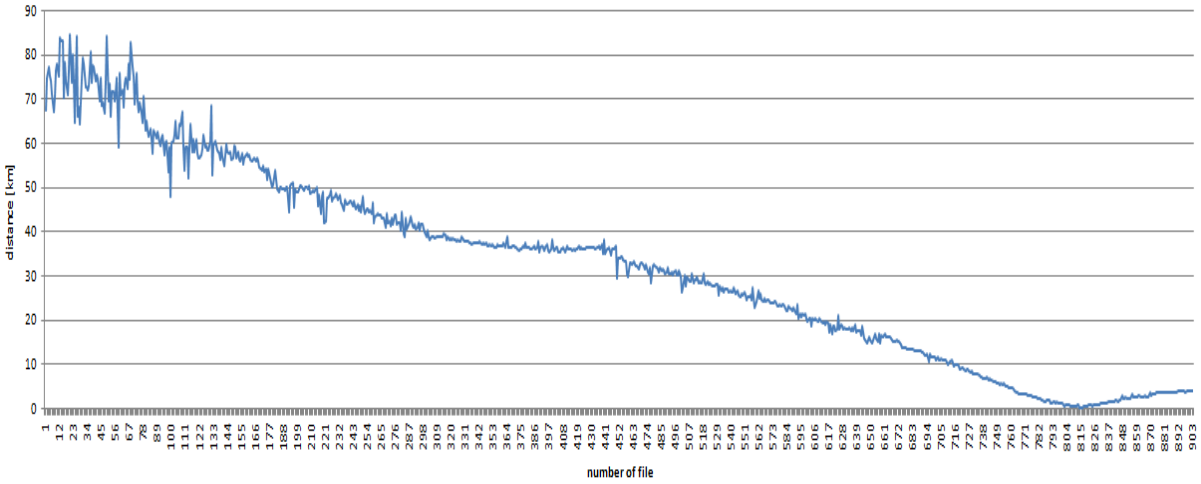

Figure 4-6: Route measurement after correlation application processing

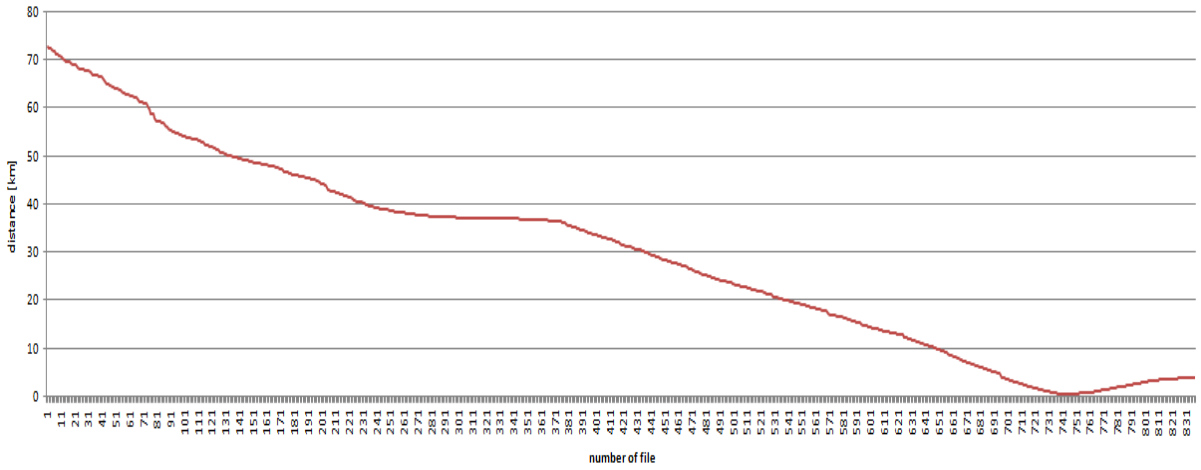

Figure 4-7: Route measurement based on GNSS and EGNOS

In order to better compare the results obtained, the charts have been superimposed in order to see the differences. The chart is presented below (fig. 4-8):

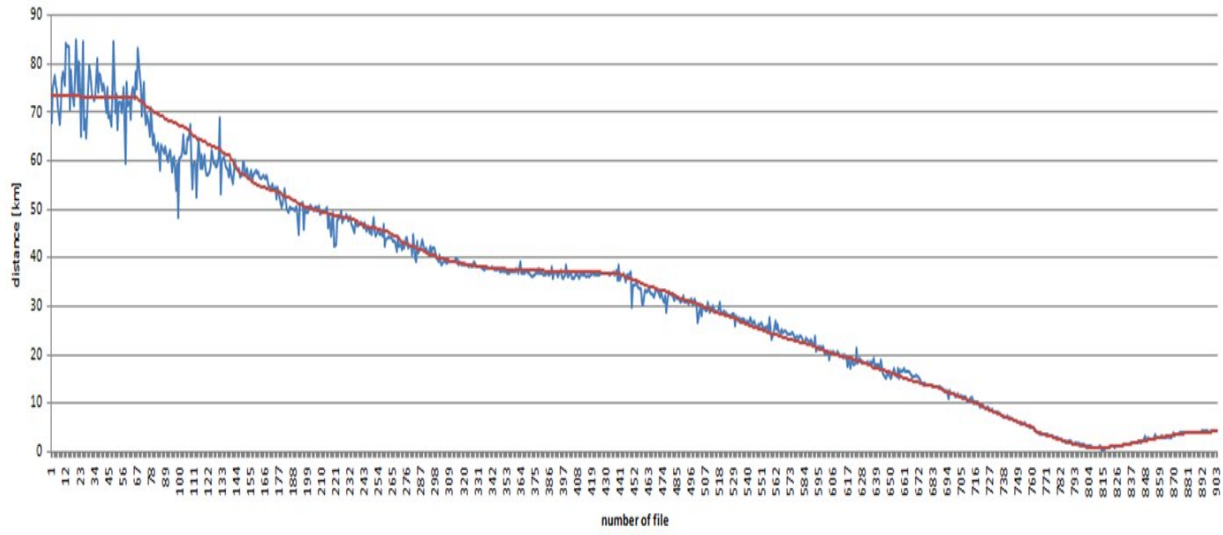

Figure 4-8: Route measurement - superimposed charts to see differences

Very similar to the previous results. In the coverage area affected approximately at 72 km. In this case, the accuracy of the distances was a little worse than for the route to Karlskrona. It can also be seen that from about 20 km up to the port of Gdynia better accuracy has already been achieved.

The next step presents the obtained SNR values on the Karlskrona-Gdynia route. Below is a graph of this relationship (fig. 4-9).

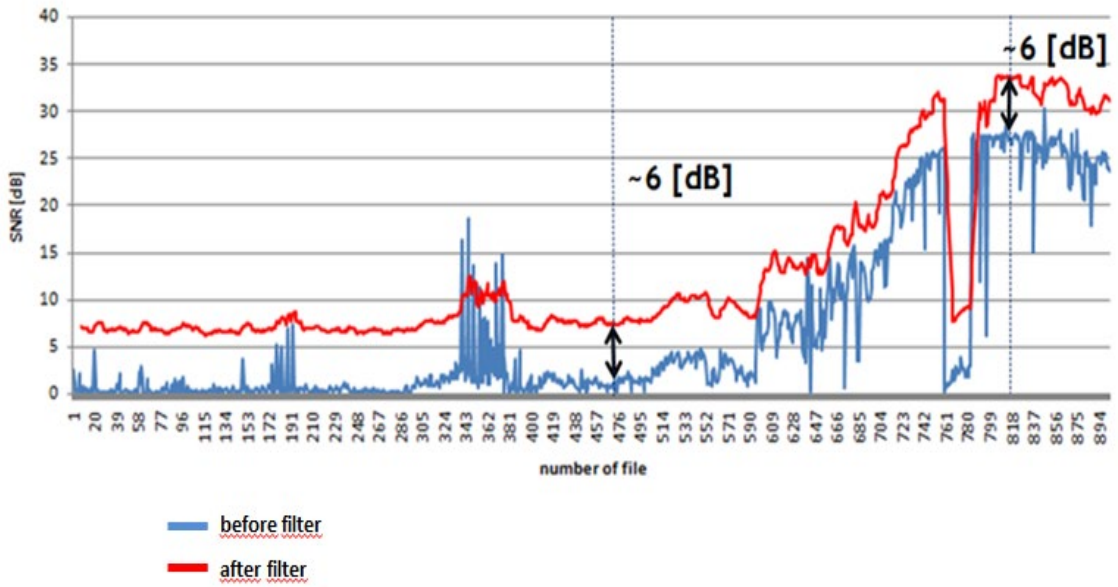

Figure 4-9: Measurements SNR at the Karlskrona – Gdynia route

The same case as in the earlier analysis of the route towards Karlskrona. The above graph shows the ratio of useful signal power to noise power. It can also be seen that, after using an additional low-pass filter, an additional 6 dB was gained in the analysis. You can see how the signal strength level fell just behind the Hel Peninsula.

The 'hole' in the power drop that was generated at the beginning of the measurements at the port could have been caused by the fact that signals from other vessels could have been received at the same frequency. After careful analysis, it was noted that at the same time it also broadcast a marine radio with a weather program. These factors could have influenced such a visible worsening of the SNR.

The ratio of the main correlation peak to side peaks was also analyzed. It can be seen on the graph (fig. 4-10) that this value deteriorated as the distance increased. The better value of this ratio, the better distance accuracy could be obtained based on correlation.

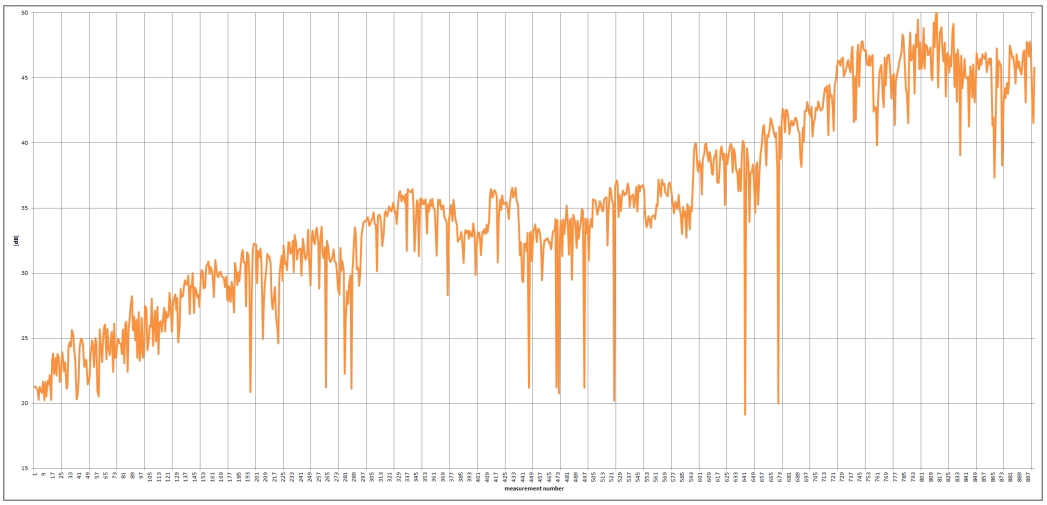

Figure 4-10: Ratio of correlation peak to side peaks

4.1.3 Analysis of all measurements

This section deals with more detailed data processing. The following are the accuracy of the distance that was obtained at a distance closer to the transmitting antenna at a high SNR value. This was compared with the accuracy result for the distance further from the transmitting antenna at low SNR. The comparison chart is below (fig. 4-11).

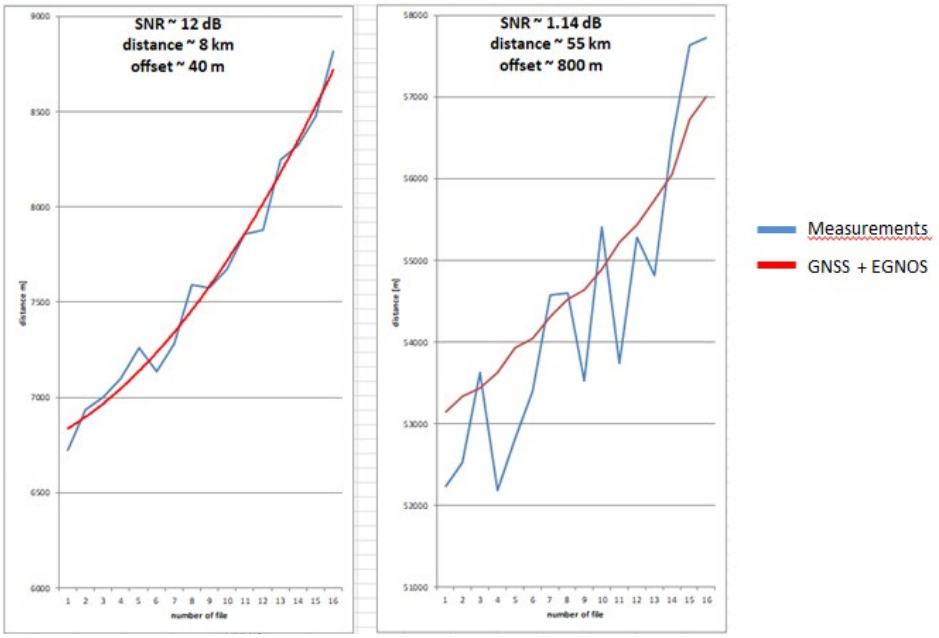

Figure 4-11: Accuracy obtained on measurements

From the above results, it can be seen that for large SNR values it was possible to achieve a distance accuracy of less than 100 m. On the other hand, this accuracy significantly decreased just behind the Hel Peninsula. At the limit of coverage, accuracy is very low.

The next graph (fig. 4-12) shows the dependence of the distance error (difference calculated from the distance calculated by the correlator and the distance from GNSS and EGNOSA) depending on the distance from the transmitting antenna located in Gdynia.

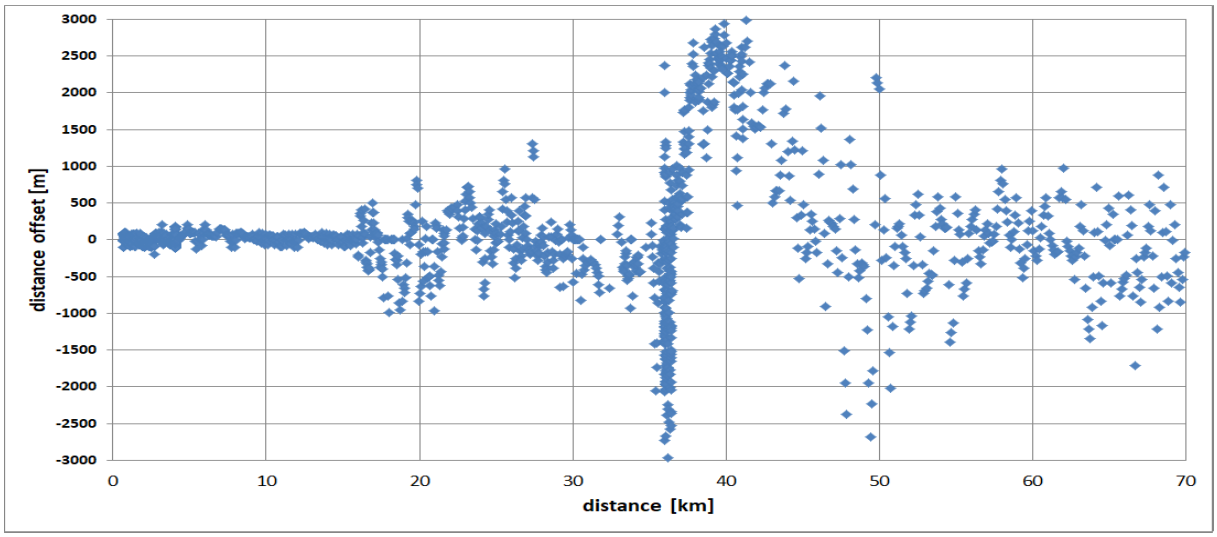

Figure 4-12: Accuracy error depending on distance

The decrease in signal strength and the impact of the terrestrial environment behind the Hel Peninsula caused a large increase in accuracy errors after 20 km. There is also a moment that the results processed in the signal correlator differ significantly from the results of GNSS and EGNOS measurements. It is a row of up to 3000 m.

Further analysis shows the RMS curve that was generated for all measurements. The chart includes (fig 4-13):

- the theoretical curve,
- curve with measurements results.

The accuracy of TOA (measurement error) can also be analyzed using the Cramer-Rao Lower Bound method. In ideal propagation conditions, with no multipath and interference phenomena considered, the ranging accuracy can be defined as a function of the signal to noise ratio and the effective signal bandwidth:

$$Acc_{CRLB} = \frac{c}{\sqrt{8\pi^2\beta^2 SNR}} \tag{7}$$

where: *c* is speed of light, $\beta^2 = \frac{\int f^2 S(f) df}{\int S(f) df}$ is the squared equivalent bandwidth. The signal to noise ratio SNR can be calculated from the ranging signal energy to noise ratio:

$$SNR = \frac{E_r}{N_0} - 10log_{10}(B) + 10log_{10}(R_r) \tag{8}$$

where: B is the system bandwidth (25 kHz for AIS and 100 kHz for VDES), $R_r = {}^1/_{T_r}$ and T_r is ranging frame length (130 ms for 5 slots AIS and 26 ms for VDES).

For the AIS system the observable differences are due to the simplification adopted in the analysis - the assumption of the rectangular wave in the first method and the real AIS spectrum shape in the Cramer-Rao method. For the purpose of the deeper analysis, the R-Mode position determination accuracy will be compared to the Cramer-Rao Lower Bound (CRLB) method. It has to be stated that this method is particularly effective for high SNR values (above 15 dB); if used for lower SNRs, however, the CRLB may be less accurate and

may introduce higher error. This theoretical assumption will be confirmed later in the paper during the analysis of the measurement data.

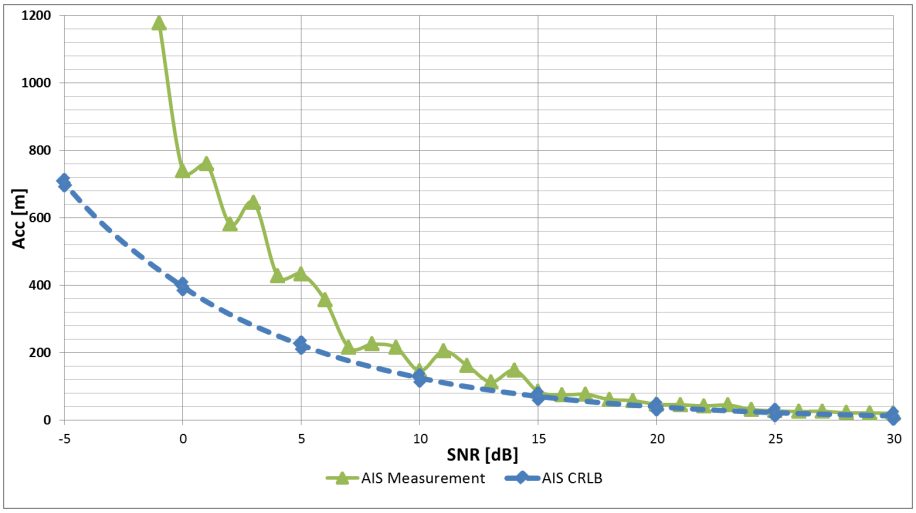

Figure 4-13: RMS curves for all measurements

As you can see, the results obtained for the AIS system, after being processed by the signal correlating application, deviate from theoretical curves. Large RMS differences that were obtained mainly for low SNR values may be due to:

- the curve takes into account large accuracy errors that occurred at the range limit,
- use of the Hann window, which gives 4 dB,
- the speed at which the vessel was traveling,
- influence of the Hel Peninsula.

The next chart (fig. 4-14) shows the RMS for the water path (until crossing the Hel Peninsula). It can be seen that RMS deviates less from theoretical curves than in the case of all measurements. Differences in error mainly decreased due to the lack of influence of the land path.

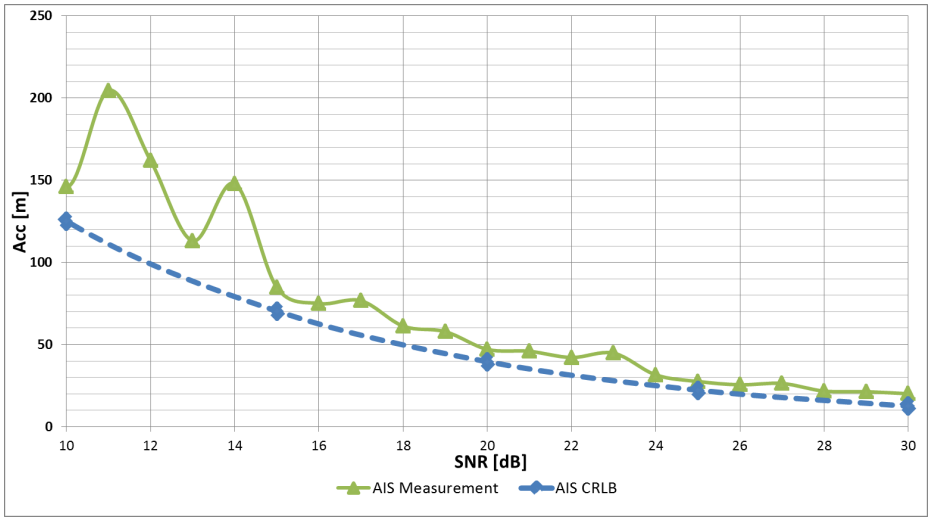

Figure 4-14: RMS curves for water path

The chart (fig. 4-15) below shows the results that were only taken into account behind the Hel peninsula. The water path is not considered here. You can see how big the distance errors are behind the peninsula.

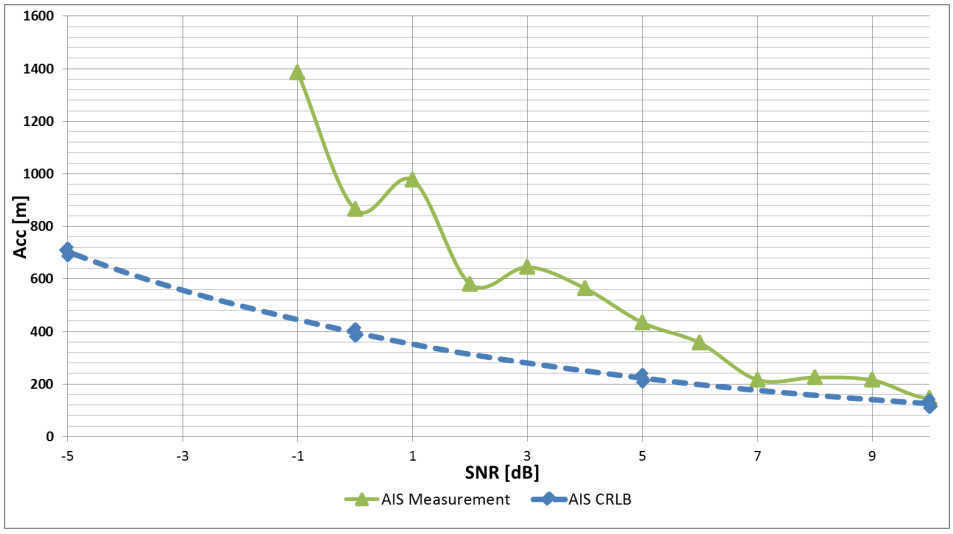

Figure 4-15: RMS curve behind the Hel Peninsula (land + water)

In addition, an analysis was made of how the width of the Hel Peninsula affects RMS. The effects are listed below (fig. 4-16):

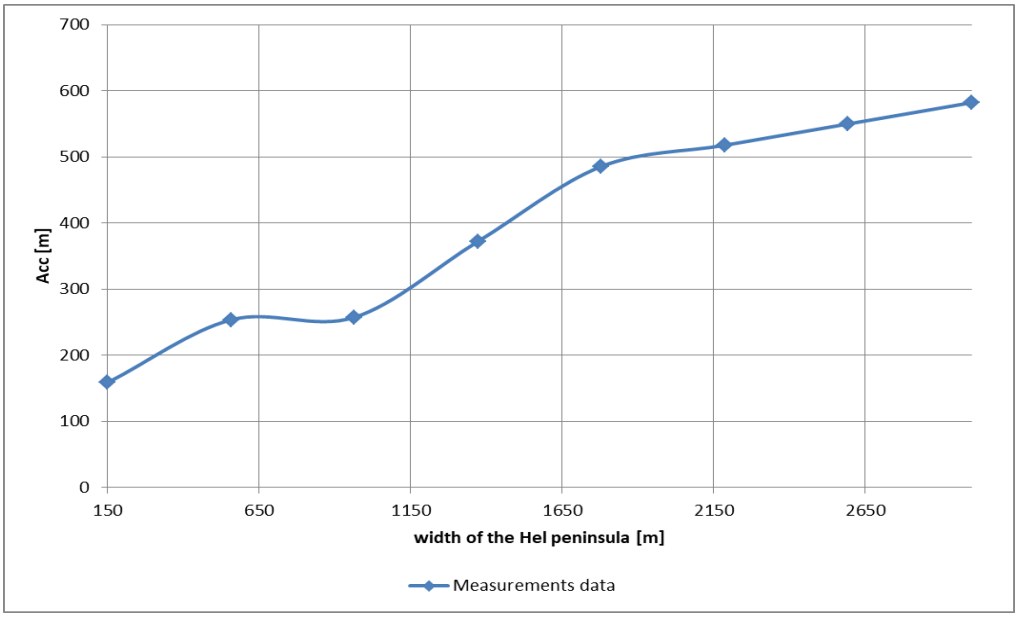

Figure 4-16: Impact of the width of the Hel Peninsula on RMS

As you can see, the influence of the width of the Hel Peninsula was large on the RMS value.

The map below (fig. 4-17) shows the obtained accuracy error. For better visualization of the range it is also applied AIS.

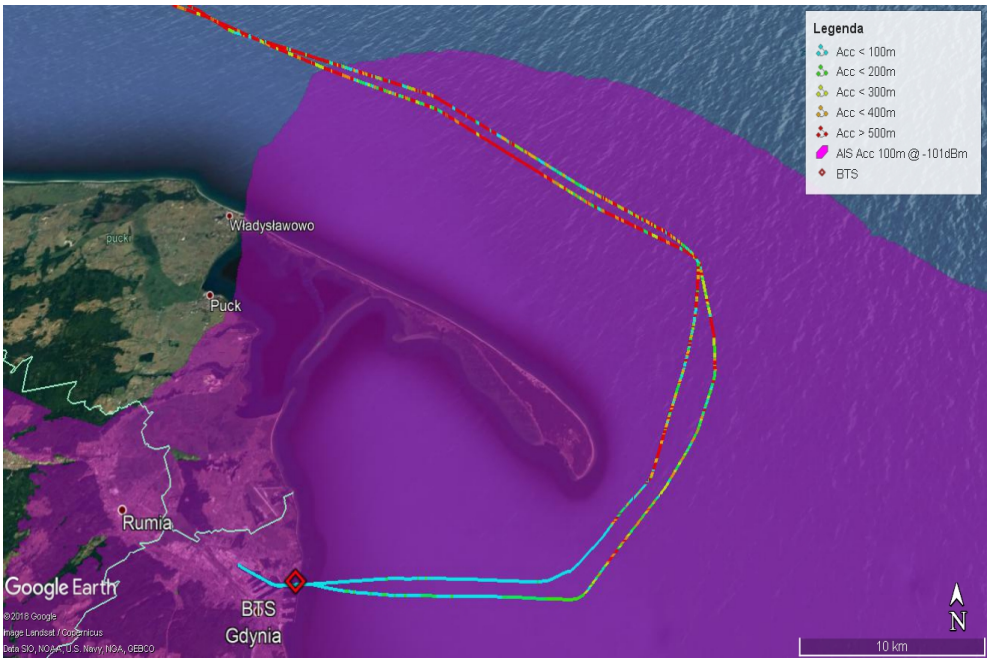

Figure 4-17: Map with distance accuracy error

4.2 Analysis of results from the VDES measurement campaign

The measurements took place on 15-16 November 2019. The table 4-3 below shows the number of files and their size, which has been processed by the application for signal correlation.

Table 4-3: Number and size of processed files for VDES

Route	Number of files	File size
Gdynia – Karlskrona	26025	581 GB
Karlskrona - Gdynia	31561	705 GB

However, the table 4-4 gives the exact start and end times of the measurements.

Table 4-4: Time of processed files for VDES

Route	Start time	End time
Gdynia – Karlskrona	07:46:25	15:17:19
Karlskrona - Gdynia	01:17:28	10:09:59

4.2.1 Analysis on the Gdynia - Karlskrona route

Below is the result in the form of the distance from the transmitting antenna from Gdynia to the receiving antenna located on the ferry. Figure 4-18 shows the distances that were

obtained by processing the files in the application for signal correlation. Figure 4-19 shows the route measurements based on GNSS and EGNOS.

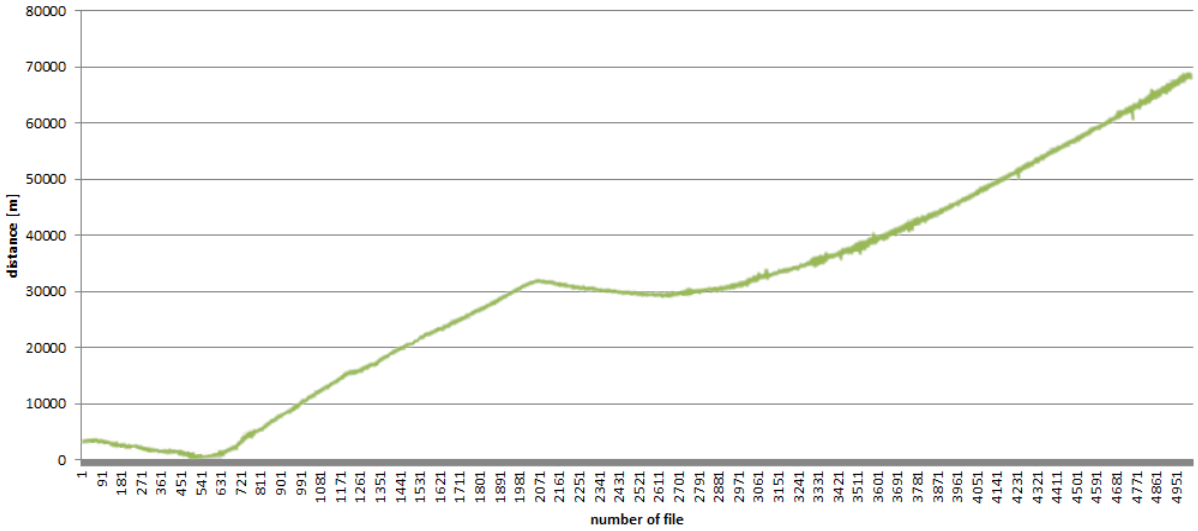

Figure 4-18: Route measurement after correlation application processing

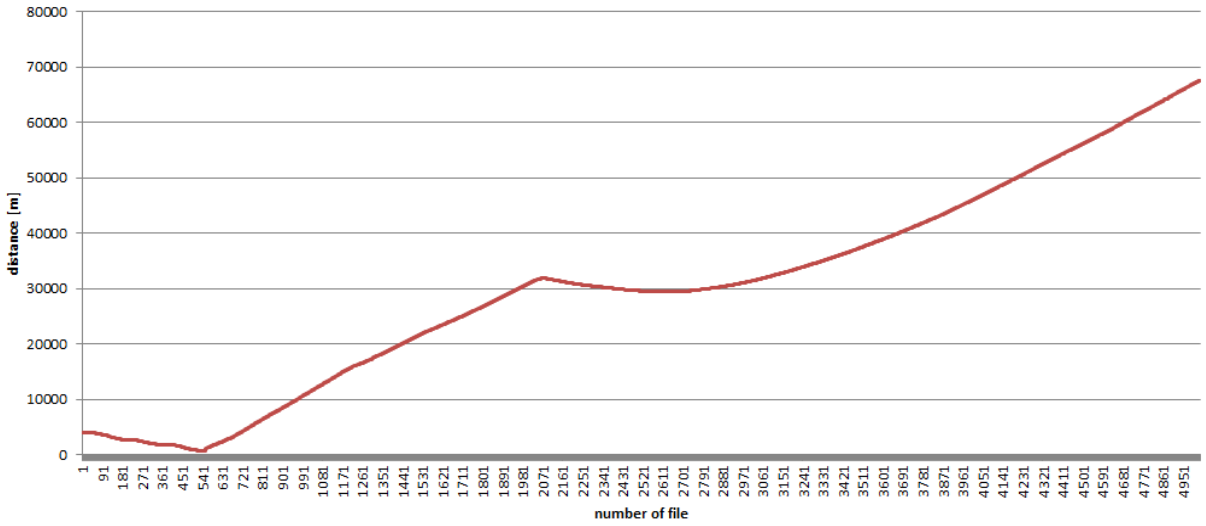

Figure 4-19: Route measurement based on GNSS and EGNOS

In order to better compare the results obtained, the charts have been superimposed in order to see the differences. The chart is presented below (fig. 4-20):

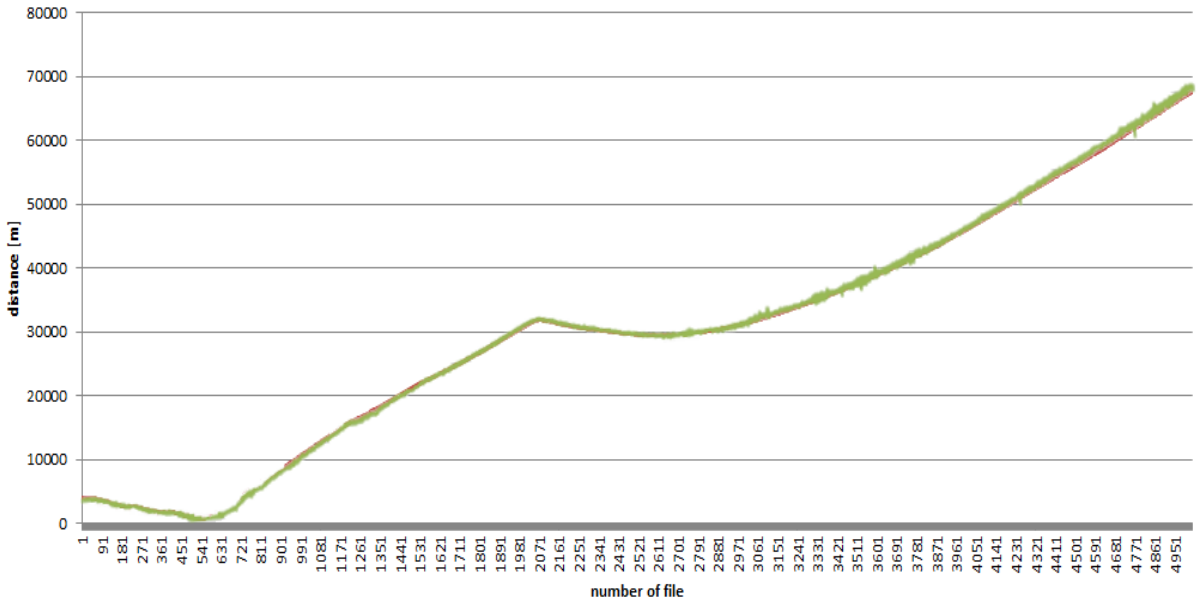

Figure 4-20: Route measurement - superimposed charts to see differences

As can be seen in the graph above, the range of 70 km has been achieved for the VDES system. Above this distance, signals could no longer be correlated. As you can see, it is only after 30 km of the route that distance accuracy begins to decrease. The results at the edge of the range are also satisfactory because no large deviations in the accuracy error were observed (on average 600 m at the end of the range).

The next step presents the obtained SNR values on the Gdynia-Karlskrona route. Below is a graph of this relationship (fig. 4-21).

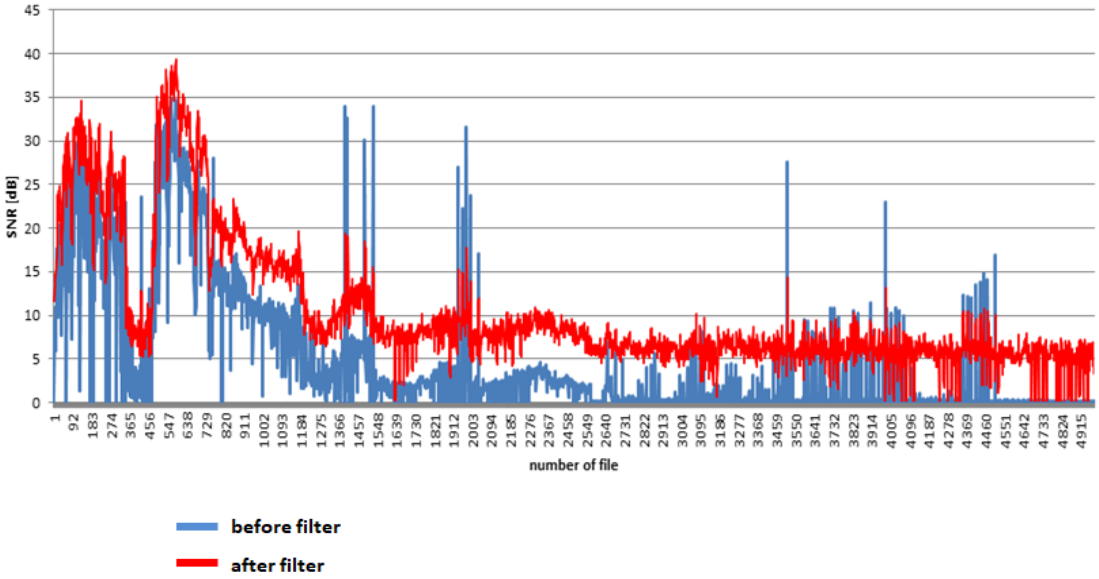

Figure 4-21: Measurements SNR at the Gdynia-Karlskrona route

The above graph shows the ratio of useful signal power to noise power. It can also be seen that, after using an additional low-pass filter, an additional 6 dB was gained in the analysis. You can see how the signal strength level fell just behind the Hel Peninsula.

The 'hole' in the power drop that was generated at the beginning of the measurements at the port could have been caused by the fact that signals from other vessels could have been received at the same frequency. After careful analysis, it was noted that at the same time it also broadcast a marine radio with a weather program. These factors could have influenced such a visible worsening of the SNR.

The ratio of the main correlation peak to side peaks was also analyzed. It can be seen on the graph (fig. 4-22) that this value deteriorated as the distance increased. The better value of this ratio, the better distance accuracy could be obtained based on correlation.

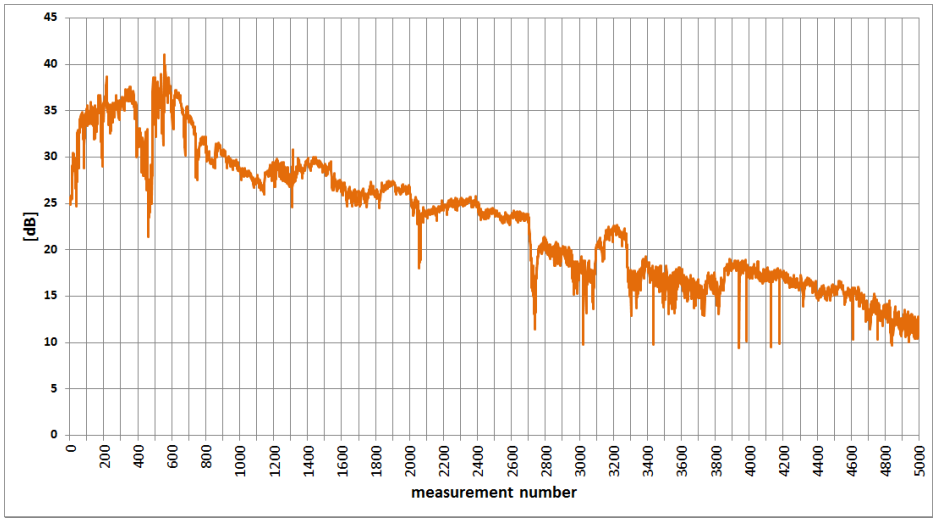

Figure 4-22: Ratio of correlation peak to side peaks

4.2.2 Analysis on the Karlskrona – Gdynia route

Below is the result in the form of the distance from the transmitting antenna from Gdynia to the receiving antenna located on the ferry. Figure 4-23 shows the distances that were obtained by processing the files in the application for signal correlation. Figure 4-24 shows the route measurements based on GNSS and EGNOS.

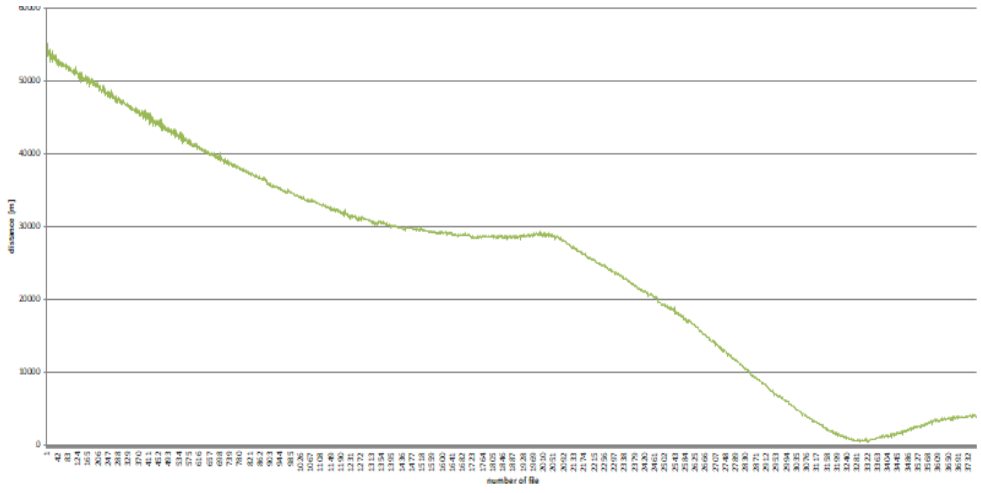

Figure 4-23: Route measurement after correlation application processing

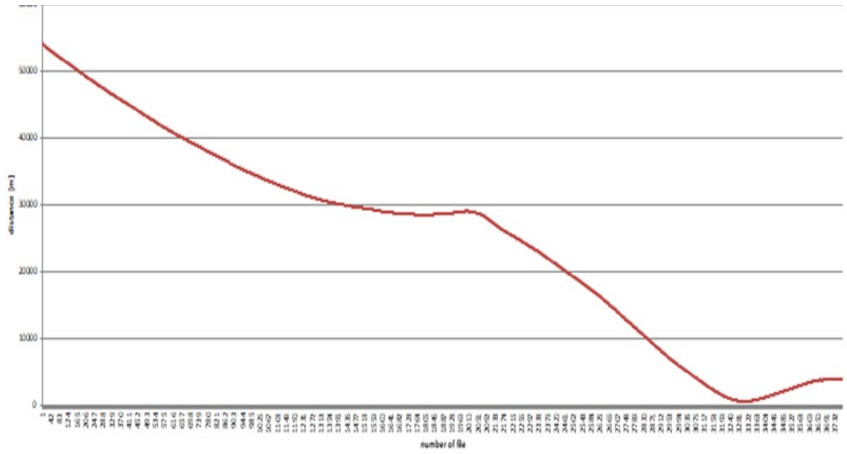

Figure 4-24: Route measurement based on GNSS and EGNOS

In order to better compare the results obtained, the charts have been superimposed in order to see the differences. The chart is presented below (fig. 4-25):

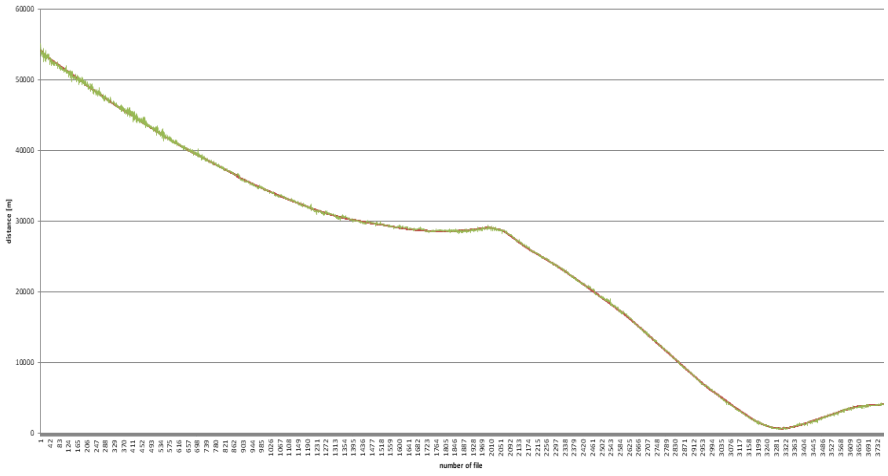

Figure 4-25: Route measurement - superimposed charts to see differences

Similarly to the route to Karlskrona, the distance accuracy was satisfactory. It can also be seen that above 30 km from the transmitting antenna, distance accuracy has decreased. The reason for this will be considered later in this report.

The next step presents the obtained SNR values on the Karlskrona-Gdynia route. Below is a graph of this relationship (fig. 4-26).

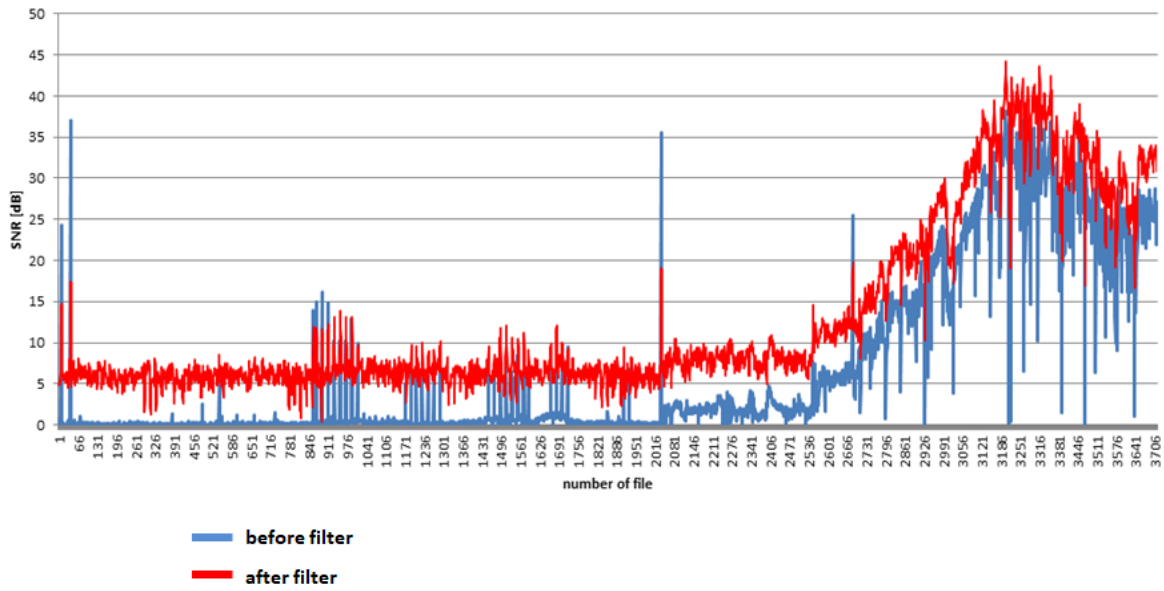

Figure 4-26: Measurements SNR at the Karlskrona – Gdynia route

It can also be seen that in this case we are not dealing with the SNR 'hole', which in previous cases appeared in the port.

The same case as in the earlier analysis of the route towards Karlskrona. The above graph shows the ratio of useful signal power to noise power. It can also be seen that, after using an additional low-pass filter, an additional 6 dB was gained in the analysis. You can see how the signal strength level fell just behind the Hel Peninsula.

The ratio of the main correlation peak to side peaks was also analyzed. It can be seen on the graph (fig. 4-27) that this value deteriorated as the distance increased. The better value of this ratio, the better distance accuracy could be obtained based on correlation.

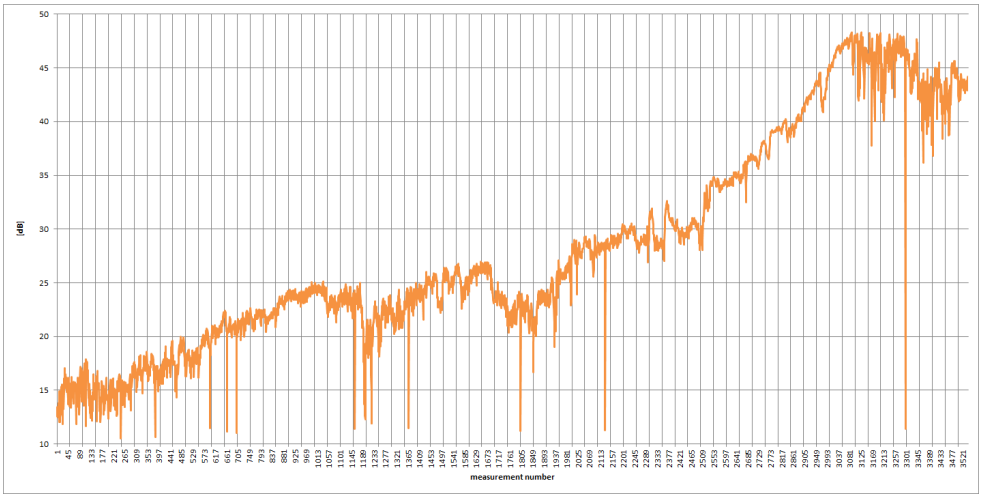

Figure 4-27: Ratio of correlation peak to side peaks

4.2.3 Analysis of all measurements

This section deals with more detailed data processing. The following are the accuracy of the distance that was obtained at a distance closer to the transmitting antenna at a high SNR

value. This was compared with the accuracy result for the distance further from the transmitting antenna at low SNR. The comparison chart is below (fig. 4-28).

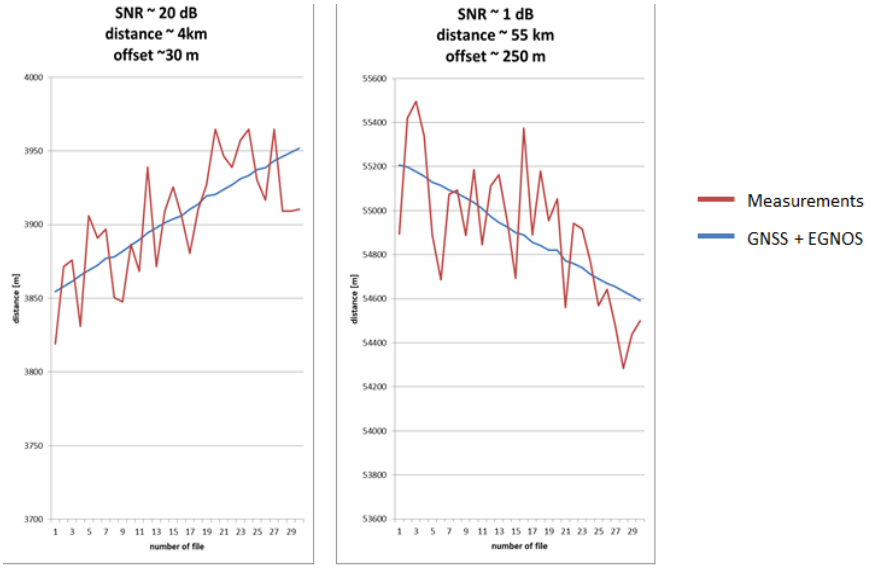

Figure 4-28: Accuracy obtained on measurements

From the above results, it can be seen that for large SNR values it was possible to achieve a distance accuracy of less than 50 m. On the other hand, this accuracy significantly decreased just behind the Hel Peninsula. Accuracy decreased to around 250 m.

The next graph (fig. 4-29) shows the dependence of the distance error (difference calculated from the distance calculated by the correlator and the distance from GNSS and EGNOSA) depending on the distance from the transmitting antenna located in Gdynia.

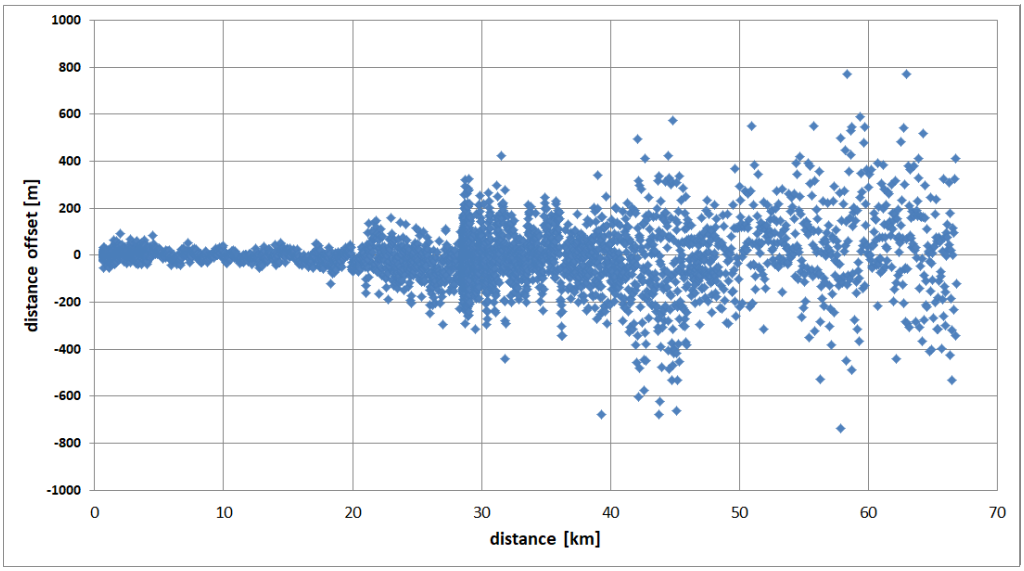

Figure 4-29: Accuracy error depending on distance

It can be seen that based on the above diagram - the accuracy of the determined position is about 50 m for a route up to 20 km. Above this distance, the accuracy error begins to increase slowly. For distances over 40 km this error is about 400 m.

Further analysis shows the RMS curve that was generated for all measurements. The chart includes (fig 4-30):

- theoretical curve,

- curve with measurements results.

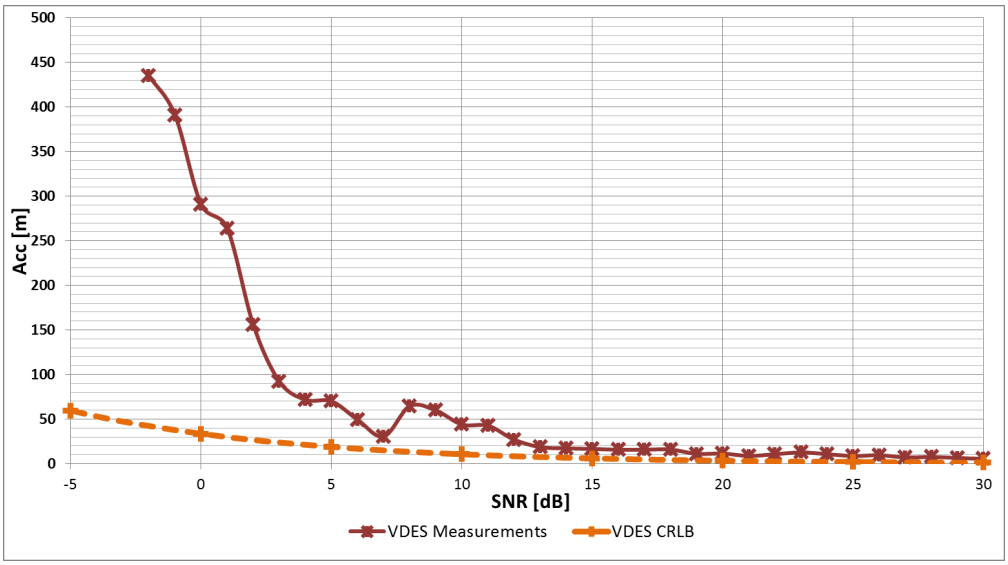

Figure 4-30: RMS curves for all measurements

In the chart above, it can be seen that the RMS for large SNR values is low, which is good evidence. However, for SNR below 5 dB it can be clearly seen that the RMS curve for data processed by the application for signal correlation is deviated from the theoretical curve. Large RMS differences that were obtained mainly for low SNR values may be due to:

- the curve takes into account large accuracy errors that occurred at the range limit,
- use of the Hann window, which gives 4 dB,
- the speed at which the vessel was traveling,
- influence of the Hel Peninsula.

The next chart (fig. 4-31) shows the RMS for the water path (until crossing the Hel Peninsula). It can be seen that RMS deviates less from theoretical curves than in the case of all measurements. Differences in error mainly decreased due to the lack of influence of the land path.

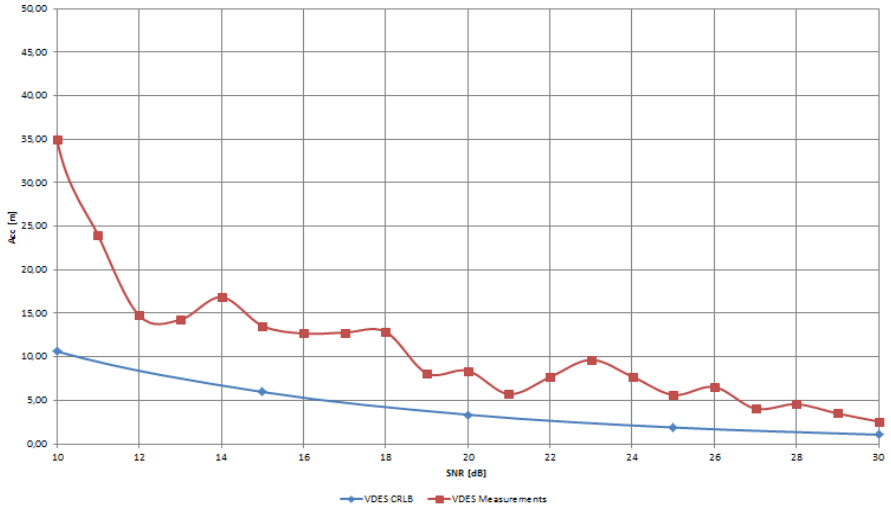

Figure 4-31: RMS curves for water path

The chart (fig. 4-32) below shows the results that were only taken into account behind the Hel peninsula. The water path is not considered here. The impact of the Hel Peninsula on the increasing accuracy error can be seen.

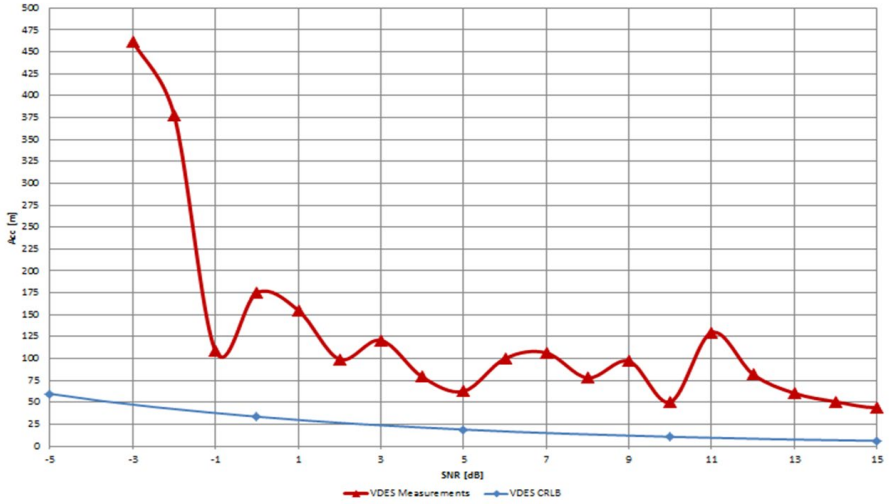

Figure 4-32: RMS curve behind the Hel Peninsula (land + water)

In addition, an analysis was made of how the width of the Hel Peninsula affects RMS. The effects are listed below (fig. 4-33):

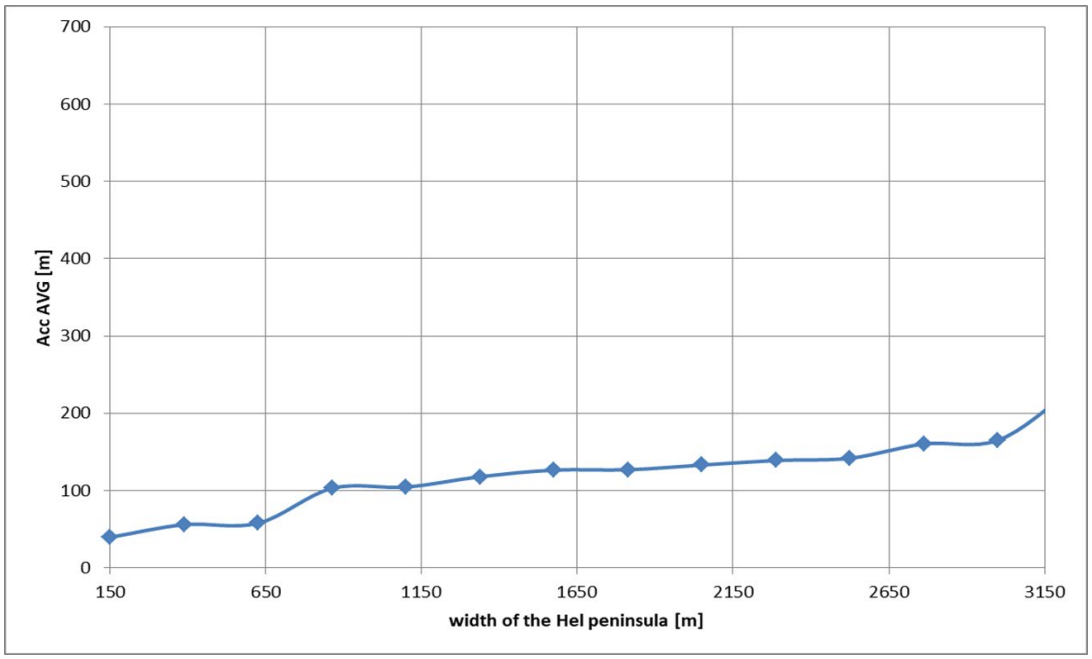

Figure 4-33: Impact of the width of the Hel Peninsula on RMS

As you can see, the influence of the width of the Hel Peninsula was large on the RMS value.

The map below (fig. 4-34) shows the obtained accuracy error. For better visualization of the range it is also applied VDES. w

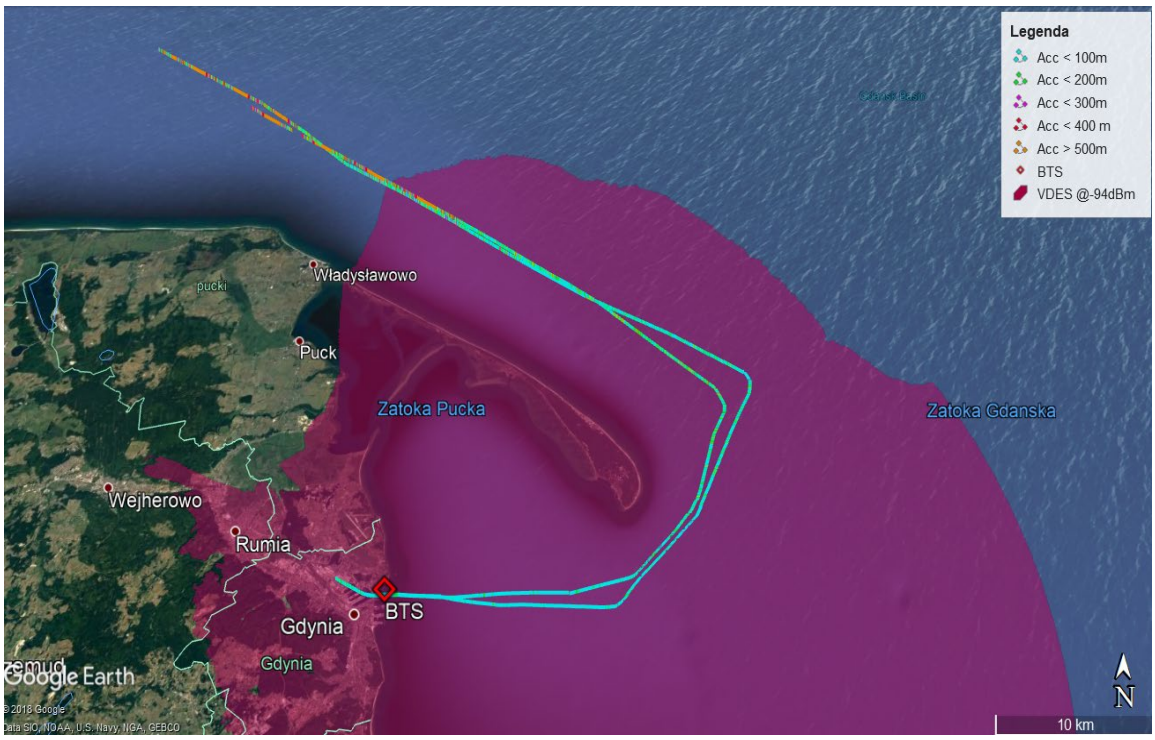

Figure 4-34: Map with distance accuracy error

4.3 Comparative analysis of the measurement campaign AIS and VDES.

This section compares the results obtained from both measurement campaigns. Thanks to the results obtained it was possible to compare, among others:

- graphs of the measured route,

- distance accuracy charts,

- RMS charts,

- RMS plots for the water path.

In the figure 4-35 and 4-36 shows the results obtained in both campaigns in both directions of the ferry route. It is clearly visible how better the distance accuracy from the broadcasting station is in the case of measurements for the VDES system. The results are better and more stable.

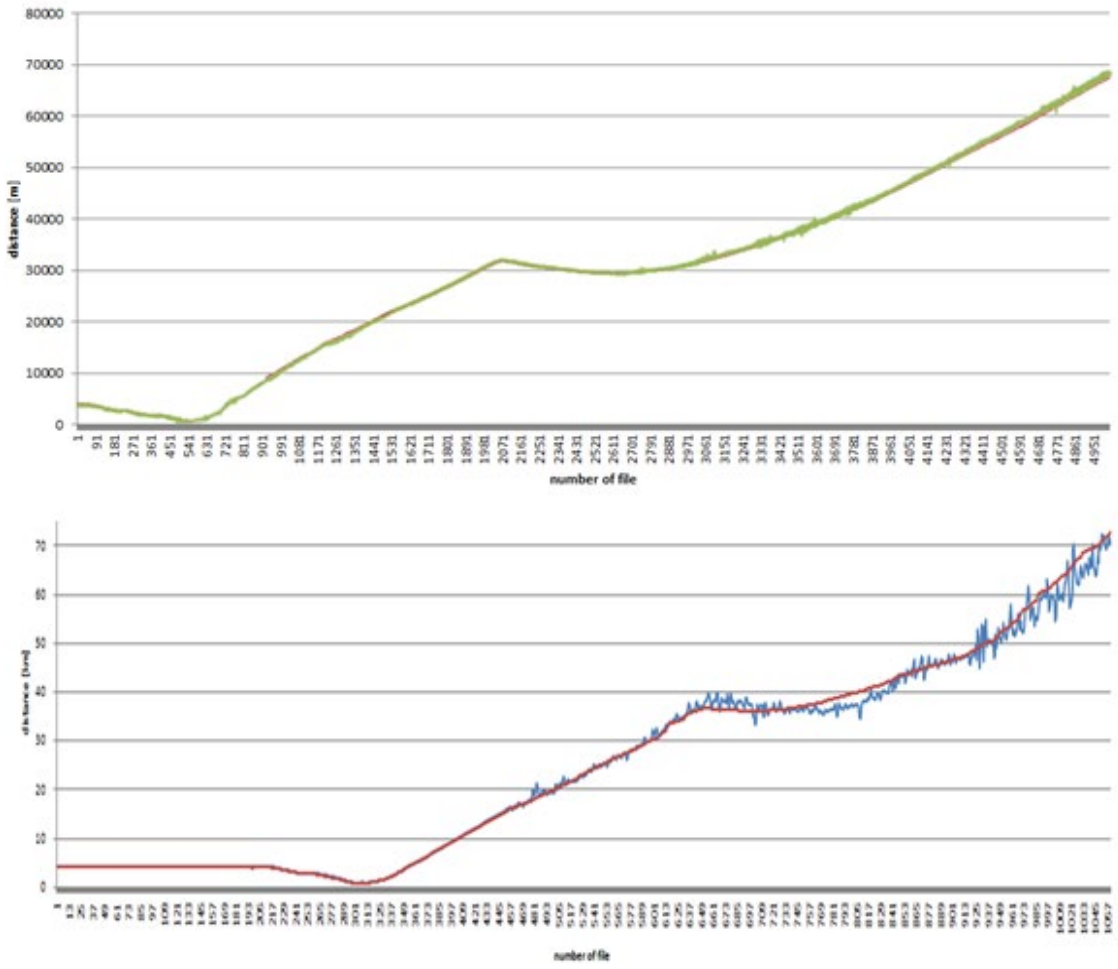

Figure 4-35: Comparative analysis of distance results obtained for the VDES and AIS system on the Gdynia-Karlskrona route.

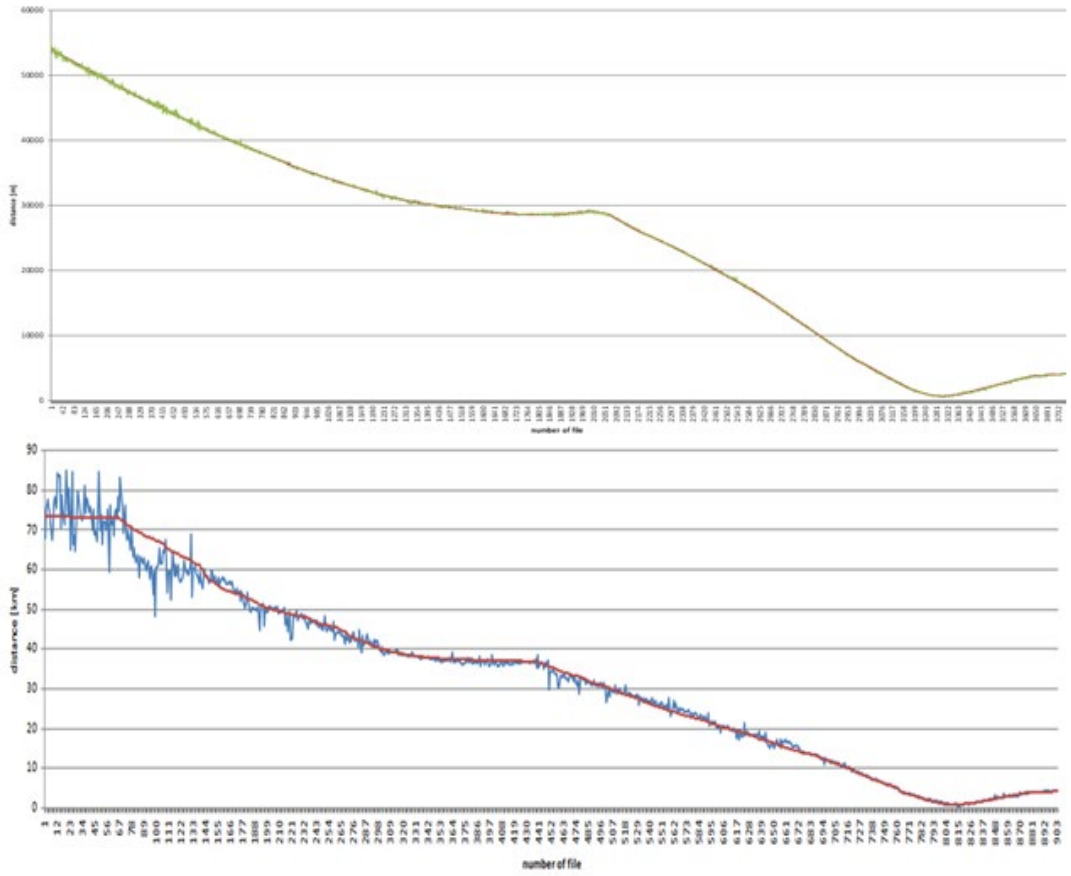

Figure 4-36: Comparative analysis of distance results obtained for the VDES and AIS system on the Karlskrona-Gdynia route.

The following figure 4-37 shows how the accuracy of the determined distance changes depending on the distance between the transmitting and receiving antennas. You can see very clearly how the accuracy error slowly increases with the distance from the transmitting antenna for the VDES system. On the other hand, for the AIS, this error starts to increase after 20 km, where it even reaches a value of 3 km. Distance accuracy error is more regular for VDES measurements than for AIS measurements.

This can be due to many properties:

- modulation type,
- the immunity of the given modulation to interference,
- weather,
- influence of the Hel Peninsula,
- vessel speed, etc.

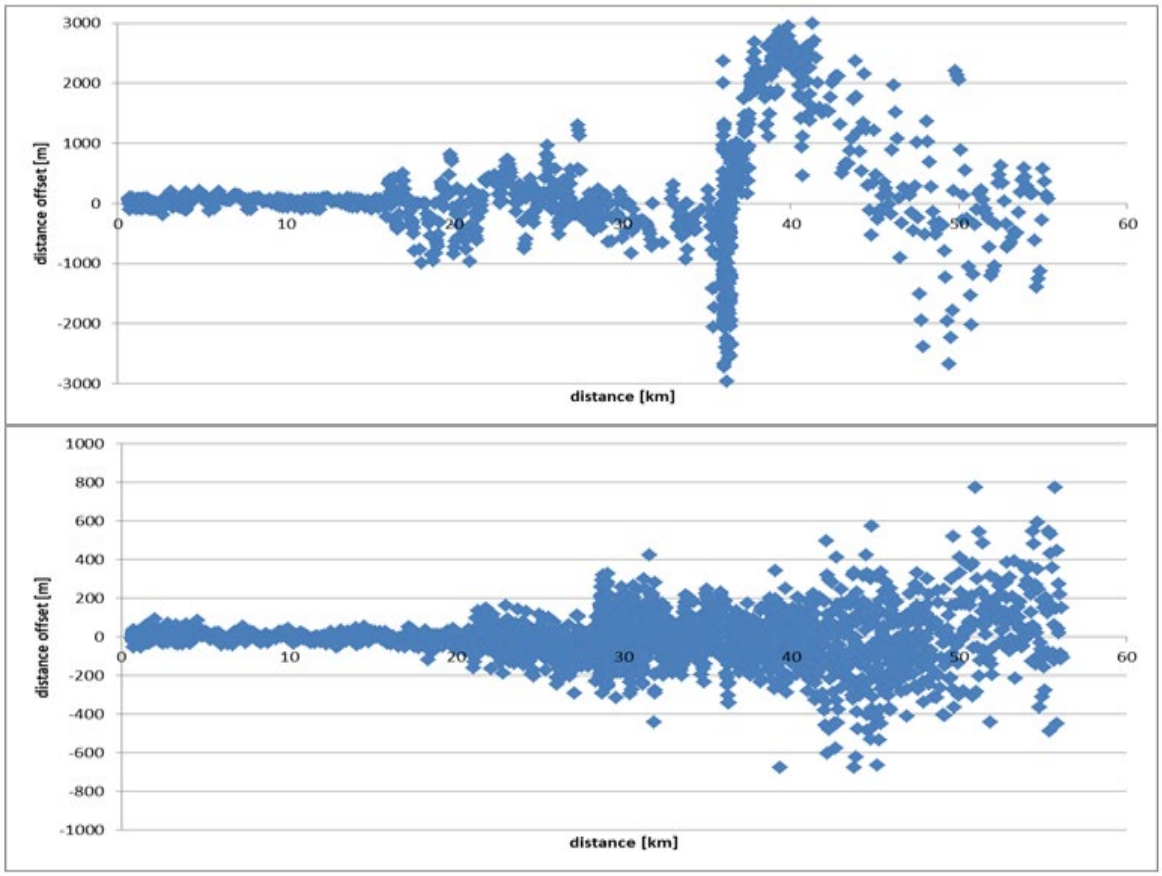

Figure 4-37: Accuracy error depending on distance for AIS and VDES system.

The figure 4-38 below shows the RMS for all measurements.

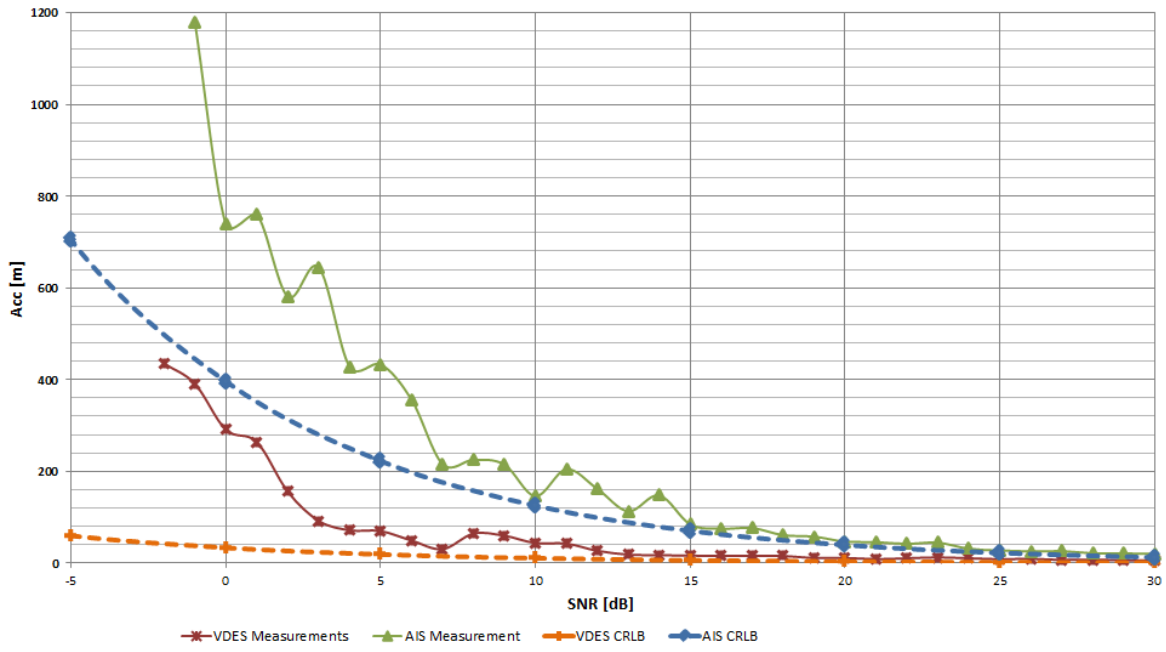

Figure 4-38: RMS curves for all measurements

The results obtained in the measurement campaigns were compared with theoretical curves calculated on the basis of the Cramer-Rao Lower Bound method. As can be seen, for very low SNR values the discrepancy between the theory and the measurements was initially very significant but it was going down as the SNR increased. The fact that for lower SNR values the accuracy of the determined distance was not satisfactory for both analyzed systems, confirms the limitation of the Cramer-Rao method mentioned earlier in this article. On the other hand, the results obtained for high SNR values almost coincided with the theoretical curves generated for the AIS and VDES systems, with the exception of the nearly constant, about 10 m difference of the RMS error . As stated earlier in the paper, much better accuracy of the determined distance was obtained for the VDES system.

Other possible sources of errors resulting (tab 4-5) in a behavior observed in fig. 4-38 which caused some deviation between theory and measurements, have been identified and are listed in table. It should be noted that some of these errors only apply to the low-SNR region, while other are valid for the entire SNR range in fig. 4-38.

Table 4-5: Sources of errors applicable for low and high SNR region

Source of error	**low SNR region**	**high SNR region**
Possible impact of residual clock errors	+	+
Errors caused by the presence of the Hel Peninsula	+	-
Errors that can be caused by lack of EGNOS and/or high HDOP	+	+
Ship’s speed too high	+	+
Weather conditions	+	+
Error resulting from passing the line of sight distance (beyond the 42.4 km mark)	+	-
Sampling rate	+	+

The relationship between RMS and the water path as well as the path taking into account the influence of the Hel peninsula are also presented in the common graphs below (fig. 4-39 and 4-40).

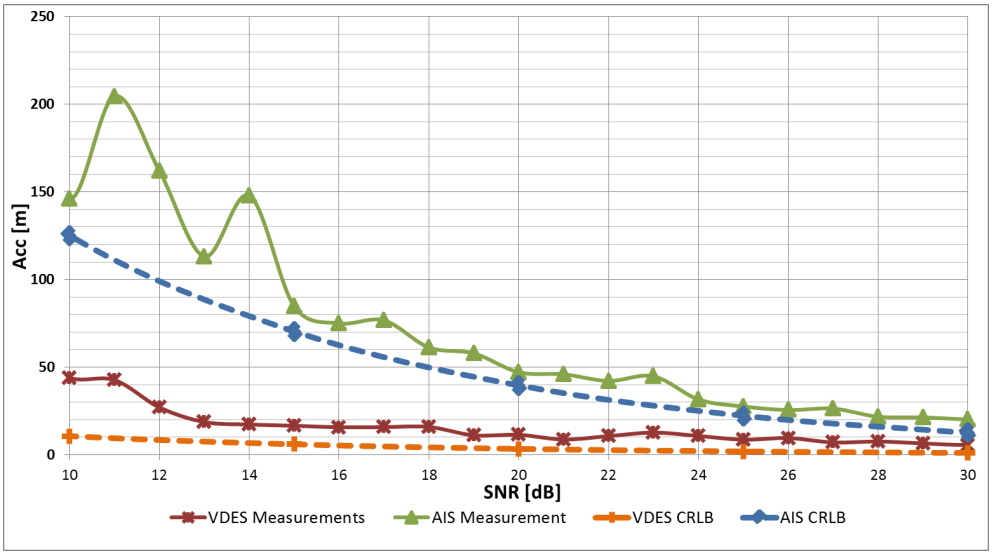

Figure 4-39: RMS curves for water path

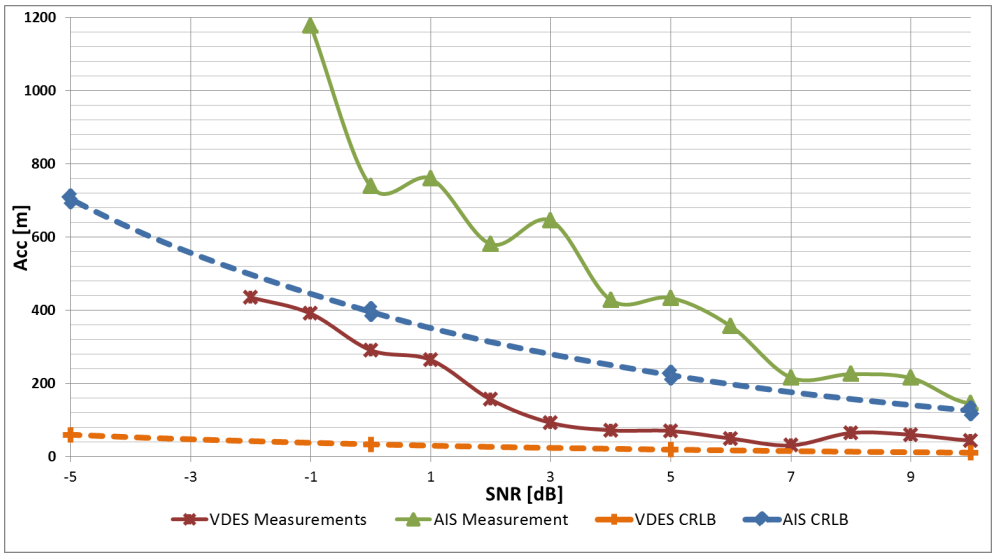

Figure 4-40: RMS curve behind the Hel Peninsula (land + water)

The conclusions are similar as in the analysis of all results. Better results were obtained for VDES measurements.

4.4 Analysis of the source of accuracy errors in measurement campaigns

This section lists potential sources of accuracy errors in the designated distance. The possible sources of error are:

- Error resulting from the momentary oscillator failure (fig. 4-41). During the measurements on the Karlskrona Gdynia route, a temporary lack of oscillator operation was observed (exactly until 07:42:45). From the results obtained it can be clearly seen that when the oscillator was not operating, an additional error was introduced, which was about 300 samples, which gives an error of about 450 m per distance.

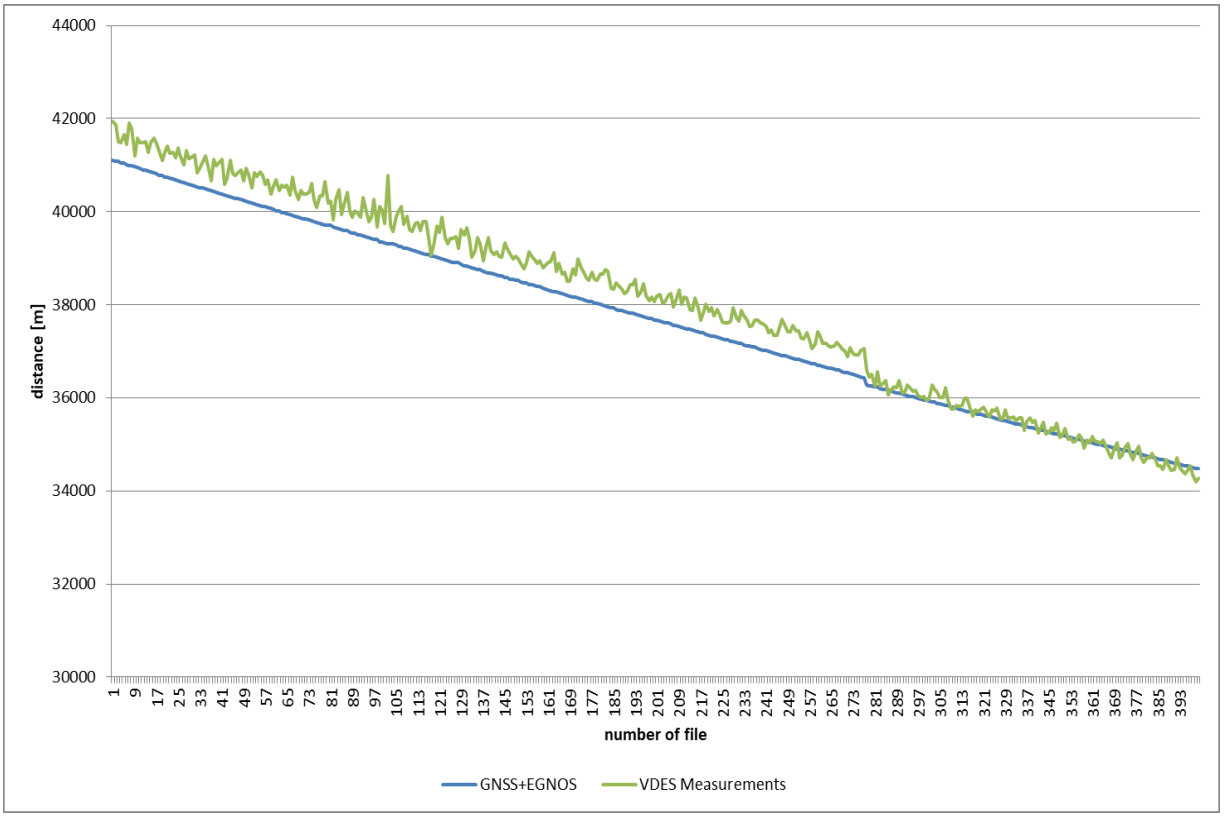

Figure 4-41: Errors caused by the failure of the oscillator

- Possible impact of residual clock errors.
- Errors caused by the presence of the Hel Peninsula. This error has already been analyzed in previous sections.
- Errors that can be generated by EGNOS.
- Too fast movement of the ship.
- Weather conditions.
- Error resulting from the line of sight distance, which after calculations is 42.4 km.

5 Summary

The activities conducted by the National Institute of Telecommunications in the R-Mode GAs 5.3 and 5.4 (and described in this report) were mostly conceptual and simulation work. Now, the results obtained up to this point need to be confirmed in the target environment (i.e. at sea).

For spring 2019, a wide measurement campaign is planned whose goal is to confirm the feasibility of the AIS-based solutions for the purposed of the planned R-Mode system. The campaign will be divided into three stages:

- Terrestrial and static tests in Gdańsk
- Onshore static/dynamic tests in Hel (on the Hel Peninsula)
- Dynamic measurements at the Baltic Sea (within the Bay of Gdansk area) which will be conducted using the Stena Line ferry travelling between Gdynia and Karlskrona. A several repetitions of this campaign are anticipated to obtain more reliable results.

As explained in the report, the vast majority of the preparations for the campaign is already completed, and some minor remaining organizational issues are being handled now.

The results that will be obtained during the campaign (alongside the software developed by the NIT) will serve a major contribution into the main R-Mode sea trial coordinated by other project partners.

Main difficulties:

- Noise + Interference
- Residual errors
- Mixed propagation path
- Weather

6 Conclusions for the next measurement campaign

The results obtained in the maritime environment indicate that the utilization of the novel VDES system for VHF ranging is more promising than the AIS system. Most notably, the accuracy of the determined position for the VDES system is better than for the AIS system, according to theoretical assumptions and actual measurement data. It should be noted, however, there are some differences between theoretical curves and obtained measurement data. The main reasons for that is the fact that theoretical curves apply mainly to high SNR values (above 15 dB), which can be seen in fig. 11, whereas for low SNR values the results are affected by the errors listed in the previous section,

For spring 2020, another measurement campaign is planned whose goal is to confirm the feasibility of the VDES-based solutions for the purpose of the planned R-Mode system. Based on the experience of the two completed measurement campaigns, a list of planned changes (on the hardware and software sides) was prepared before the next measurement campaign scheduled for March/April 2020:

- VDES signal without Hann Window – to improve transmitted signal power,
- transmission without physical VHF filter – to improve transmitted signal power,
- noise reduction in the receiver – utilization of another LNA and filter type is being considered,
- Low Noise Amplifier with less gain – to eliminate the need for an attenuator at the USRP input,
- reconfiguration of the ublox module (reference positioning system) – to maximize the number of GPS and Galileo satellites used.

In addition to that, yet another campaign is anticipated, which will deal with the signals developed by one of the project's partners – German Aerospace Center (DLR).

It is planned to maintain the R-Mode test station installed in the Port Gdynia until the end of the R-Mode Baltic project and, possibly, throughout its extension (until 2021).

All measurement results obtained will be utilized in the implemented positioning software based on the distance measurements from several reference R-Mode stations using TOA (*Time of Arrival*) method. This software is critical for further evaluation of the R-Mode system capabilities because it will ultimately allow us to analyze not only ranging accuracy but also to estimate the actual positioning errors, which otherwise would not be possible as currently we only have just one R-Mode station. That being said, in the future there are plans to develop a multi-station test bed in the R-Mode project as well.

7 References

[2-1] R-Mode Baltic - Baseline and Priorities

[2-2] Recommendation ITU-R M.1371-5 (02/2014), *Technical characteristics for an automatic identification system using time division multiple access in the VHF maritime mobile frequency band*

[2-3] 3GPP TS 25.213 V15.0.0, 2018, “Technical Specification Group Radio Access Network; Spreading and modulation (FDD)”.

[3-1] ITU-R P.1546-5, 2013, “Method for point-to-area predictions for terrestrial services in the frequency range 30 MHz to 3 000 MHz”

[4-1] ITU-R M.1371-5, 2014,“Technical characteristics for an automatic identification system using time division multiple access in the VHF maritime mobile frequency band”.

[4-2] National Instruments, 2012, “NI USRP™-2920 Specifications: 50 MHz to 2.2 GHz Tunable RF Transceiver”.

[4-3] Quartzlock E80-GPS Specification: GPS Disciplined Rubidium Frequency & Time Reference

[4-4] ITU-R M.2092-0, 2015, "Technical characteristics for a VHF data exchange system in the VHF maritime mobile band".

[5-1] ITU-R P.1546-5, 2013, “Method for point-to-area predictions for terrestrial services in the frequency range 30 MHz to 3 000 MHz”.

[7-1] Report ITU-R M.2123-2007; Long range detection of automatic identification system (AIS) messages under various tropospheric propagation conditions